# RECONSTRUCTION OF SEA LEVEL FLUCTUATION AND ENVIRONMENTAL CHANGES IN KHAO SAM ROI YOT NATIONAL PARK, CHANGWAT PRACHUAP KHIRI KHAN DURING THE LATE HOLOCENE

Miss Worakamon Nudnara



A Thesis Submitted in Partial Fulfillment of the Requirements
for the Degree of Master of Science in Geology
Department of Geology
Faculty of Science
Chulalongkorn University
Academic Year 2019

# การจำลองการเปลี่ยนแปลงของระดับน้ำทะเลและสภาพแวดล้อมบริเวณอุทยานแห่งชาติเขาสามร้อยยอด จังหวัดประจวบคีรีขันธ์ ในสมัยโฮโลซีนตอนปลาย

น.ส.วรกมล นัดนะรา



วิทยานิพนธ์นี้เป็นส่วนหนึ่งของการศึกษาตามหลักสูตรปริญญาวิทยาศาสตรมหาบัณฑิต
สาขาวิชาธรณีวิทยา ภาควิชาธรณีวิทยา
คณะวิทยาศาสตร์ จุฬาลงกรณ์มหาวิทยาลัย
ปีการศึกษา 2562

| | |
|---|---|
| Thesis Title | RECONSTRUCTION OF SEA LEVEL FLUCTUATION AND ENVIRONMENTAL CHANGES IN KHAO SAM ROI YOT NATIONAL PARK, CHANGWAT PRACHUAP KHIRI KHAN DURING THE LATE HOLOCENE |
| By | Miss Worakamon Nudnara |
| Field of Study | Geology |
| Thesis Advisor | Assistant Professor AKKANEEWUT JIRAPINYAKUL, Ph.D. |
| Thesis Co Advisor | Paramita Punwong, Ph.D. |

Accepted by the Faculty of Science, Chulalongkorn University in Partial Fulfillment of the Requirement for the Master of Science

............................................................ Dean of the Faculty of Science

(Professor POLKIT SANGVANICH, Ph.D.)

THESIS COMMITTEE

............................................................ Chairman

(Assistant Professor VICHAI CHUTAKOSITKANON, Ph.D.)

............................................................ Thesis Advisor

(Assistant Professor AKKANEEWUT JIRAPINYAKUL, Ph.D.)

............................................................ Thesis Co-Advisor

(Paramita Punwong, Ph.D.)

............................................................ Examiner

(Professor MONTRI CHOOWONG, Ph.D.)

............................................................ External Examiner

(Trongjai Hutangkura, Ph.D.)

วรกมล นัดนะรา : การจำลองการเปลี่ยนแปลงของระดับน้ำทะเลและสภาพแวดล้อมบริเวณอุทยานแห่งชาติเขาสามร้อยยอด จังหวัดประจวบคีรีขันธ์ ในสมัยโฮโลซีนตอนปลาย. ( RECONSTRUCTION OF SEA LEVEL FLUCTUATION AND ENVIRONMENTAL CHANGES IN KHAO SAM ROI YOT NATIONAL PARK, CHANGWAT PRACHUAP KHIRI KHAN DURING THE LATE HOLOCENE) อ.ที่ปรึกษาหลัก : ผศ. ดร.อัคนีวุธ จิรภิญญากุล, อ.ที่ปรึกษาร่วม : ดร.ปรมิตา พันธ์วงศ์

การศึกษาการเปลี่ยนแปลงของระดับน้ำทะเลโดยรอบอ่าวไทยในสมัยโฮโลซีนมีความสำคัญเนื่องจากพื้นที่ในบริเวณนี้ไม่ได้รับผลกระทบจากการเปลี่ยนแปลงทางธรณีสัณฐาน ในการศึกษานี้ได้ทำการเก็บตัวอย่างแท่งตะกอนจำนวน 9 ตำแหน่งจากทุ่งสามร้อยยอด จังหวัดประจวบคีรีขันธ์ ซึ่งมีลักษณะเป็นพื้นที่ชุ่มน้ำในบริเวณชายฝั่งตะวันตกของอ่าวไทย เพื่อทำการศึกษาการกระจายตัวของตะกอน ต่อมาได้เลือกแท่งตะกอน CP-4 มาทำการศึกษาอย่างละเอียด ประกอบด้วยการหามวลที่หายไปจากการเผา การกระจายตัวของขนาดตะกอน และการวิเคราะห์ละอองเรณู เพื่อทำการจำลองการเปลี่ยนแปลงของระดับน้ำทะเลและสภาพแวดล้อมของพื้นที่บริเวณนี้ ตะกอนที่พบในพื้นที่ชุ่มน้ำสามารถจำแนกออกได้ 3 หน่วย ได้แก่ หน่วย A มีลักษณะเป็นตะกอนโคลนสีเทาเข้มปะปนด้วยตะกอนขนาดทรายถึงทรายแป้ง หน่วย B มีลักษณะเป็นตะกอนโคลนสีน้ำตาลอ่อนที่ถูกปะปนด้วยตะกอนขนาดทรายถึงทรายแป้ง และหน่วย C ได้แก่ตะกอนทะเลสาบสีน้ำตาลเข้าถึงสีเทาเข้ม ผลการศึกษาละอองเรณูบ่งบอกว่าในบริเวณนี้อยู่ในสภาพแวดล้อมที่ได้รับผลจากน้ำขึ้นน้ำลง และถูกปกคลุมด้วยป่าชายเลนเมื่อประมาณ 3500 - 1700 ปีก่อนช่วงปัจจุบัน โดยหลักฐานจากละอองเรณูบ่งบอกว่ามีช่วงแห้งแล้งเกิดขึ้นเป็นระยะเวลาสั้น ๆ เมื่อประมาณ 3300 ปีก่อนช่วงปัจจุบัน หลังจากนั้นพบว่าระดับน้ำทะเลค่อนข้างคงที่เมื่อประมาณ 3000 - 1700 ปีก่อนช่วงปัจจุบัน ต่อมาในบริเวณนี้เกิดสภาพแวดล้อมแบบหลังป่าชายเลนขึ้นเมื่อ 1700 - 1600 ปีก่อนช่วงปัจจุบัน บ่งบอกถึงระดับน้ำทะเลที่ลดลง สภาพแวดล้อมเปลี่ยนแปลงกลับมาเป็นป่าชายเลนเนื่องจากระดับน้ำทะเลเพิ่มขึ้นอีกเล็กน้อยเมื่อประมาณ 1600 - 1000 ปีก่อนช่วงปัจจุบัน หลังจากนั้นเกิดสภาพแวดล้อมหลังป่าชายเลนขึ้นอีกครั้งเมื่อประมาณ 1000 - 400 ปีก่อนช่วงปัจจุบัน ระดับน้ำทะเลลดลงอย่างต่อเนื่องร่วมกับอิทธิพลของน้ำจืดที่เข้ามาในพื้นที่ ทำให้สภาพแวดล้อมในบริเวณทุ่งสามร้อยยอดเปลี่ยนแปลงไปเป็นพื้นที่ชุ่มน้ำจนถึงปัจจุบัน



| | | |
|---|---|---|
| สาขาวิชา | ธรณีวิทยา | ลายมือชื่อนิสิต ............................................... |
| ปีการศึกษา | 2562 | ลายมือชื่อ อ.ที่ปรึกษาหลัก ............................. |
| | | ลายมือชื่อ อ.ที่ปรึกษาร่วม .............................. |

# # 6072092223 : MAJOR GEOLOGY
KEYWORD: sea level, paleoenvironment, lake sediment, pollen analysis

Worakamon Nudnara : RECONSTRUCTION OF SEA LEVEL FLUCTUATION AND ENVIRONMENTAL CHANGES IN KHAO SAM ROI YOT NATIONAL PARK, CHANGWAT PRACHUAP KHIRI KHAN DURING THE LATE HOLOCENE. Advisor: Asst. Prof. AKKANEEWUT JIRAPINYAKUL, Ph.D. Co-advisor: Paramita Punwong, Ph.D.

The Gulf of Thailand is generally provided the efficiency evidences of sea level fluctuation according to the lack of tectonic events. Sam Ro Yot National Park (SRY) is located in the west coast of the Gulf of Thailand with its elevation approximately at sea level. Sedimentary sequences from SRY wetland has been obtained. This sedimentary sequence can be divided into 3 units, comprised dark grey silty to sandy clay of unit A, beige clay of unit B, and gyttja sediment of unit C. An intensive analysis was focused on core CP-4 because it is the longest core and compose of all sedimentary units. Environmental reconstruction was accomplished by pollen analysis, grain size analysis, Loss on Ignition (LOI) and radiocarbon dating. This area was under intertidal environment and dominated by *Rhizophora*-mangroves since c. 3500 - 1700 cal year BP with a temporary dry conditions at c. 3300 cal year BP. Mangrove subsequently transferred to back mangroves at c. 1700 – 1600 cal year BP according to sea level regression. A minor transgression occurred later at c. 1600 – 1000 cal year BP, displaced this area by *Avicenia*-mangroves. Thereafter, mangrove zonation was prograde seaward due to the second regression, effected this area prominent by back mangroves at c. 1000 - 400 cal year BP. Freshwater wetland was finally replaced from c. 400 cal year BP to present.



| | | |
|---|---|---|
| Field of Study: | Geology | Student's Signature ............................... |
| Academic Year: | 2019 | Advisor's Signature ............................. |
| | | Co-advisor's Signature ......................... |

# ACKNOWLEDGEMENTS

First, I would like to express my gratitude for my thesis advisor, Assistant Professor Akkaneewut Jirapinyakul, Ph.D. who always educate and give a helpful advice that help me to accomplish my thesis. Furthermore, he also provides a lot of supports in my real life which gain me a grateful experience and extraordinary occasions.

Second, my co-adviser, Dr. Paramita Punwong from Faculty of Environment and Resource studies, Mahidol University, for the advice in palynological study and laboratory techniques.

My appreciation goes further to Mr. Robin Nohall, Ms. Chawisa Phujareanchaiwon and Ms. Apichaya Englong for helping me in fieldworks. Without their support, the data in my thesis would not be completed as it is.

Next, I would like to thank Mrs. Assuma Sainakum for assisting me in laboratory works and helping me to solve technical problem.

Finally, my deepest thanks go to my family. They always support everything I do, and their trust always comfort me. I cannot get to my goal without their encouragement.

Worakamon Nudnara

TABLE OF CONTENTS

## Tables

Page

# Figures

Page

# CHAPTER 1 INTRODUCTION

## 1.1 Background

Environmental changes, which are generally related with climate variability, widely impact on human living in both direct and indirect ways (Galbraith et al., 2002; Kemp et al., 2013; Michener et al., 1997). The sea level rise, for example, is associated with the global warming (Church et al., 2013; Milne et al., 2009; Nicholls and Cazenave, 2010). Recent studies suggest that the warmer temperature disrupted the ice sheet mass balance in Greenland and Antarctica and raised the sea level between the $19^{th}$ and $20^{th}$ centuries (Bindoff et al., 2007; Church et al., 2013; Milne et al., 2009; Nicholls and Cazenave, 2010). Moreover, the sea level rise subsequently increases the coastal erosion through coastal flooding and wetland losses, and the saltwater intrusion into both the surface water and groundwater (Church et al., 2013; Nicholls and Cazenave, 2010). Although the physical impacts of sea level changes are well known, long-term observation is still necessary to understand their spatial and temporal variabilities. Geological archives therefore have been introduced to fulfill the gap of instrumental observation.

The Gulf of Thailand has been considering to be an important area for investigating history of the sea level. Since its location in the tropical climate and lack of tectonic evidences, the relative sea level in the Gulf of Thailand possibly reflected the eustatic change (Culver et al., 2015; Horton et al., 2005; Tjia, 1992). The investigation on the sea level changes in the Gulf of Thailand has generally been based on the radiocarbon dating of peat layers, pollen analysis and shell layers attached on the sea notch (Chaimanee, 1987; Choowong et al., 2004; Hutangkura, 2012; Sinsakul, 1992; Somboon, 1988; Thiramongkol, 1984; Tjia, 1996). A few sequential radiocarbon dates in these studies make it difficult to follow the abrupt sea level changes. Recent studies in this area, however, have focused on a coastal and delta development and been based on high resolution dating (Li et al., 2012; Nimnate et al., 2015; Surakiatchai et al., 2018; Tamura et al., 2009).

Sam Roi Yot National Park is located in the northwestern side of the Gulf of Thailand in Prachuap Khiri Khan Province. Center of the national park is Permian Limestone Mountain surrounded by flat area, which is approximately elevated at recent sea level (Koskelainen, 2014). East of the area is a beach, while the west is a wetland with a year-round stagnant condition called Thung Sam Roi Yot. The environmental changes in the eastern part of the study area were well reported by many studies, while the environmental reconstruction from the western wetland was paucity (Choowong, 2002; Dusitapirom, Choowong, and Daorerk, 2008; Surakiatchai et al., 2018). The detail of these studies was reported in the literature reviews (Chapter II). Although, many proxies were using for the environmental reconstruction in this area, the mangrove succession based on pollen analysis has never been reported.

Pollen is male gametophyte of the flowering plants, which have their own specific morphology, i.e. aperture, sculpture and size. Moreover, the pollens do not disperse far from their source (Somboon, 1988). These altogether make them sufficient proxy for the environmental assessment. In the sea level reconstruction, pollen is wildly used, since the mangrove succession is directly influenced by the sea level changes (Ellison, 2008). Therefore, the response of mangrove to sea level changes based on pollen analysis was recognized to be a main principle in this study.



**1.2 Research objectives**

1. To reconstruct environmental changes in Khao Sam Roi Yot National Park
2. To compare and discuss history of the sea level changes during the late Holocene in the Gulf of Thailand

**3. Scope of study**

This study focuses on reconstruction of the sea level fluctuation occurring in Khao Sam Roi Yot National Park (12° 04´ to 12° 21´N and 99° 51´ to 100° 02´E). Sediment cores were collected from nine locations in the Sam Roi Yot wetland located in the western part of the national park. According to its the longest sedimentary sequence and including all sedimentary units, CP-4 was here selected for the further study by loss on Ignition (LOI), grain size and pollen analysis at 2, 4, and 5-cm intervals, respectively. For the pollen analysis, pollen grains were enumerated in an attempt to achieve a count of 300 pollen grains by sample. The chronology for sediment core CP-4 is based on nine radiocarbon dates of microscopic charcoal. The mangrove succession associated with chronology was discussed in term of the temporal variability of the sea level fluctuation.

**4. Benefit**

The temporal variability of the sea level changes in Khao Sam Roi Yot National Park.

# CHAPTER 2 LITERATURE REVIEW

## 2.1 Sea level changes during the Holocene in the Gulf of Thailand

The Gulf of Thailand has been considered to be an important area for studying history of sea level changes because it is located in tropical climate and tectonic stability (Geyh, Streif, and Kudrass, 1979; Hanebuth, Stattegger, and Bojanowski, 2009; Horton et al., 2005; Tam et al., 2018). Therefore, the influences of isostatic adjustment and tectonic movement can be separated from the sea level changes. Many studies reported the sea level fluctuation in this area based on various techniques, e.g. geomorphology (Choowong et al., 2004; Dusitapirom et al., 2008; Nimnate et al., 2015; Surakiatchai et al., 2018), dating of peat layer (Bird et al., 2007; Geyh et al., 1979; Sinsakul, 1985) and shall layer attached on the sea notch (Dusitapirom et al., 2008; Surakiatchai et al., 2018; Thiramongkol, 1984), pollen and sediment analysis (Horton et al., 2005; Li et al., 2012; Somboon, 1988). Results of studies were summarized and further constructed to draw the sea level curves of the Gulf of Thailand (Bird et al., 2007; Choowong et al., 2004; Horton et al., 2005; Sinsakul, 1985).

The Gulf of Thailand was emerged during the last glacial maximum (c. 23,000-19,000 cal year BP) when the sea level decreased and reached its lowstand of approximately 120 m below modern sea surface (bmss) owing to advance of continental ice sheet in the Northern Hemisphere (Bird et al., 2007; Hanebuth, Stattegger, and Grootes, 2000) (Figure 1). The emerged Gulf of Thailand connected the Southeast Asian mainland with Sumatra, Java and Boneo (Hanebuth et al., 2011). Many proxies indicate the sea level rise together with climate changes after the retreat of continental ice sheet during the deglaciation (after c. 19,000 cal year BP). The sea level curve at Singapore constructed by Geyh et al. (1979) suggested that the sea level rapidly rose during the early Holocene (11700 – 8200 cal year BP), reached its highstand in the mid Holocene, and gradually decreased thereafter. Later studies however provided the further information on sea level fluctuation (Bird et al., 2007; Hanebuth et al., 2000; Hanebuth et al., 2009; Hesp et al., 1998; Horton et al., 2005; Somboon, 1988). The sea level in the Gulf of Thailand was rapidly rose in a rate of approximately 10 mm/year (Hanebuth et al., 2009) to 5.5 mm/year (Horton et al., 2005) during the early Holocene. Exact date of the mid Holocene sea level highstand however has been debated by many studies, i.e. c. 4500 cal year BP (Geyh et al., 1979), c. 6500 cal year BP (Somboon, 1988), c. 3800 cal year BP (Hesp et al., 1998), 4850-4450 cal year BP (Horton et al., 2005) and c. 6500 cal year BP (Nimnate et al., 2015; Surakiatchai et al., 2018) (Figure 2). Despite the outbreak of regression after the mid Holocene sea level highstand was varied, it is well consistent that the rate of sea level fall was lower than the early Holocene transgression (Choowong et al., 2004; Geyh et al., 1979; Horton et al., 2005; Nimnate et al., 2015; Somboon, 1988; Surakiatchai et al., 2018). Horton et al. (2005), for example, proposed that the rate of regression was about 1.1 mm/year.

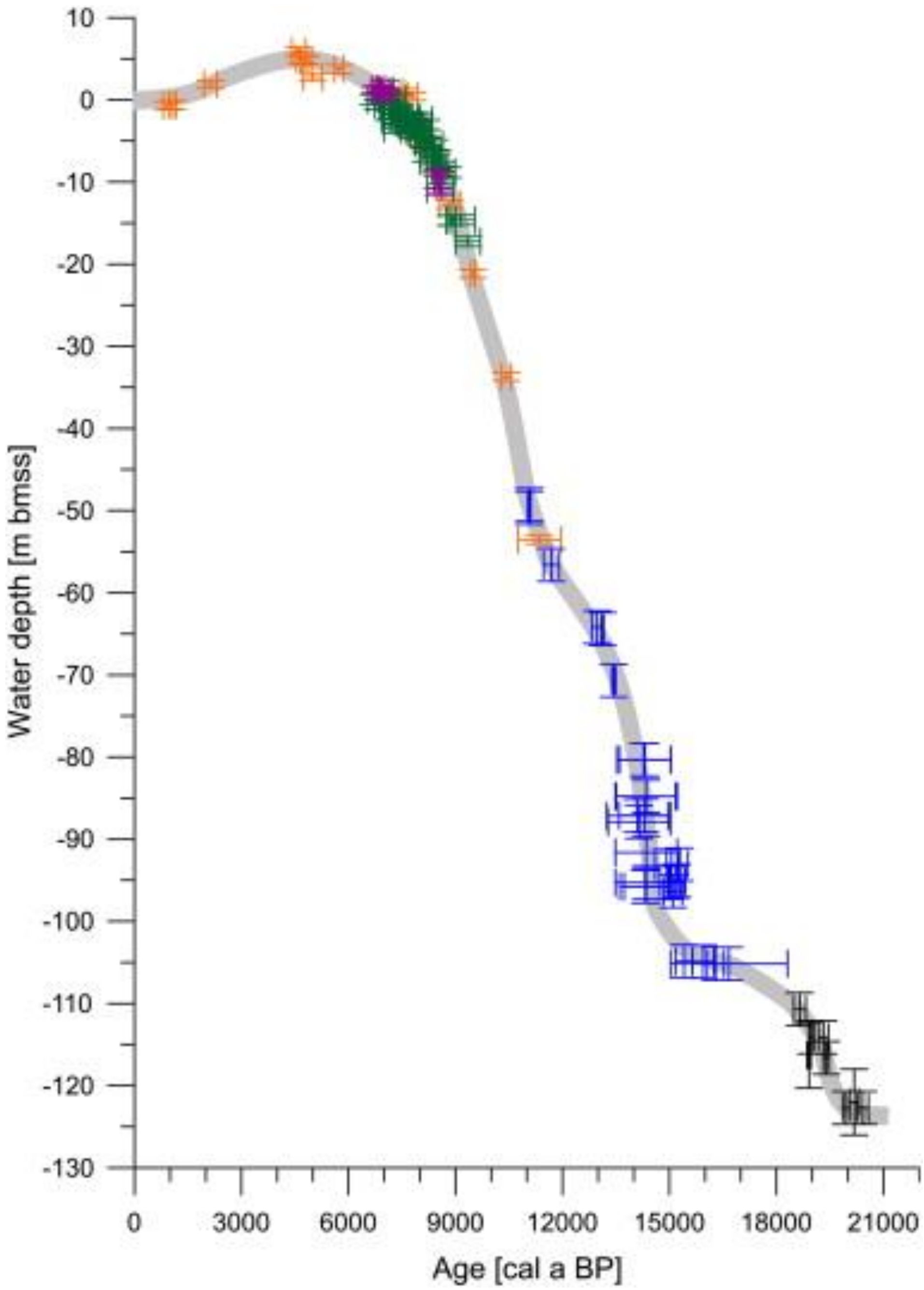


**Figure 1** Reconstruction of sea level history for the past 21 ka showing all data recently available from the Sunda core region. Data compiled from Geyh et al. (1979) (orange; Strait of Malacca), Hesp et al. (1998) (purple; Singapore), Hanebuth et al. (2009) (black; Sunda Shelf). (Hanebuth et al., 2011)

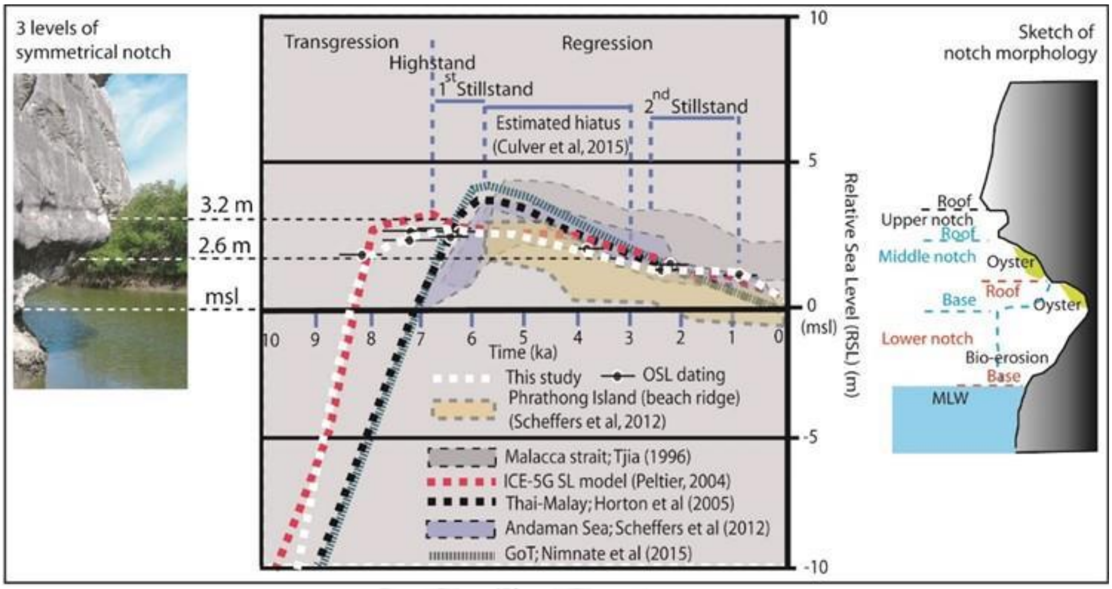


**Figure 2** Compilation of sea level curves from Southeast Asia and South China Sea. Three levels of sea notch (left) and sketch of notch morphology (right) showed correlation with sea level curve. Proposed sea level curve derived from Surakiatchai et al. (2018) shows in whit dash-line (Surakiatchai et al., 2018)

In contrast, the curve which were constructed by Tjia (1996), Sinsakul (1992) and Bird et al. (2007) show a more complicated fluctuation of sea level. The reconstructed sea level which was associated with well chronology in Singapore by Bird et al. (2007) suggest a rapid sea level rise from -17 to -3 m bmss between c. 9500 and 8000 cal year BP (Figure 5). The sea level was relatively stable than that between c. 8000 to 7000 cal year BP, when it was varied from +4 to +2 m above modern sea surface (amss). And the sea level high was +1.5 m amss at c. 6500 cal year BP. Tjia (1996) proposed that the sea level increased 3 times during the mid-late Holocene, i.e. c. 6000-4000 cal year BP, 3,000-2,000 cal year BP, and after 1,000 cal year BP (Figure 3). These intervals of transgression were intervened by the excursions of sea level fall 4,000-3,000 cal year BP and 2,000-1,000 cal year BP. And the sea level reached its highstand at c. 5000 cal year BP (Tjia, 1996). These were slightly shifts in time from those reconstructed by Sinsakul (1992) who propose the sea level rise c. 7,000-6,500 cal year BP, 4,200-3,500 cal year BP, and 2,500-1,800 cal year BP, and sea level fall in between these intervals and after 1,800 cal year BP (Figure 4).

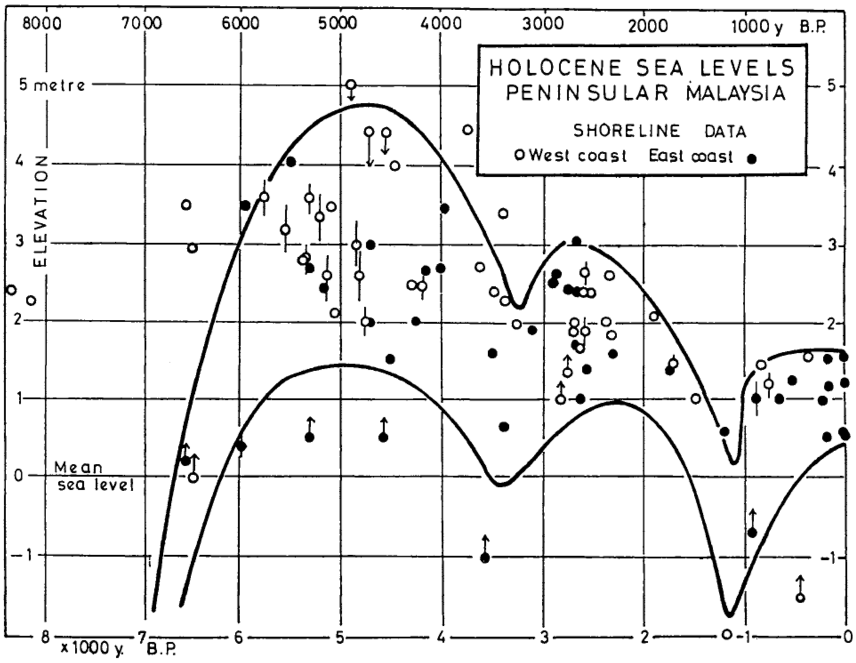


**Figure 3** The reconstructed sea level curve by Tjia (1996). It demonstrated the Holocene sea level fluctuation with sea level highstand at c. 5000 and 2800 cal year BP.

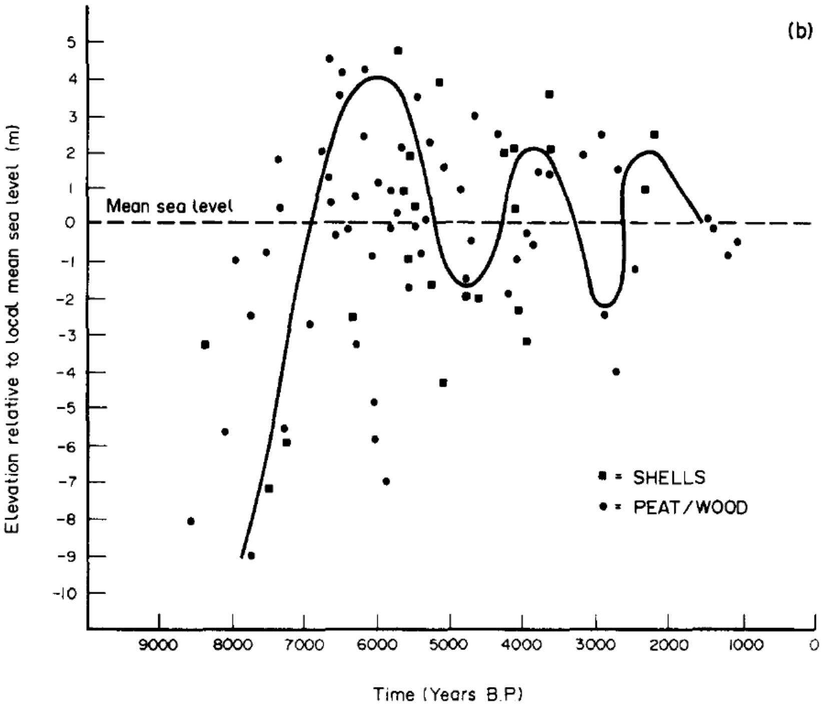


**Figure 4** The reconstructed sea level curve by Sinsakul (1992).

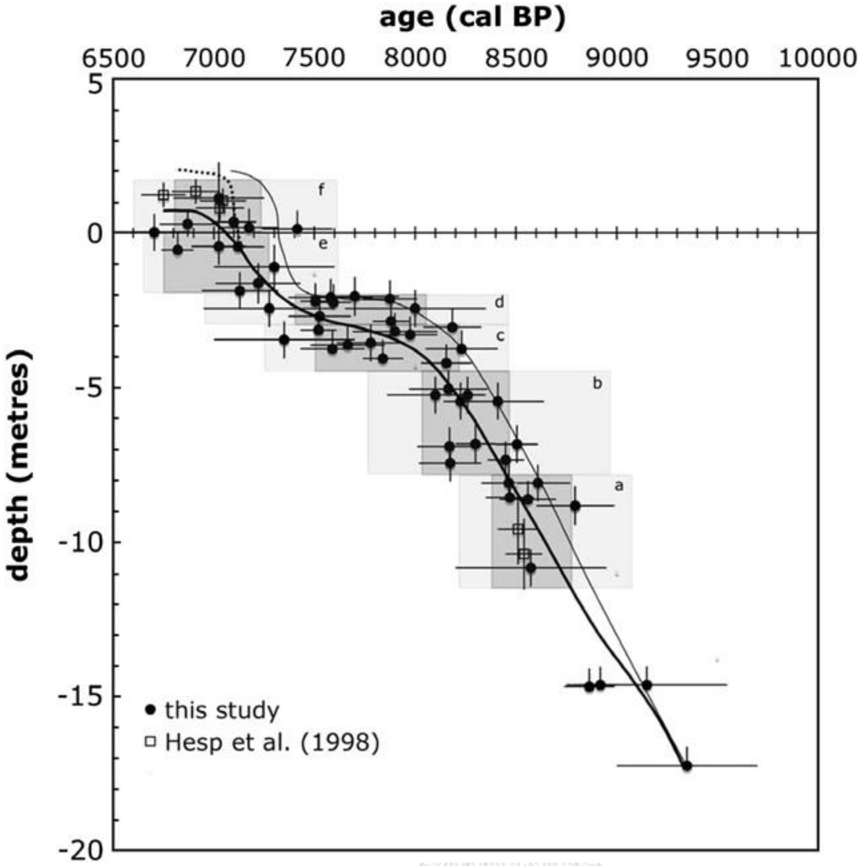


**Figure 5** The reconstructed sea level change in Singapore (Bird et al., 2007).

**2.2 Response of mangrove to sea level changes**

Mangrove is an assemblage of tree and shrubs that thrive along tropical and subtropical coasts (Ellison, 2008; Li et al., 2012; Lugo and Snedaker, 1974; Santisuk, 1983). These plants have evaluated and developed their specific physiological characteristics and morphological adaptation that allows them to survive under the intertidal environment (Ellison, 2008; Li et al., 2012; Lugo and Snedaker, 1974). Mangrove community is generally controlled by many parameters, i.e. inundation frequency, soil salinity, soil composition, tide and wave energy (Li et al., 2012; Lugo and Snedaker, 1974). Watson (1928) suggested that the frequency of inundation is possibly a key role on mangrove dynamics. This parameter can be classified in to five classes (Table 1)

**Table 1** Tidal inundation class modified from Watson (1928)

| Class | Flood type | Frequency (times per month) |
|---|---|---|
| **1** | All high tides | 56 - 62 |
| **2** | Medium high tides | 45 - 59 |
| **3** | Normal high tides | 20 - 45 |
| **4** | Spring tides | 2 – 20 |
| **5** | Abnormal of equinoctial tides | 0 - 2 |

The mangrove can be divided into 2 groups in regarding to the frequency of inundation, i.e. swampy mangrove or mangroves, and tidal mangrove or back mangrove (Qureshi, 1959). Swampy mangroves or mangroves are generally submerged under the seawater during the high tide. However, the seawater can reach to the tidal mangroves or back mangroves during very high tide, e.g. spring tide or exceptional tide. Santisuk (1983) further classified the distribution of mangrove trees and shrubs in Thailand based on Watson's (1928) (Table 2). The mangroves are consistent with class 1-3, while back mangroves can be referred to class 4-5 (Table 1).

**Table 2** Mangrove tree and shrubs distribution in Thailand based on Watson's (1928) inundation classes modified from Santisuk (1983)

| Scientific name | Family | Ecological appearance | |
|---|---|---|---|
| | | Mangroves | Back mangroves |
| *Acrostichum aureum* | Pteridaceae | | ✓ |
| *Acrostichum speciosum* | Pteridaceae | | ✓ |
| *Avicennia alba* | Avicenniaceae | ✓ | |
| *Avicennia marina* | Avicenniaceae | ✓ | |
| *Avicennia officinalis* | Avicenniaceae | ✓ | |
| *Baringtonia asiatica* | Baringtoniaceae | | ✓ |
| *Baringtonia racemosa* | Baringtoniaceae | | ✓ |
| *Brownlowia tersa* | Tiliaceae | | ✓ |

| | | | |
|---|---|---|---|
| *Bruguiera cylindrica* | Rhizophoraceae | ✓ | |
| *Bruguiera gymnorrhiza* | Rhizophoraceae | ✓ | |
| *Bruguiera parviflora* | Rhizophoraceae | ✓ | |
| *Bruguiera sexangula* | Rhizophoraceae | | ✓ |
| *Ceriops decandra* | Rhizophoraceae | ✓ | |
| *Ceriops tagal* | Rhizophoraceae | ✓ | |
| *Lumnitzera littorea* | Combretaceae | | ✓ |
| *Lumnitzera racemosa* | Combretaceae | | ✓ |
| *Melaleuca leucadendron* | Myrtaceae | | ✓ |
| *Nypa fructicans* | Arecaeae | | ✓ |
| *Oncosperma tigillaria* | Arecaeae | | ✓ |
| *Pluchea indica* | Asteraceae | | ✓ |
| *Rhizophora apculata* | Rhizophoraceae | ✓ | |
| *Rhizophora mucronata* | Rhizophoraceae | ✓ | |
| *Sonneratia alba* | Sonneratiaceae | ✓ | |
| *Sonneratia caseolaris* | Sonneratiaceae | | ✓ |
| *Sonneratia griffithii* | Sonneratiaceae | | ✓ |
| *Sonneratia ovata* | Sonneratiaceae | | ✓ |
| *Suaeda maritima* | Chenopodiaceae | | ✓ |
| *Xylocarpus gangeticus* | Miliaceae | | ✓ |
| *Xylocarpus granatum* | Miliaceae | | ✓ |
| *Xylocarpus moluccensis* | Miliaceae | | ✓ |



Because the mangrove zonation directly relates with the inundation frequency, pollen analysis of mangrove succession is widely used as a proxy to assess the changes in sea level (Ellison, 2008; Horton et al., 2005; Li et al., 2012). In this case, pollen records can provide temporal variability of mangrove dynamics reflecting sea level fluctuation (Li et al., 2012)

A palynological study by Rugmai et al. (2008) suggests that mangrove and inland pollen taxa were the indicator of the sea level rise and a tropical vegetation in

Songkhla Lake, Southern Thailand during the late Pleistocene. The presence of mangrove pollen assemblages indicate that this area was a tidal zone and a transgression at c. 30950 cal year BP. However, the sparse of pollen together with yellowish brown mottled point to a poor preservation caused by oxidation reflecting a regression after c. 30950 cal year BP.

Hutangkura (2012) demonstrated paleogeographical changes in the lower Central Plain of Thailand in regarding to environmental and sea level change. The presence of mangrove covered from Suphan Buri, Ang Thong, to Samut Sakhon and Samut Prakarn indicated the Holocene maximum transgression at 8400 cal year BP. Sea level was covered the most part of the Central Plain and Suphan Buri. The sea level decreased after 7000 cal year BP. The continuous fall of sea level caused of the paleo-shoreline and mangrove zone shifted southward to the Gulf of Thailand (Figure 6).

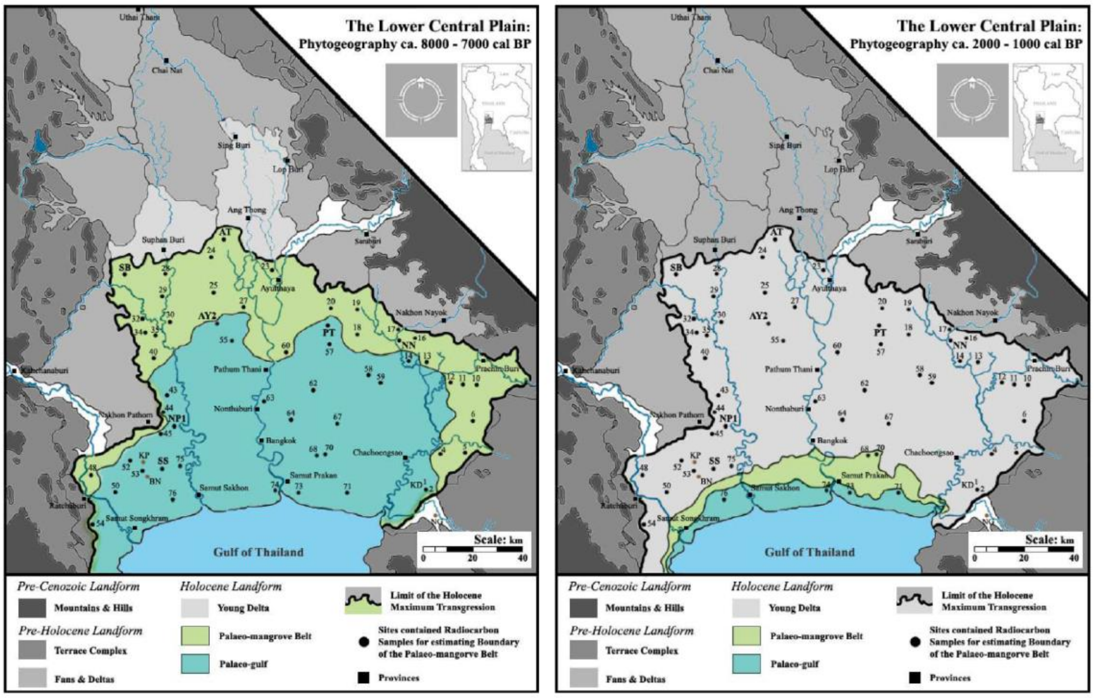


**Figure 6** Paleogeography of the Lower Central plain in Thailand (Hutangkura, 2012)

Palynological record from the lower Central Plain of Thailand demonstrates that freshwater-derived pollen assemblage was occupied by mangrove pollen taxa reflecting a transgression at c. 8600 - 8400 cal year BP (Somboon, 1988).

Horton et al. (2005) revealed an environmental and sea level change in Malay-Thai Peninsula by using palynological record in sedimentary sequence from the Great Songkhla Lake, Songkhla, Thailand. The pollen analysis suggests that this area was the mangrove environment at 8420-8190 cal year BP and was replaced by freshwater swamp at 7880-7680 cal year BP. These results suggest the declination of marine influence or regression during this time interval.

The investigation of mangrove succession in sedimentary sequence from the upper Mekong River delta, Cambodia showed the abundance of *Sonneratia alba* and *Sonneratia caseolaris* which are pioneer taxa at 8300 cal year BP. *Sonneratia* was subsequently replaced by *Rhizophora apiculate* and *Bruguiera* spp. indicated the regressive mangrove succession and the declination of the sea level (Li et al., 2012).

The sea level fluctuations in Ong Kharak district, Nakhon Nayok province was investigated by Punwong (2007). The sedimentary sequences can be divided into three units; the Pleistocene stiff clay, the Holocene marine clay (Bangkok clay), and the recent floodplain deposit. Pollens have been found only in Bangkok clay. Mangrove pollen taxa was dominated the sediment at approximately c. 7620 cal year BP. Back mangrove pollen assemblage was subsequently occupied at c. 7460 cal year BP inferred the sea level rise. Mangrove pollen again increased and reached the highest percentage at approximately 6000 cal year BP that was consist well in time with the sea level highstand (Sinsakul, 1992; Somboon, 1988). Back mangrove had again increased till 5050 cal year BP owing to the regression. The slight changes in mangrove and back mangrove suggested that the sea level was relatively stable than that the previous period after 5050 cal year BP. However, this interval of steady sea level was possibly interrupted by the excursions of regression and transgression (Sinsakul, 1992; Somboon, 1988). The decrease in mangrove pollen taxa corresponded well with an increase in back mangrove and lowland forest that points to the Holocene final regression. However, dating results, which can refer to an absolute age of the last regression, had not yet accomplished.

Although many studies demonstrated the sea level changes based on geomorphology in the Khao Sam Roi Yot National Park, the mangrove succession in regarding to pollen records have never been reported from this area (Choowong et al., 2004).

### 2.3 Study area

Khao Sam Roi Yot National Park (12° 04´ to 12° 21´N and 99° 51´ to 100° 02´E) is located in the west coast of the Gulf of Thailand, covered the area of approximately 98.8 $km^2$ (Koskelainen, 2014; Surakiatchai et al., 2018) (Figure 7). The center of national park is a mountain, which composes of the Permian limestone. The mountain is surrounded by wetland and beach in the west and east directions. The wetland is called Thung Sam Roi Yot, which covers the area of approximately 36.8 $km^2$ (Koskelainen, 2014). Koskelainen (2014) mentioned that this wetland is a freshwater marsh. The marsh and its surrounding areas are approximately at mean sea level (MSL) (Koskelainen, 2014).

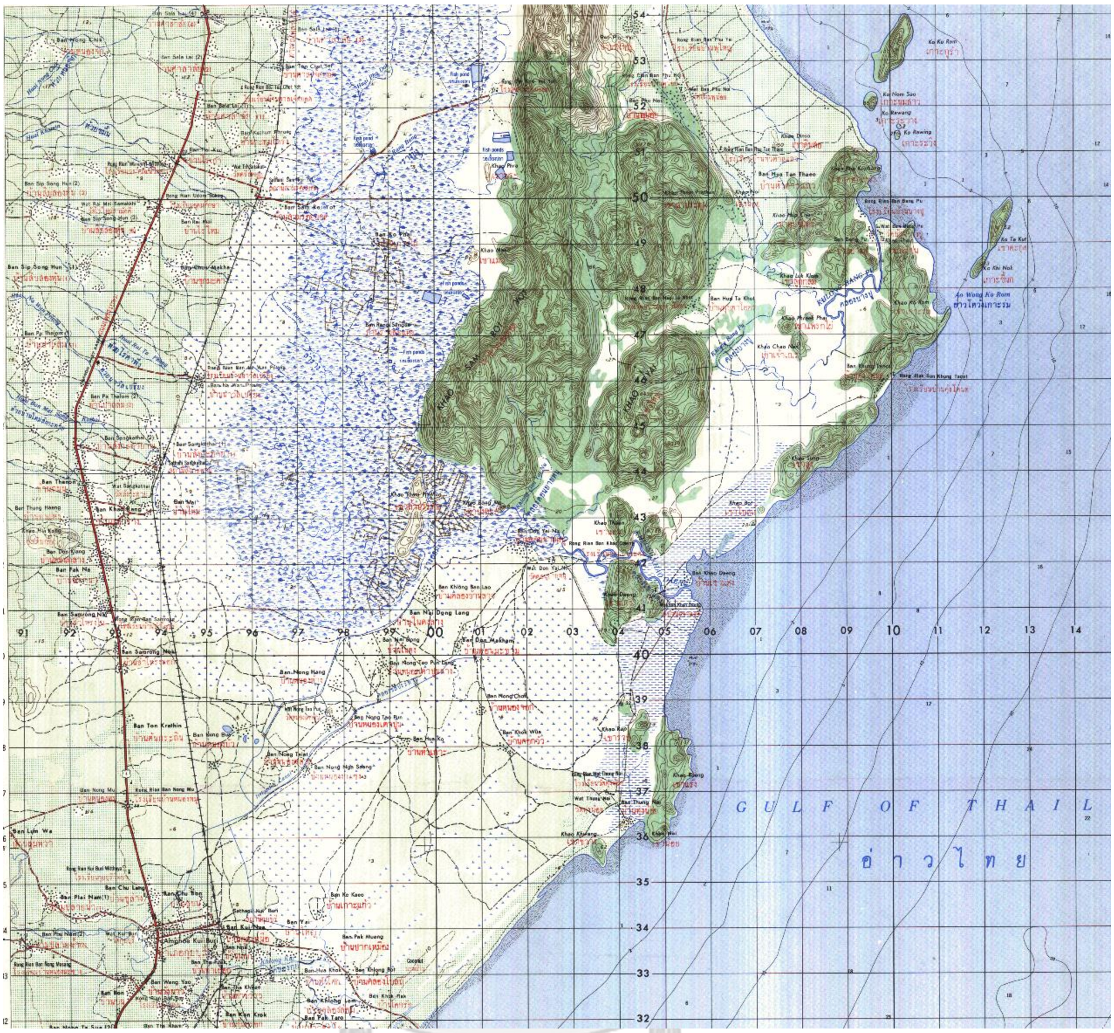


**Figure 7** Khao Sam Roi Yot National Park topographic map



The limestone mountain is flourished by evergreen and deciduous tree and shrubs, which generally thrive in the thin soil and the barren rocks (Koskelainen, 2014). However, vegetation found in the marsh is mainly Poaceae associated with Cyperaceae. The eastern part of the mountain is dominated by mangrove forest. However, *Casuarina*, which usually classified as associated mangrove, can be found in the beach area (Koskelainen, 2014).

Geomorphological evolution of this area was described by Surakiatchai et al. (2018) who suggested the development of coastal bay, beach ridge plain, and tombolos caused by the Holocene transgression at approximately 6500 – 6000 cal year BP. The tombolos were gradual developed and connected the limestone island with the mainland at 3000 – 1000 cal year BP. The landform was progressively transferred to a tidal flat. The coastal evolution agree well in time with the dating of shells attached on the sea notch that indicated the stillstand of sea level at 6000 and 3000 cal year BP (Figure 8). Thiramongkol (1984) either report radiocarbon dating of two level of sea notches in this area which are c. 6700 cal year BP from 2 m and 3500 cal year BP for 1 m. Absolute age provided by Thiramongkol (1984) and Surakiatchai et al. (2018) are rather consistent. These results agree well with Choowong et al. (2004) who suggested a gradual fall of the sea level after the mid Holocene.

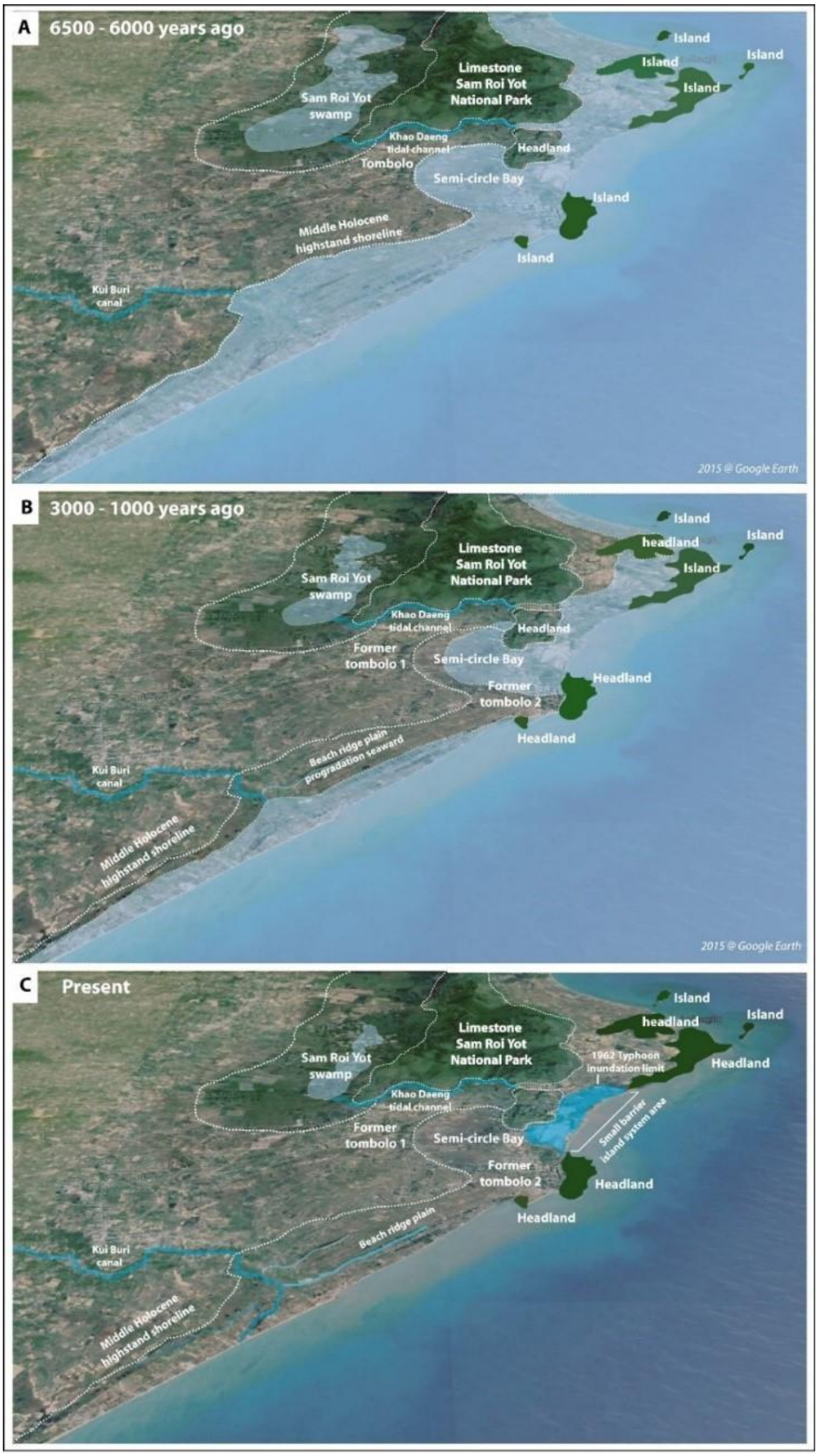


**Figure 8** The reconstruction of paleogeography in Khao Sam Roi Yot National Park (Surakiatchai et al., 2018)

# CHAPTER 3 MEDTHODOLOGY

## 3.1 Sample collection

Sediment cores were collected from Thung Sam Roi Yot by using Russian corer, 1-meter long and approximately 10 centimeters diameter, on the modified inflatable boat. In each coring site, the sediment cores had been taken meter by meter till penetration was impossible. The platform then moved approximately 50-30 centimeters further from the first hole and the overlap sediment cores of depth of 50 cm were taken. The sediment cores were taken from seven coring points along the north-south transect. Sites CP-3 and CP-7 in the western part of wetland were further observed in order to compare with the previous studies by Koskelainen (2014). The sediment cores were placed in the PVC tubes, transported to the Department of Geology, Chulalongkorn University, and keep in the refrigerator for the further analysis.

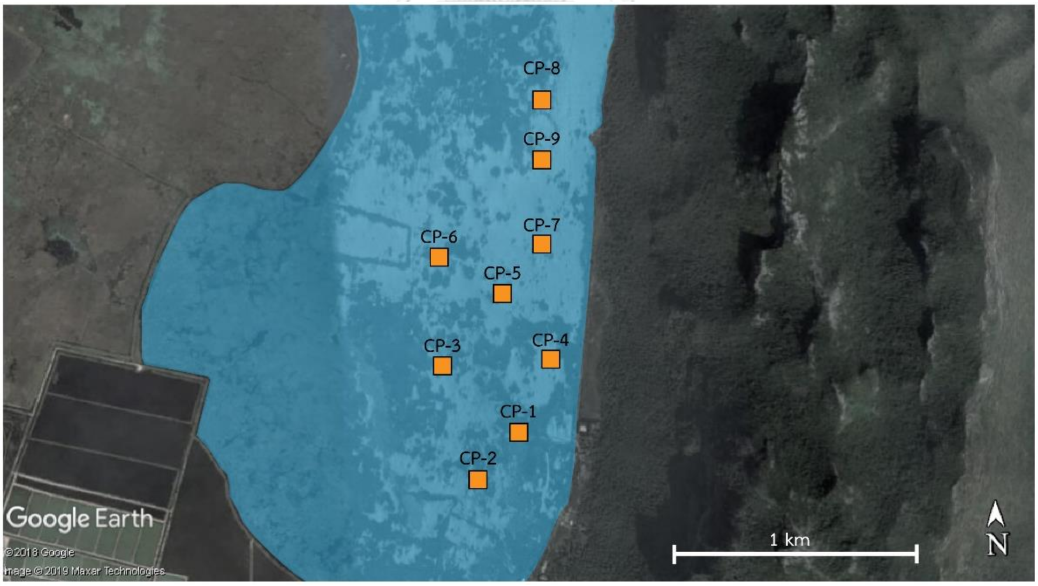


**Figure 9** Location map of coring points

**Figure 10** Coring method

**Figure 11** A sedimentary core obtained from the lake

**3.2 Laboratory works**

Surface of sedimentary sequences was carefully cleaned and described in detail based on their physical properties, e.g. sediment color and grain size. The overlap sediment cores were then correlated in order to construct composite depth and lithostratigraphic column for each coring point. The lithostratigraphic columns from each site were subsequently correlated in order to investigate sediment distribution in the wetland. Core SRY CP-4 was selected for studying in detail because it is the longest sedimentary sequence and composing of all sedimentary units. The further studies compose of loss on ignition (LOI), grain size distribution, pollen analysis and radiocarbon dating.

3.2.1 Loss on ignition (LOI)

The consecutive 2-cm samples were prepared for the LOI followed the procedure of Heiri, Lotter, and Lemcke (2001). Crucibles and about 1 $cm^3$ of sediment samples were weight and then dried at 105°C for 12 hours. The dried samples were subsequently combust at 550°C for 6 hours. The relative organic carbon content can be estimated by the percentage of weight loss at 550°C followed the equation (1).

Equation (1);

$$LOI_{550} = \frac{DW_{105} - DW_{550}}{DW_{105}} \times 100$$

Where $LOI_t$ = weight loss on ignition at t °C (g)

$DW_t$ = dry weight of samples at t °C (g)

After that, the samples were again combust 950°C for 3 hours to eliminate carbonate content in the form of $CO_2$. The weight loss at 950°C can be calculated followed the equation (2).

Equation (2);

$$LOI_{950} = \frac{DW_{550} - DW_{950}}{DW_{105}} \times 100$$

$CaCO_3$ in the sample was transferred to $CO_2$ and CaO by combustion at 950°C (3). $CO_2$ is the weight loss. Consequently, the weight loss at 950°C was multiplied by 2.27 in order to assess the carbonate content ($CaCO_3$) in the sample (4).

Equation (3);

$$CaCO_3 \rightarrow CaO + CO_2$$

Equation (4);

$$\frac{CaCO_3}{CO_2} = \frac{MW_{CaCO_3}}{MW_{CO_2}} = \frac{100.086\ g/mol}{44.009\ g/mol} = 2.27$$

Where MW = Molecular weight (g/mol)

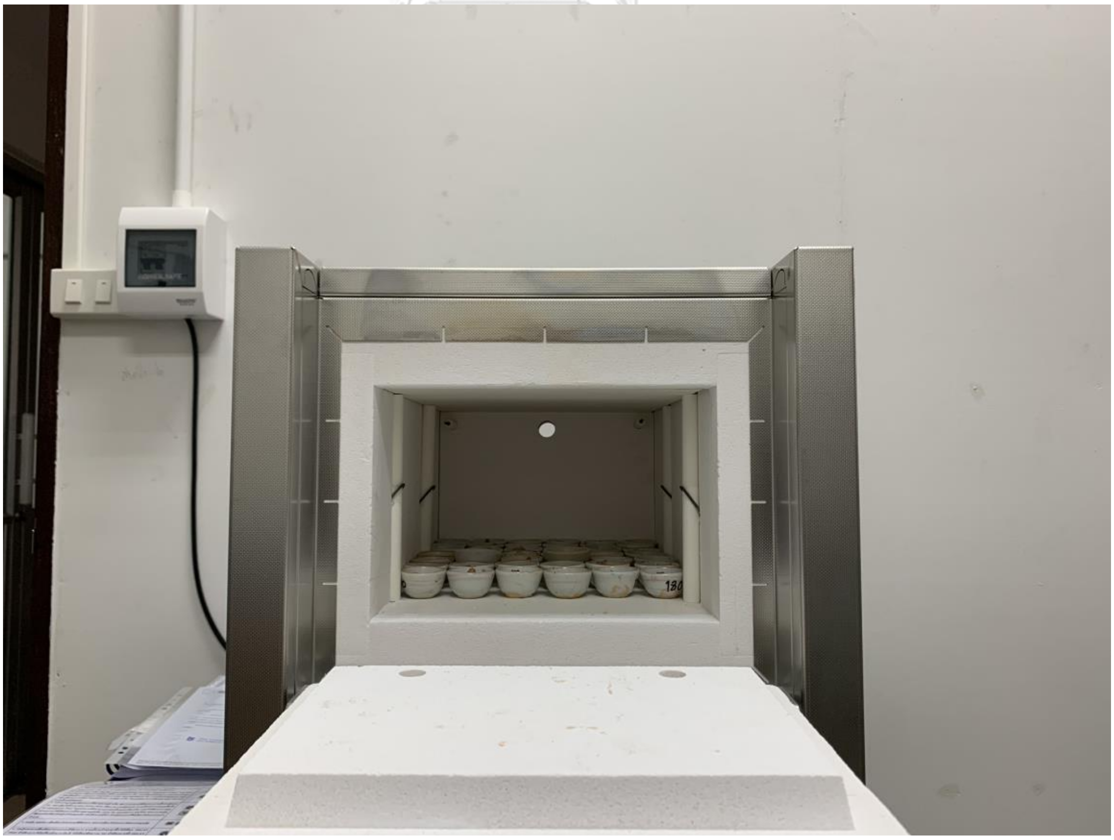

**Figure 12** LOI samples in furnace

3.2.2 Grain size analysis

Samples for the grain size analysis were prepared for each consecutive 4-cm depth following Rowell (2014). Each subsample was treated by 20 ml of 10% (v/v) HCl, and 20 ml of 10 and then 30% $H_2O_2$ in order to eliminate carbonate and organic contents, respectively. The prepared samples were cleaned by deionized water 3 times and soak in 5% Sodium Hexametaphosphate ($Na_6O_{18}P_6$; Calgon) to disperse the particle. The samples were eventually sent to analyze the grain size distribution by laser diffraction technique at Scientific and Technological Research Equipment Center Chulalongkorn University (STREC).

The grain size distribution was calculated to mean size particle by the following equation (5).

Equation (5);

$$D[4,3] = \frac{\sum_i^n D_i^4 v_i}{\sum_i^n D_i^3 v_i}$$

Where D [4,3] = the mean diameter over volume

$D_i$ = mean of dacile i

$v_i$ = dacile i




**Figure 13** Organic content elimination in sample by $H_2O_2$

3.2.3 Pollen analysis

For pollen analysis, samples were prepared based on Ellison (2008). Subsamples (about 1 $cm^3$) were taken at 5-cm intervals and samples were treated by 10 ml of 10% KOH to disperse the sediment. They were subsequently sieve with a mesh size of 0.2 mm. The sieve remains were treated by glacial acetic ($CH_3COOH$), and mixed acetic anhydride ($CH_3CO_2O$) and 96% sulfuric acid ($H_2SO_4$). Sodium polytungstate ($3Na_2WO_4 \cdot 9WO_3 \cdot H_2O$), which density is 2.0 g/$cm^3$, and water were added in the sample, respectively. The prepared samples were centrifuged with the speed of 2000 rpm for 2 minutes. The heavy liquid with pollen was separated from the solvent by using dropper. The samples were washed by alcohol, add silicone oil and dry at 60 °C for 12 hours to eliminate alcohol. The samples were eventually mouth on slide glass and pollens were identified by stereomicroscope based on their morphology including aperture, sculpture, and size. Pollens were identified in regarding to Punwong (2007).

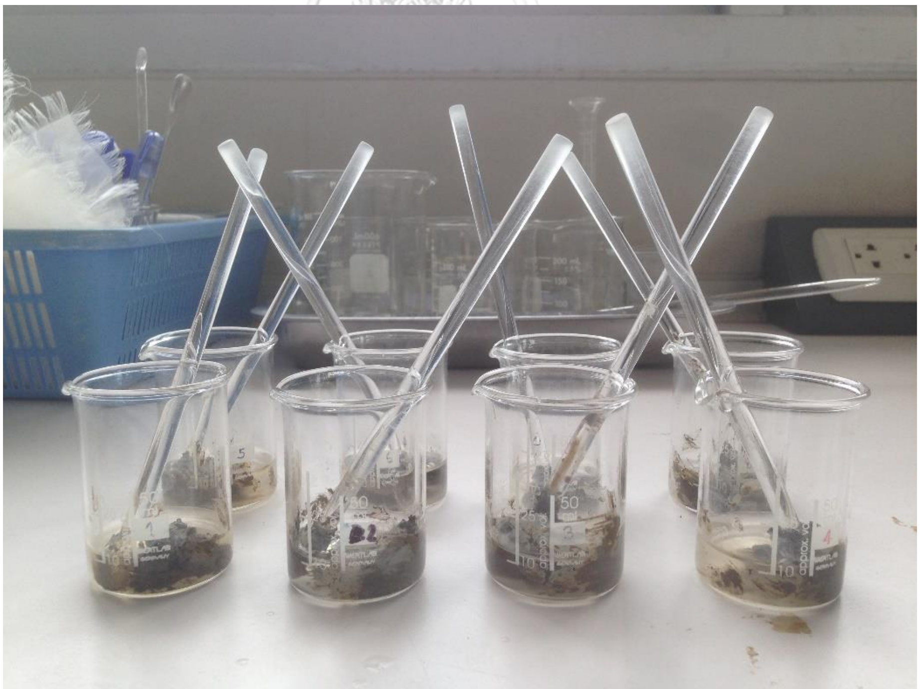

**Figure 14** Pollen sample preparation

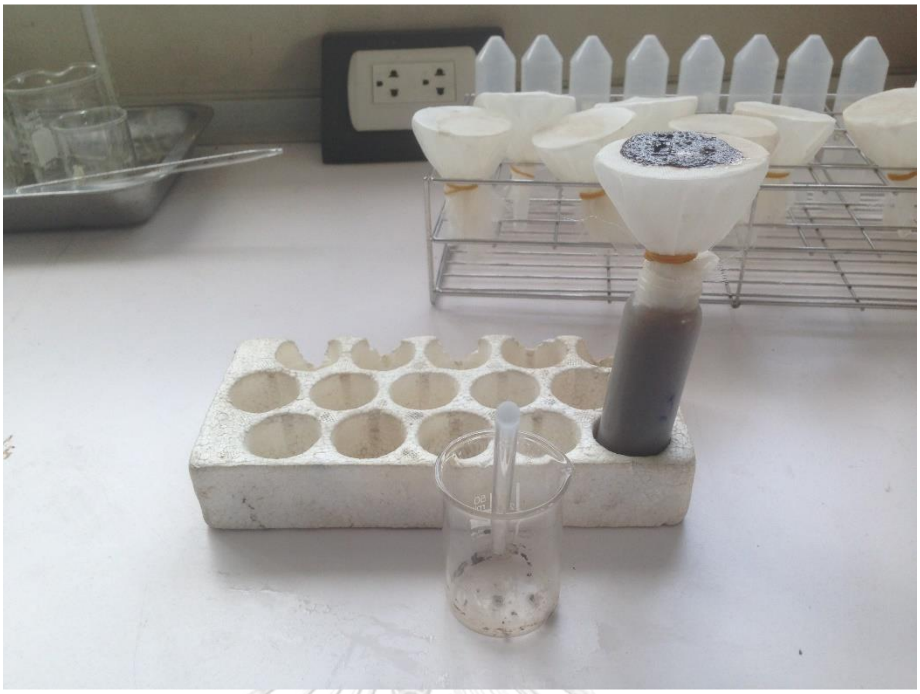

**Figure 15** A sample was sieve with 0.2 mm mesh size

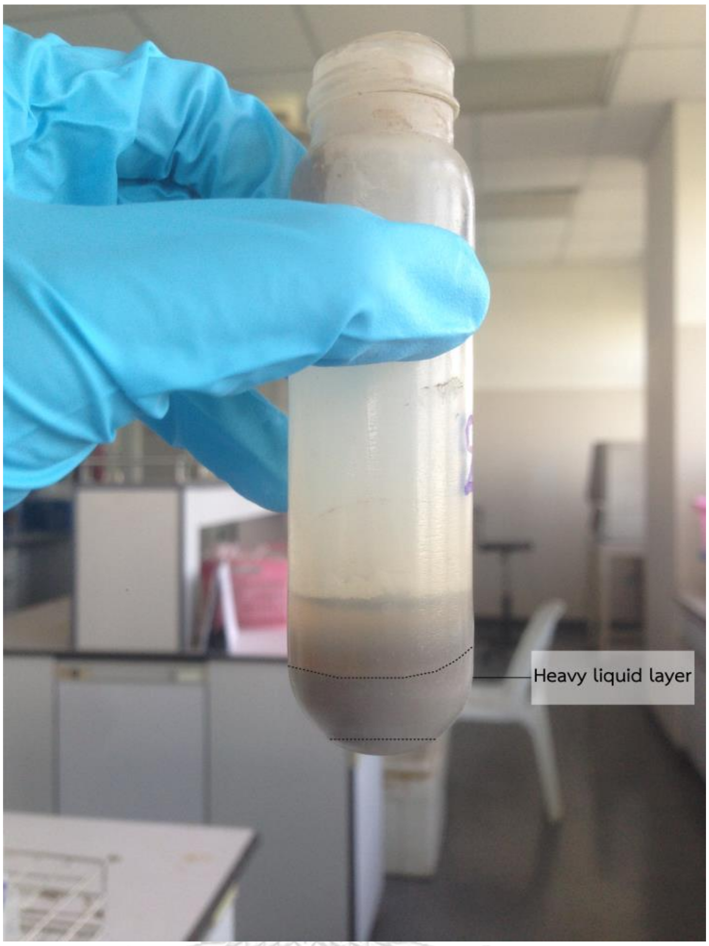


**Figure 16** Heavy liquid separation



3.2.4 Radiocarbon dating

The samples for radiocarbon dating were prepared by the procedure of Björck and Wohlfarth (2002). The selected samples were soak in 5% Sodium Hexametaphosphate ($Na_6O_{18}P_6$; Calgon) and then sieve under running tab water with mesh size of 500-µm. The sieve remains were identified under a binocular microscope. The leaves, charcoal, small twigs and wood fragments were picked and clean with deionized water 2-3 times. The cleaned samples were dried at 60°C for 12 hours. The dried samples were pretreated following the acid-base-acid method (De Vries and Barendsen, 1952), where 1M HCl and NaOH were used to remove carbonate and fluvic and humic acids, respectively. The samples were cleaned by deionized water 3 times and then dried at 60 °C for 12 hours. The prepared samples were sent to analyze by using the Accelerated Mass Spectrometer (AMS) at directAMS, the USA.

The radiocarbon dating results were calibrated by using calibration curve of InCal13 (Reimer et al., 2013). And the age-depth model was constructed for CP-4 by BACON, which is a Bayesian statistic based program (Blaauw and Christen, 2005, 2011).

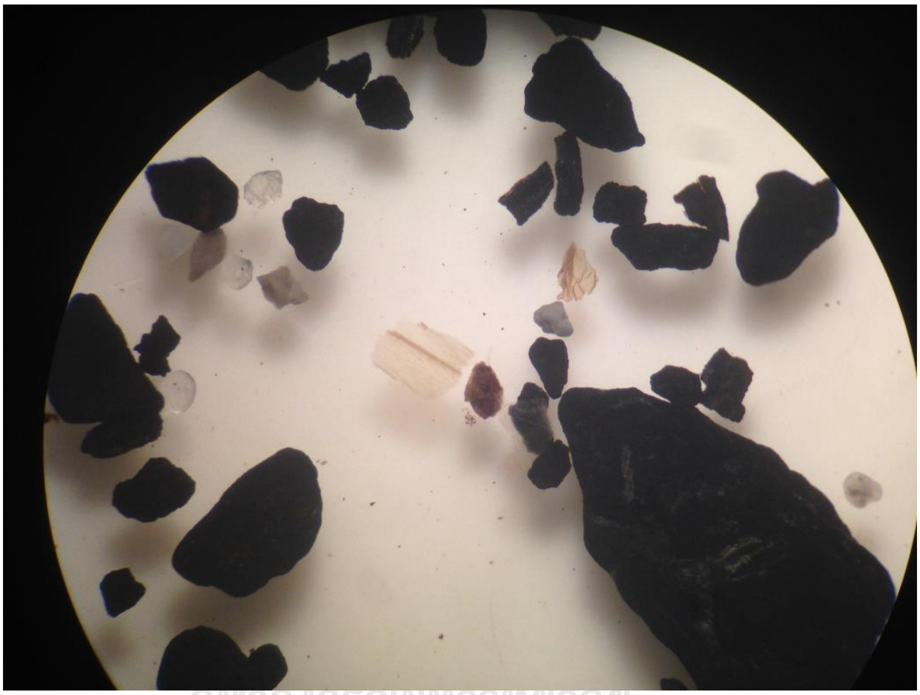



**Figure 17** Microscopic charcoal under microscope

# CHAPTER IV RESULTS

Six sedimentary sequences were collected in the north-south transect that consist of CP-2, CP-1, CP-4, CP-7, CP-9 and CP-8 (Figure 18). The additional coring sites, which are sites CP-3, CP-5 and CP-6, were taken in the western part of Sam Roi Yot (SRY) wetland in order to compare with the previous studies by Koskelainen (2014) (Figure 18).

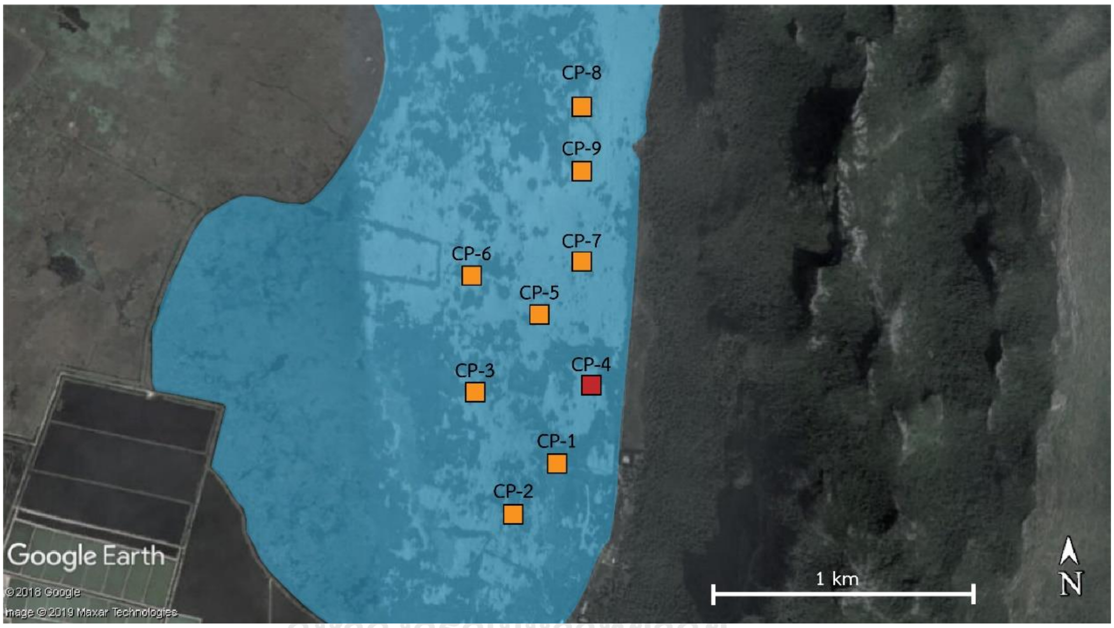


**Figure 18** Coring location in SRY wetland



## 4.1 Lithostratigraphic correlation

The sedimentary sequences obtained from SRY generally consist of 3 sedimentary units, i.e.

*Unit A*

Unit A is the dark grey clay mixed with silt and sand. This unit is typically laid in the lowermost part of all sedimentary sequences (Figure 19). However, it cannot be determinable in core CP8. Unit A is underlain by the light grey clay in core CP1 and a layer of gravel and shell fragments in core CP4 (Figure 19). In core CP5, the layer of gravel and shall fragments has been found intervened between sedimentary unit A from 3.1 to 2.98 m DBWS (Figure 20). Interestingly, the oxidized layers of clay were noticeable from 3.37 to 3.31 m DBSW and from 3.2 to 3.1 m DBSW in sediment cores CP-1 and CP-4, respectively (Figure 19). The upper part of sedimentary unit A is *c.* 2.6 m DBSW and gradually transfers to unit B (Figure 19 and 20).

*Unit B*

The sediments in unit B are clay mixed with silt and sand, which resemble with unit A, but they are beige, brown and grey colors. Sedimentary unit B is approximately 0.6 and 1.2 m thick in the eastern and western wetland, respectively (Figure 19 and 20). The lower most layer of unit B is beige clay mixed with silt and sand, which is continued to the top of the cores and transfer to unit C in sediment core CP1, CP4 and CP7 (Fig. 19). In core CP2, the layer of beige clay mixed with silt and sand is overlain by yellowish brown sand, which is c. 20 cm thick. The brown silty or sandy clay layer has been found over the beige sediments in CP8, CP9, CP6 and CP3. However, light grey silty clay is overlain by the layer of beige clay mixed with silt and sand. The top of unit B is suddenly transferred to Unit C (Figure 19, 20 and 21).



*Unit C*

Unit C composes of organic rich clay overlaid by gyttja. The boundary between unit B and C has been found at approximately 1.8-1.9 m DBSW in cores CP-1, CP4, CP7, CP9 and CP8 (Figure 19). The thickness of unit C varies from *c.* 10 to 20 cm in these cores (Figure 19, 20, 21). This unit however presents in relatively shallow depths of c. 1.7 to 1.4 m DBSW in core CP2, CP3, CP5 and CP6 (Figure 19, 20, 21). Gyttja is dominated in the upper part of core CP-1. However, it is indeterminable or disappears in core CP-4 and CP-5. The uppermost layers of core CP-4 and CP-5 have been classified to clayey gyttja and gyttja clay, respectively (Figure 19, 20).

Since core CP-4 was been taken from the deepest part of the wetland and composes of all sedimentary units, it was here selected for the further study and to represent the Sam Roi Yot wetland.

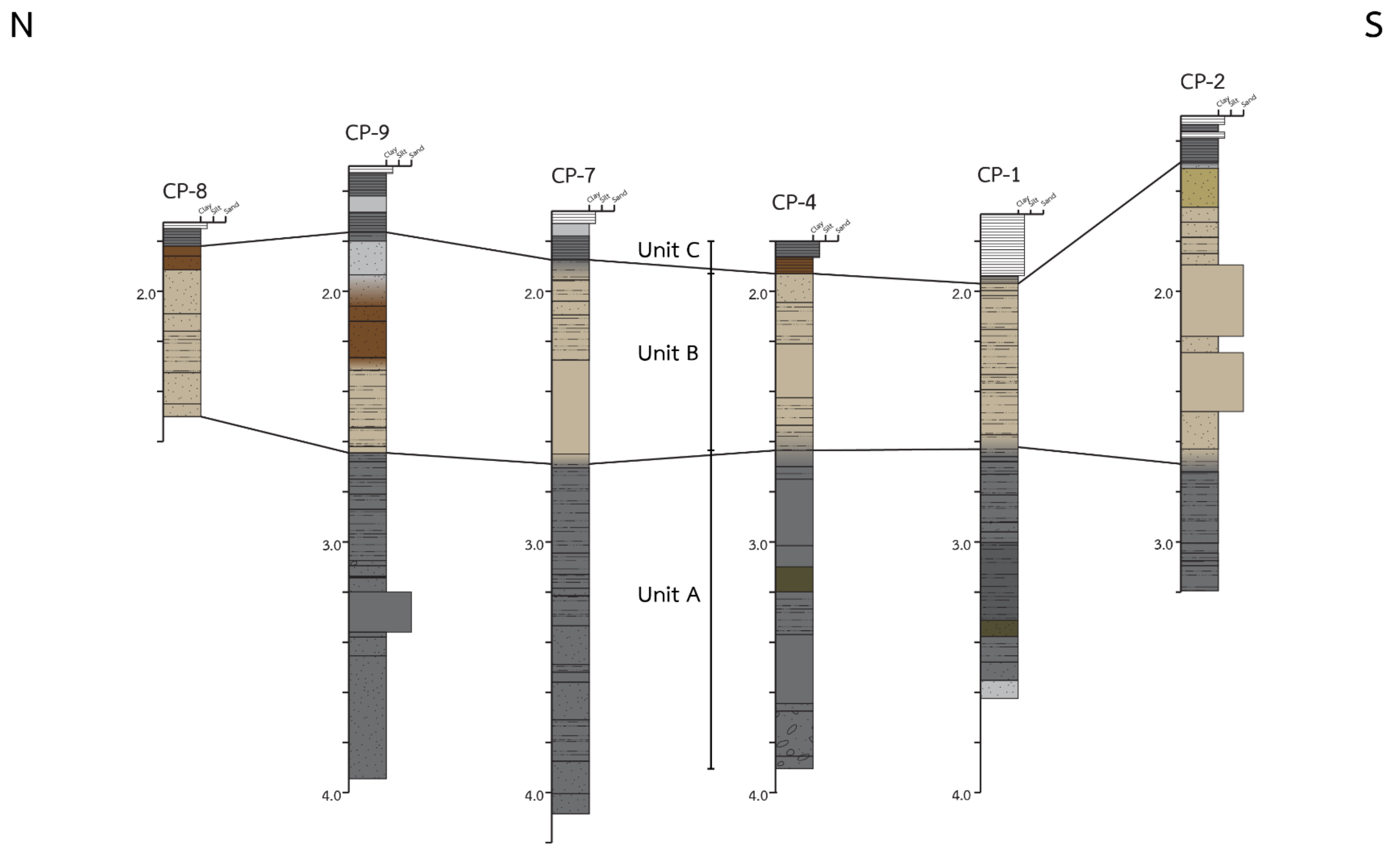


**Figure 19** Stratigraphic correlation of SRY in N-S

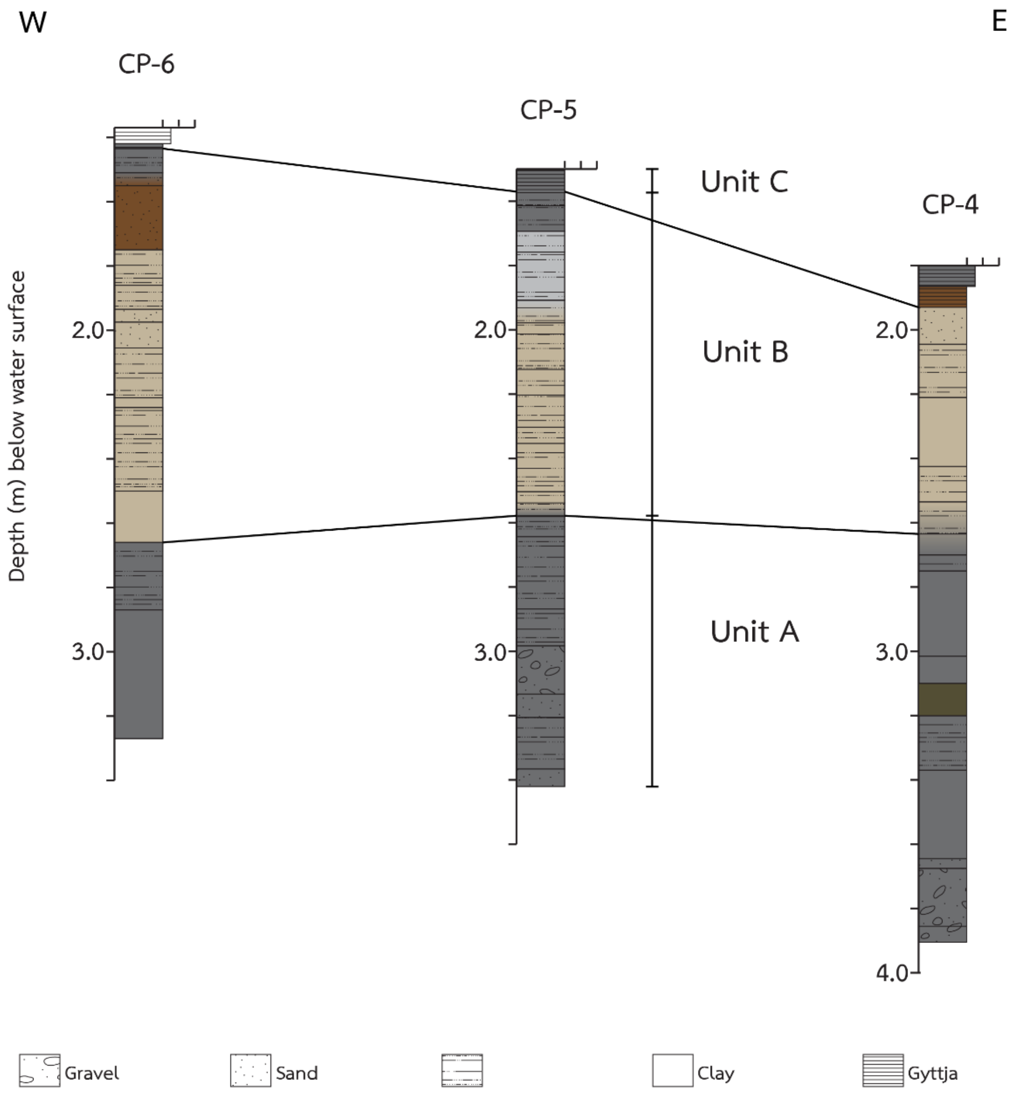


**Figure 20** Stratigraphic correlation of SRY in E-W transect

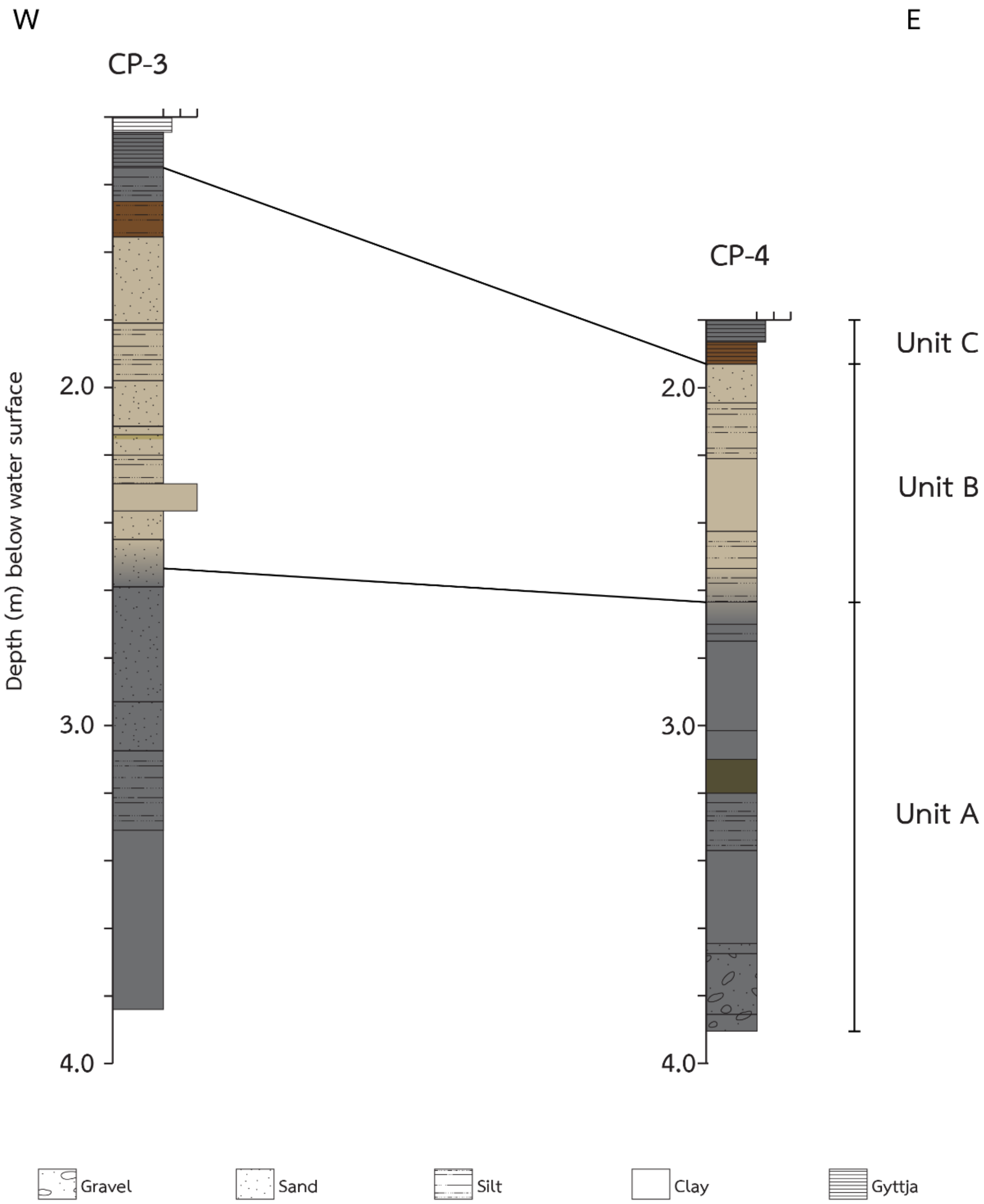


**Figure 21** Stratigraphic correlation of CP-3 and CP-4

### 4.2 Lithostratigraphy of CP-4

Sedimentary sequence of CP-4 is 2.1 m thick, and water depth at this site is approximately 1.8 m. This core can be divided into 13 layers (Table 3). Units A, B and C compose of layer 1-7, 8-11, and 12-13, respectively (Table 3).

The lowermost layer of this core is the dark grey silty to sandy clay, which is mixed by limestone gravel and shall fragments, from 3.9 to 3.675 m DBWS (layer 1) (Table 3). Despite layers 2 (3.675-3.645 m DBWS) and 3 (3.645-3.37 m DBWS) are dark grey sandy clay, sand spots have been found in layer 3. The dark grey sandy clay layers are overlaid by dark grey silty clay (layer 4, 3.37-3.2 m DBWS) and dark grey clay (layer 5, 3.2-3.1 m DBWS and layer 6, 3.1-2.75 m DBWS). These layers possibly point to a sedimentary structure of normal grading. The uppermost layer of unit A is dark grey silty clay (layer 7, 2.75-2.6 m DBWS).

The lower most part of unit B is beige silty clay of layer 8 (2.6-2.415 m DBWS) (Table 3). The grain size increases in units 9-11 that are beige clay (2.415-2.21 m DBWS), beige silty clay (2.21-2.045 m DBWS) and beige sandy clay (2.045-1.93 m DBWS) (Table 3).

Unit C is the brown gyttja clay overlain by clayey gyttja of unit 12 (1.93-1.865 m DBWS) and 13 (1.865-1.8 m DBWS), respectively (Table 3).

**Table 3** Sedimentary unit of CP-4

| Depth (m) below water surface | Lithostratigraphic description | Unit | Layer |
|---|---|---|---|
| 1.865 – 1.8 | Clayey gyttja | C | 13 |
| 1.93 – 1.865 | Brown gyttja clay | | 12 |
| 2.045 – 1.93 | Beige sandy clay | B | 11 |
| 2.21 – 2.045 | Beige silty clay | | 10 |
| 2.415 – 2.21 | Beige clay | | 9 |
| 2.6 – 2.415 | Beige silty clay | | 8 |
| 2.75 – 2.6 | Dark grey silty clay | A | 7 |
| 3.1 – 2.75 | Dark grey clay | | 6 |
| 3.2 – 3.1 | Dark grey clay (oxidized) | | 5 |
| 3.37 – 3.2 | Dark grey silty clay | | 4 |
| 3.645 – 3.37 | Dark grey clay with sand spot | | 3 |
| 3.675 – 3.645 | Dark grey sandy clay | | 2 |
| 3.9 – 3.675 | Dark grey sandy clay with gravel | | 1 |

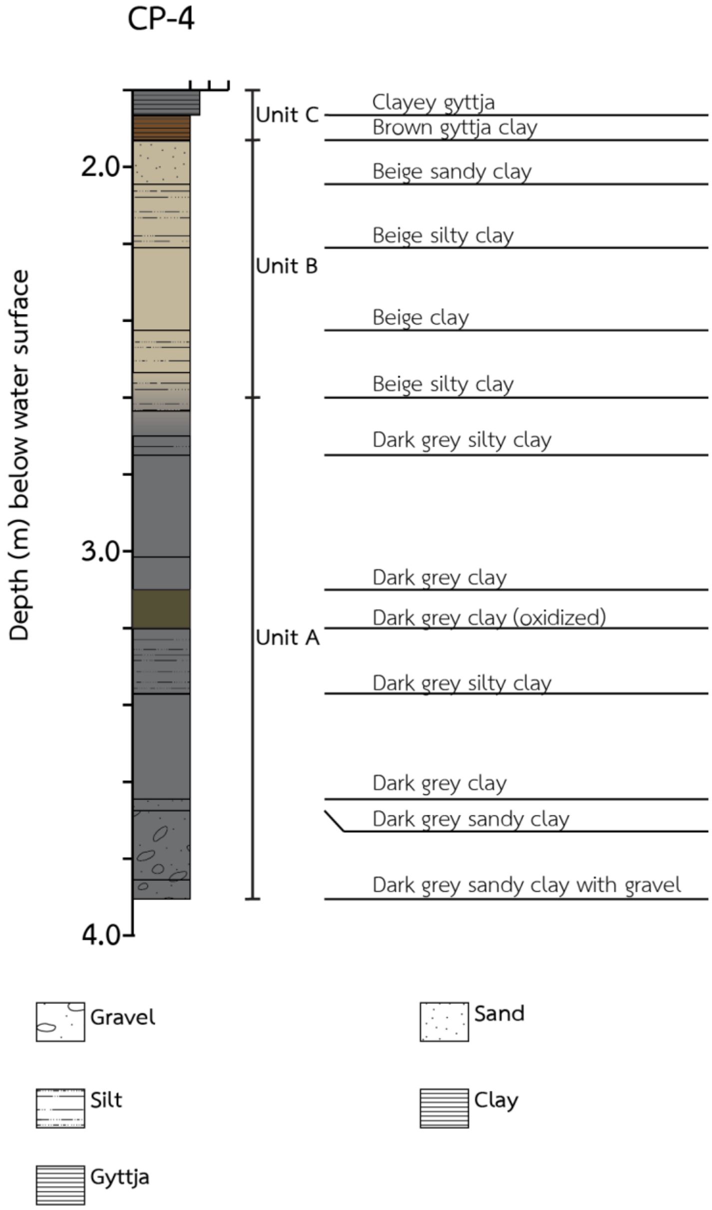


**Figure 22** Stratigraphic description of CP-4

### 4.3 Loss on Ignition (LOI)

The consecutive 2-cm depth of sediment samples from CP-4 were combusted at 550°C ($LOI_{550}$) and 950°C ($LOI_{950}$) to achieve the qualitative changes in organic and carbonate content.

The $LOI_{550}$ values gradually increase from 3% to 10% in sedimentary unit A (Figure 23). In unit B, the $LOI_{550}$ values decline from 10% at the bottom of this unit to 2.40 m DBWS. It again increases to 10% at 2.10 m DBWS where it is insignificant change till 2.0 m DBWS. The $LOI_{550}$ suddenly change and reach 20% from 2.045 to 2.0 m DBWS. It is varied approximately 16-18% in the brown clayey gyttja layer of unit C. The $LOI_{550}$ values reach its maximum of c. 28% in gyttja layer (Figure 23).

$LOI_{950}$ values gradually decline from 7 to 4% in unit A. In unit B, the LOI remains decrease and reach the minimum of 3% at 2.4 m DBWS (Figure 23). It becomes insignificant change from 2.3 to 2.1 m DBWS. The $LOI_{950}$ values slightly increase to 4% in the upper part of unit B and unit C (Figure 23).

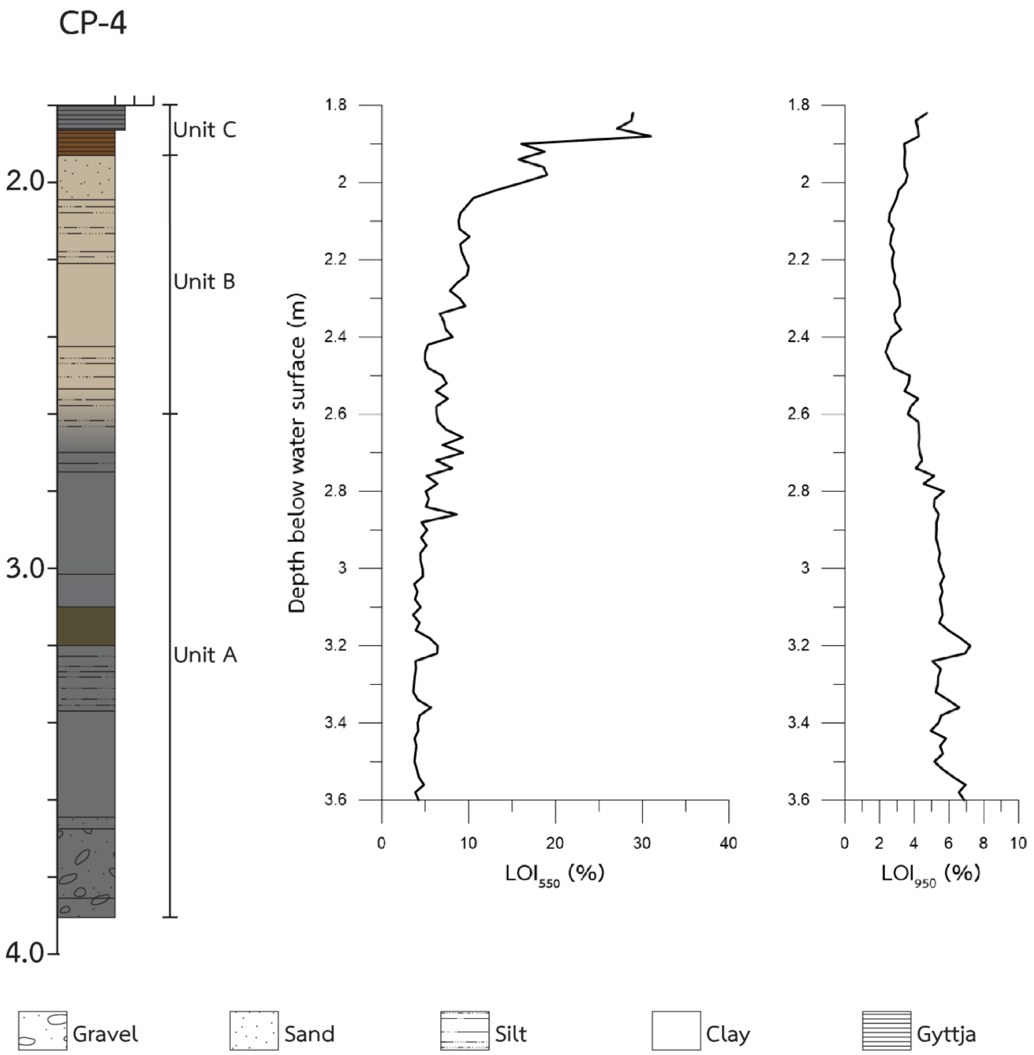




**Figure 23** $LOI_{550}$ and $LOI_{950}$ in CP-4

**4.4 Grain size distribution**

Grain size distribution obtained by laser diffraction technique suggests that silt is the most abundant sediment in core CP-4. Silt component gradually increases from 70 to 80% in unit A and layer 9, which is the lower part of unit B (Figure 24). Despite the concentration of silt decreases from 80 to 60% hereafter, it is intervened by a layer of abruptly increase in this sediment at the boundary between unit B and C. The concentration of clay is varied from 30 to 45% and is mirrored with that of silt

(Fig. 24). Sand has been generally found in a low concentration from 1 to 5%. It significantly increases and reach 5% near the boundary between unit A and B.

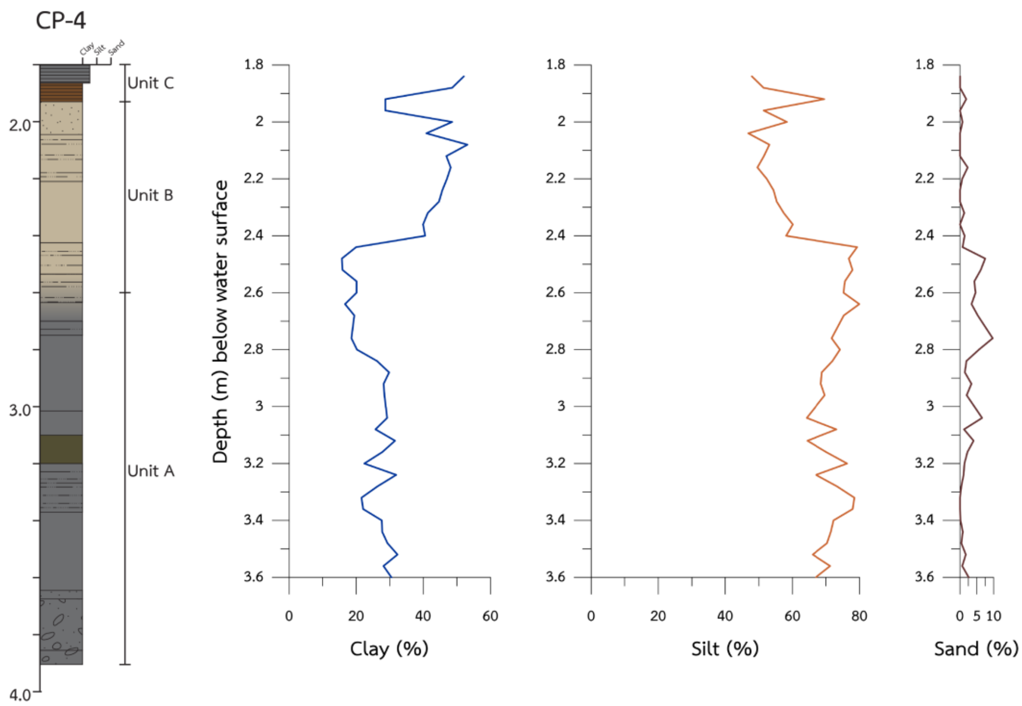


**Figure 24** Clay, silt, and sand distribution in CP-4



According to the volumetric mean (D[4,3]), the size of sediments in core CP-4 was varied from 6 to 25 μm (Figure 25). Although the volumetric mean diameter generally increases from 12.5 to 25 μm between 3.6 and 2.75 m DBWS, it is intervened by a layer of the relatively finer sediment between 3.0 and 2.8 m DBWS. The volumetric mean is c. 22.5 μm and slightly change close to the unit A and B boundary from 2.75 to 2.4 m DBWS. It becomes sudden decrease, reaches 7.5 μm at 2.4 m DBWS, and insignificantly changes hereafter. This relatively constant volumetric mean is hampered by a layer of abrupt increase in the volume metric mean near the boundary between unit B and C.

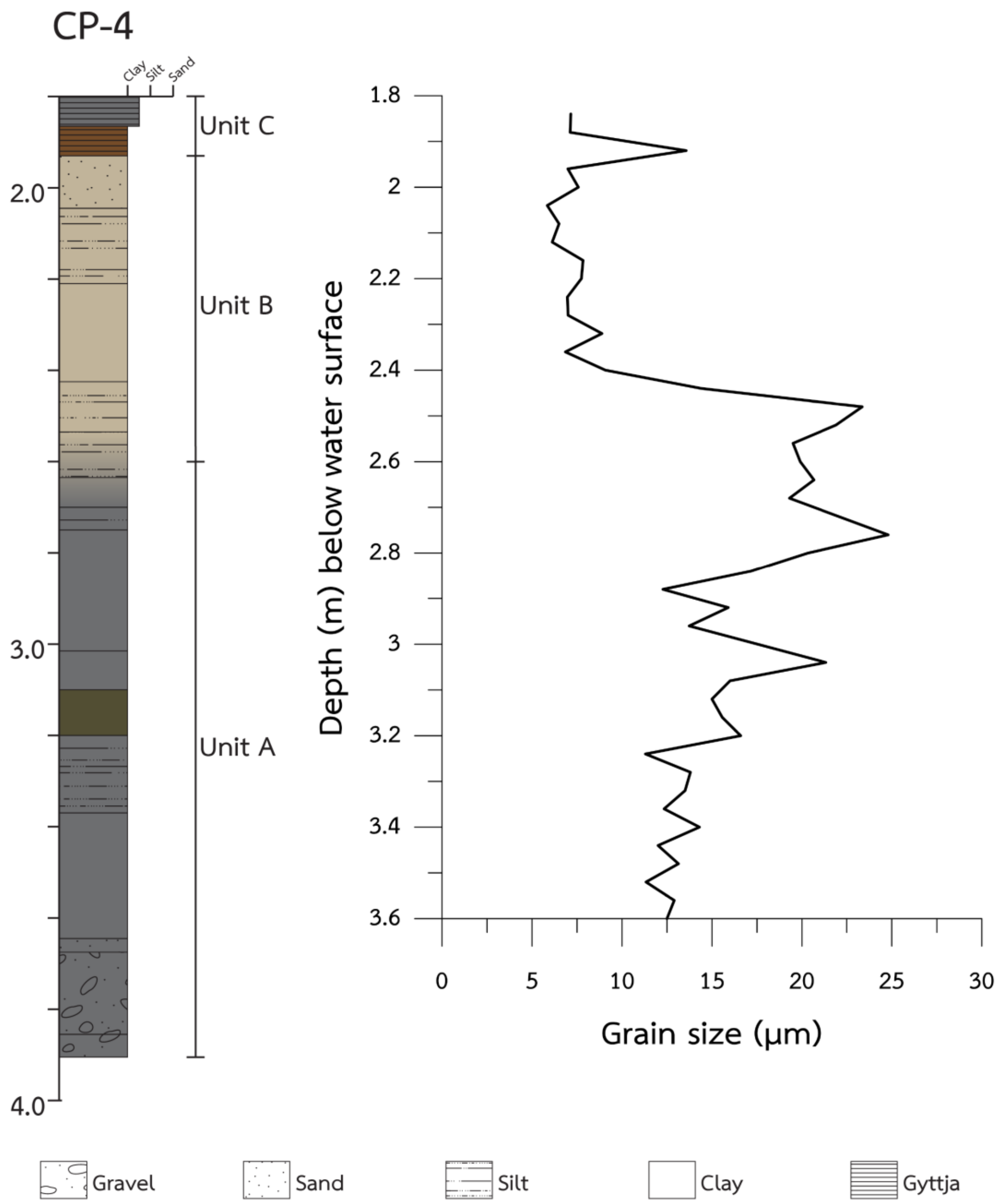


**Figure 25** Volumetric mean grain size of CP-4

### 4.5 Palynology

Eighteen pollen taxa have been found in core CP-4 that can be divided into 4 assemblages, i.e. mangrove, back mangrove, terrestrial herbaceous, non-mangrove arboreal, and unidentified taxa (Table 4). The classifications of mangrove taxa and back mangrove taxa, and terrestrial herbaceous taxa and non-mangrove arboreal taxa assemblages were here based on Santisuk (1983) and Punwong (2007), respectively. The pollen stratigraphy can be divided into 2 pollen zones, i.e. SRY-1 and SRY-2, based on cluster analysis by CONISS software (Figure 26).

**Table 4** Pollen assemblage of CP-4

| Assemblage | Assemblage name | Plant assemblage |
|---|---|---|
| 1 | Mangrove taxa | *Rhizophora*, *Avicennia*, *Sonneratia*, and *Bruguiera* |
| 2 | Back mangrove taxa | *Suaeda*, *Acrostichum*, *Oncosperma*, and *Xylocarpus* |
| 3 | Terrestrial herbaceous taxa | Asteraceae, *Ceratopteris*, Cyperaceae, Poaceae, Polygalaceae, and *Stenochlaena* |
| 4 | Non-mangrove arboreal taxa | *Barringtonia*, *Casuarina*, and Myrtaceae |
| 5 | Unidentified taxa | - |

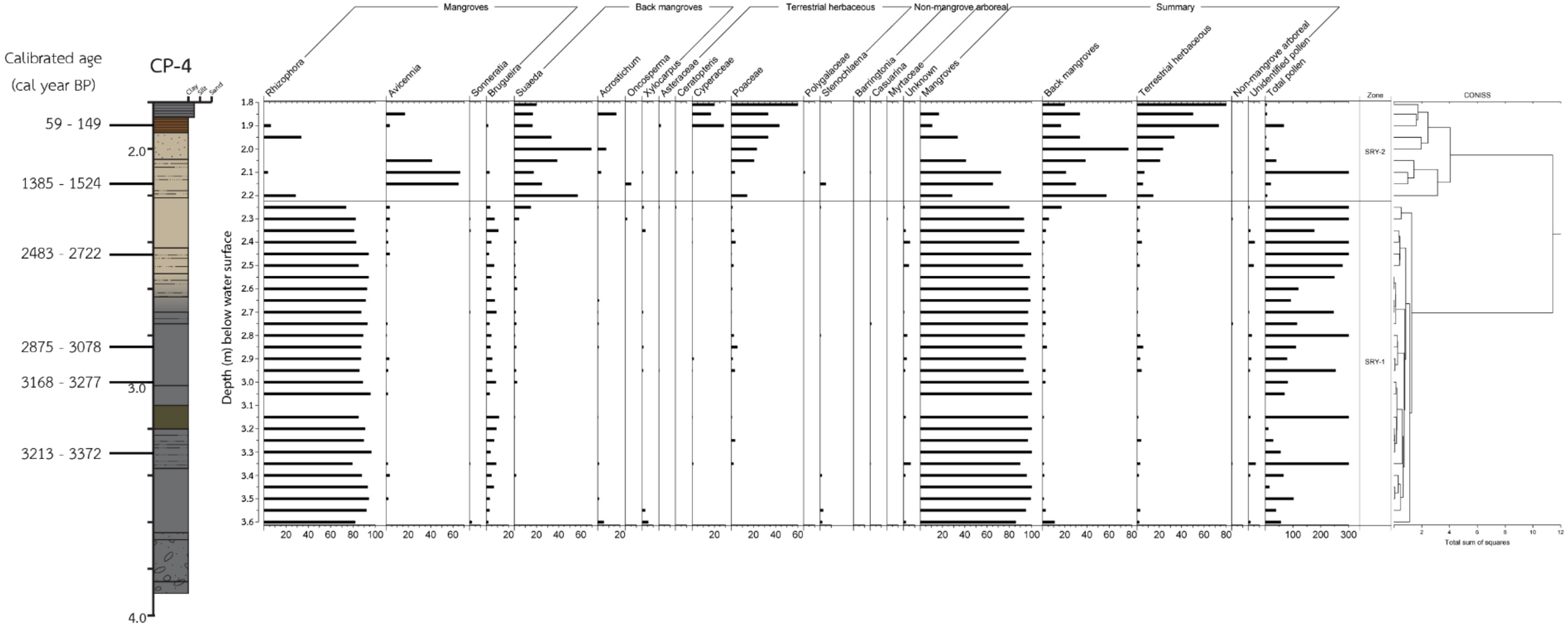


**Figure 26** Pollen assemblage of CP-4 shown in percentage

4.5.1 SRY-1 (3.6-2.25 m DBWS)

Mangrove pollen taxa are dominated in SRY-1 from 3.6 to 2.25 m DBWS (Figure 26). Despite pollen grains have been generally presence throughout the sedimentary sequence, they became disappear or indeterminable at 3.1 m DBWS, which was remarked as a barren zone of pollen. *Rhizophora*, especially, has been found higher than 80% in this pollen zone (Figure 26). *Bruguiera* is the second high abundance pollen taxon fluctuating between 1 and 12%. The other mangrove pollen taxa including *Avicennia* and *Sonneratia* have been occasionally found by less than 5%. *Suaeda*, which is the back mangrove plants, can be determinable of approximately 5% from 3 to 2.2 m DBWS (Figure 26). It suddenly increases and reaches 15% at the top of pollen zone SRY-1. *Xylocarpus* has been also found of approximately 5% at the top of this zone (Figure 26). Poaceae occasionally presented in some depth of about 5%. However, it is the most predominance of terrestrial herbaceous taxa assemblage.

4.5.2 SRY-2 (2.25-1.8 m DBWS)

*Suaeda* remarkably increased and reached its maximum of 70% at the bottom of SRY-2 (Figure 26). The percentage of this pollen taxon declines to 20% and is occupied by *Avicennia*, which is approximately 60%, between 2.15 and 2.05 m DBWS. *Suaeda* again abruptly increase to 70% at 2 m DBWS, and decrease to 20% hereafter. Interestingly, *Rhizophora* and *Avicennia* have been found 40 and 20% at 1.95 and 1.85 m DBWS (Figure 26). *Acrostichum*, which is another back mangrove plant, gradually increased from 3 to 15% in pollen zone SRY-2 (Figure 26). The pollen of terrestrial herbaceous taxa assemblage, especially Poaceae and Cyperaceae, dominated in the upper part of SRY-2 (Figure 26). Poaceae generally increased from 20 to 60% between 2.25 and 1.8 m DBWS. Pollen grains of Cyperaceae presented distinctively of 16-28% between 1.90 and 1.80 m DBWS (Figure 26). Other terrestrial herbaceous taxa and non-mangrove arboreal pollen grains were found in a small percentage.

**4.6 Chronology**

Chronology of core CP-4 is based on nine radiocarbon dates of microscopic charcoal found in the core (Table 5). According to the age-depth model of BACON, this sedimentary sequence is of the Late Holocene ranging from 3500 to 117 cal year BP (Walker et al., 2012). Although most of these sequential dates are fitting well with the age-depth curve, three samples (D-AMS 030466, D-AMS 034856 and D-AMS 032441) are outliners, which will be discussed in detail next chapter.

The oldest age obtained from 3.59-3.645 m DBWS (D-AMS 030466) is approximately 3296 cal year BP. The following radiocarbon dates of sample no. D-AMS 032444 (3.25-3.31 m DBWS), D-AMS 032443 (2.97-3.015 m DBWS), and D-AMS 032442 (2.8-2.85 m DBWS) are approximately 3293, 3249, and 2993 cal year BP, respectively. The depositional rate from 3.8 to 2.58 m DBWS is 0.28 cm/yr.

The samples no D-AMS 034856 and D-AMS 032441 were obtained from the same depth at 2.58-2.635 m DBWS. Radiocarbon date of D-AMS 034856 is 3372 cal year BP, which is about 150 year younger than that of D-AMS 032441. However, These two dates are older than that of lower samples (no. D-AMS 032444, D-AMS 032443 and D-AMS 032442).

The sample no D-AMS 034857 (2.43-2.46 n DBWS) and D-AMS 30465 (2.12-2.15 m DBWS) are approximately 2586 and 1466 cal year BP, respectively. The youngest date obtained from sample no. D-AMS 034858 (1.88-1.9 m DBWS) is approximately 117 cal year BP. The depositional rate from 2.58 to 1.8 m DBWS is 0.02 cm/yr.

**Table 5** $^{14}C$ dated for CP-4

| Lab ID | Depth (m) below water surface | Material | $^{14}C$ date age (BP ± 1σ) | Calibrated age (cal year BP) | Unit |
|---|---|---|---|---|---|
| D-AMS 034858 | 1.88 – 1.9 | Charcoal | 129 ± 20 | 149 - 59 | C |
| D-AMS 030465 | 2.12 – 2.15 | Charcoal | 1550 ± 25 | 1524 - 1385 | B |
| D-AMS 034857 | 2.43 – 2.46 | Charcoal | 2489 ± 26 | 2722 - 2483 | B |
| D-AMS 034856 | 2.58 – 2.635 | Charcoal | 3032 ± 26 | 3272 - 3161 | B |
| D-AMS 032441 | 2.58 – 2.635 | Charcoal | 3145 ± 32 | 3447 - 3328 | B |
| D-AMS 032442 | 2.8 – 2.85 | Charcoal | 2870 ± 36 | 3078 - 2875 | A |
| D-AMS 032443 | 2.97 – 3.015 | Charcoal | 3042 ± 28 | 3277 - 3168 | A |
| D-AMS 032444 | 3.25 – 3.31 | Charcoal | 3084 ± 32 | 3372 - 3213 | A |
| D-AMS 030466 | 3.59 – 3.645 | Charcoal | 3090 ± 30 | 3376 - 3225 | A |

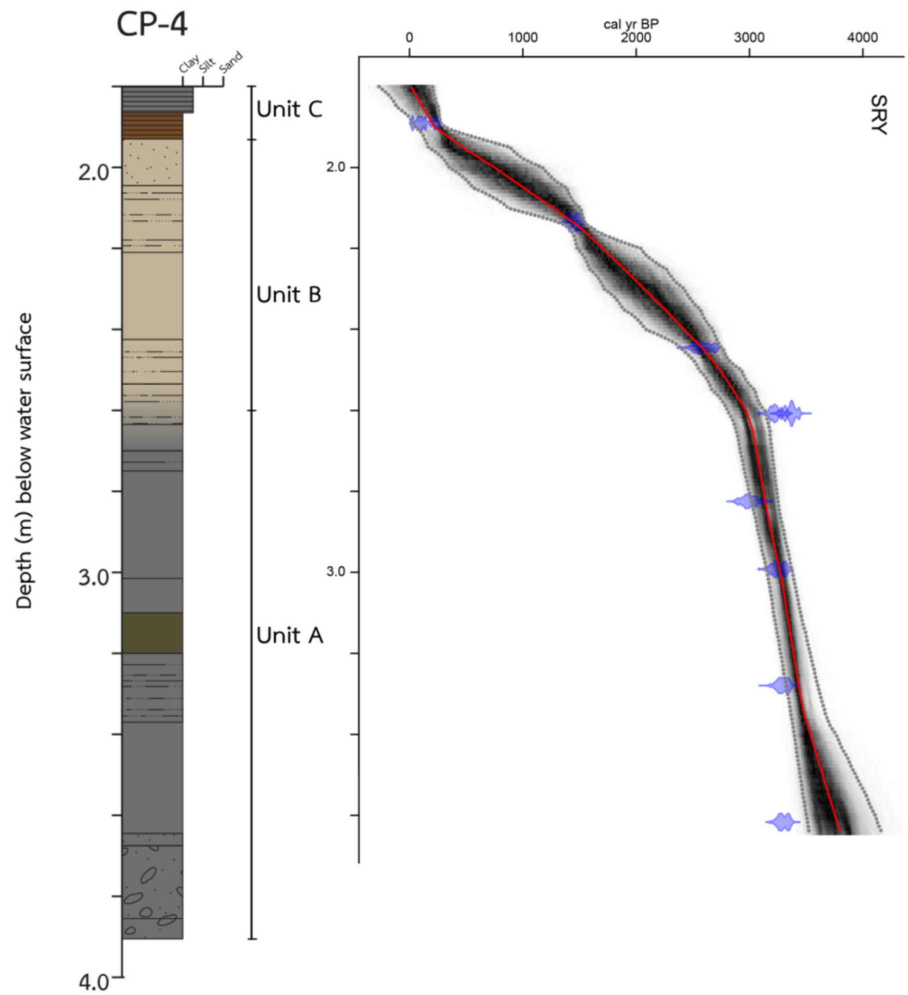


**Figure 27** Age-depth relationship of CP-4

# CHAPTER 5 DISCUSSION

## 5.1 Chronology

Chronology of core CP-4 was constructed by using Bacon based on nine radiocarbon dates (Table 5). Most of the sequential radiocarbon dates agreed well with the age-depth model. However, sample no. D-AMS 030466 (3.59 – 3.645 m DBWS; 3296 cal year BP), D-AMS 032441 (2.58 – 2.635 m DBWS; 3372 cal year BP) and D-AMS 034856 (2.58 – 2.635 m DBWS; 3232 cal year BP) are outliers (Figure 27).

Sample D-AMS 030466 was picked from the layer which is adjacent to limestone gravel layer (Layer 1) (Table 3). This layer was possibly disturbed by slump from the neighboring limestone mountain cause of sediment mixing up. Sample no. D-AMS 034856 and D-AMS 034856 were taken from the same depth. This depth is a boundary between unit A and unit B, that suggest a change in sedimentation. Alternatively, the depositional environment is expected to be under intertidal condition, which is abundance of mangrove flora and fauna. Both sediment dynamics and mangrove living creatures can be disturbed the sedimentation by digging up. Therefore, the dating results of these samples were older than expected.

Age-depth model show a continuous deposition of sedimentary sequence of CP-4. Since hiatus of remarkably changes in other sequential proxies cannot be determinable tectonic was here neglect (Figure 23, 25, 26 and 27). Sedimentation rate of unit A is approximately 10 times higher than unit B, that can infer the deposition of unit A occurred under relative high energy condition compared to unit B.

## 5.2 Environmental reconstruction of Thung Sam Roi Yot

Pollen, LOI and grain size distribution records indicate that the environmental changes can be divided into 8 stages in the SRY wetland between c. 3500 and 120 cal year BP (Figure 28).

5.2.1 Stage I (c. 3500 cal year BP)

Grey clay mixed up with clastic sediments suggests that the deposition was under intertidal environment. High $LOI_{950}$ and low $LOI_{550}$ values, and the high percentage of silts can be possibly inferred to the marine-dominated coastline during c. 3500 cal year BP. Moreover, SRY wetland was possibly covered by mangrove forest since mangrove pollen, especially *Rhizophora*, was dominated in this stage.

5.2.2 Stage II (c. 3300 cal year BP)

The yellowish grey color sediment, which was interbedded with sedimentary unit A, was caused by oxidation. This oxidized layer can possibly be explained by an exposure of the sediments reflecting sea level decrease during c. 3300 cal year BP. LOI and grain size values were insignificant changes. Pollen was suddenly disappeared or indeterminable which can be defined as a barren pollen zone. These results indicate that the occasionally dry conditions of intertidal environment at SRY wetland became longer than the previous period.

5.2.3 Stage III (3300 – 3000 cal year BP)

The gradual increase in organic content and the slight decrease in carbonate content suggest that the marine influence became decline between 3300 and 3000 cal year BP. However, the predominance of mangrove pollen assemblage point to the thrive of mangrove forest surrounding this area.

5.2.4 Stage IV (3000 – 1700 cal yr BP)

Dark grey color of sediment was gradually transferred to beige clay sediment. Grain size was abruptly changed from silt- to clay-dominated sediment at approximately 2500 cal year BP. It suggested the decline in transportation energy. LOI values were relatively stable. Mangrove pollen assemblage remained dominated until the period before c. 1800 cal year BP when it slightly decreased. The results can be inferred to the stillstand of sea level before it started to fall at c. 1800 cal year BP.

5.2.5 Stage V (1700 – 1600 cal year BP)

The slight changes in LOI values and grain size compared to the stage before can be noticeable from 1700 to 1600 cal year BP. However, pollen record suggests an environmental change in the study area during this period since back mangrove pollen assemblage occupied mangrove pollen taxa, which were predominance in the period before. The occupation of back mangrove can be explained by the progradation of mangrove zonation owing to the declination of sea level.

5.2.6 Stage VI (1600 – 1000 cal year BP)

LOI values and grain size were slightly changed. Mangrove pollen assemblage became again replace the back mangrove pollen taxa from 1600 to 1000 cal year BP. However, *Avicennia* became more dominated than *Rhizophora*, which have been found in the highest percentage from 3500 to 1700 cal year BP. The predominance of *Avicennia* instead of *Rhizophora* presented. Although *Avicennia* has wide range of salinity preferences, its presence associated with back mangrove taxa suggests mangrove zonation shifted landward due to an increase of sea level. However, the sea level rise did not reach to the same level as the previous period.

5.2.7 Stage VII (1000 – 400 cal year BP)

$LOI_{550}$ values suddenly increase reflecting relatively high organic content. The dominance of back mangrove pollen assemblage and increase in terrestrial herbaceous pollen assemblage have been found from 1000 to 400 cal year BP. The replacement of back mangrove indicated the sea level fall, which consists well with the higher freshwater influence in regarding to the increase in terrestrial herbaceous pollens.

5.2.8 Stage VIII (400 cal year BP – present)

Beige clay was suddenly transferred to gyttja clay corresponded with the increase in $LOI_{550}$. Terrestrial herbaceous pollen assemblage replaced the back mangrove pollen taxa after 400 cal year BP. This result indicates that the intertidal environment was completely transferred to the freshwater wetland like in the present.

**Table 6** SRY evolution stage according to LOI, grain size and pollen analysis

| Stage | Age (cal year BP) | Sedimentary unit | $LOI_{550}$ (%) | $LOI_{950}$ (%) | Grain size (µm) | Dominance taxa | Environment | Sea level stage |
|---|---|---|---|---|---|---|---|---|
| VIII | 400 – recent | C | 20 – 30 | 5 – 6 | 7 – 15 | Poaceae | Freshwater swamp | - |
| VII | 1000 - 400 | B | 10 - 20 | 3 - 5 | 6 - 15 | *Suaeda* | Back mangrove | Regression |
| VI | 1600 - 1000 | B | 9 - 10 | 3 | 6 - 8 | *Avicennia* | Mangrove | Minor transgression |
| V | 1700 - 1600 | B | 9 - 10 | 3 | 8 | *Suaeda* | Back mangrove | Regression |
| IV | 3000 - 1700 | B | 5 - 10 | 3 - 5 | 7 - 24 | *Rhizophora* | Mangrove | Stillstand |
| III | 3300 - 3000 | A | 5 - 10 | 5 - 6 | 12 - 25 | *Rhizophora* | Mangrove | Transgression |
| II | c. 3300 | A | 5 | 6 | 15 - 22 | - | Mangrove (dry) | Regression |
| I | 3500 - 3300 | A | 5 - 7 | 5 - 7 | 10 - 17 | *Rhizophora* | Mangrove | Regression |

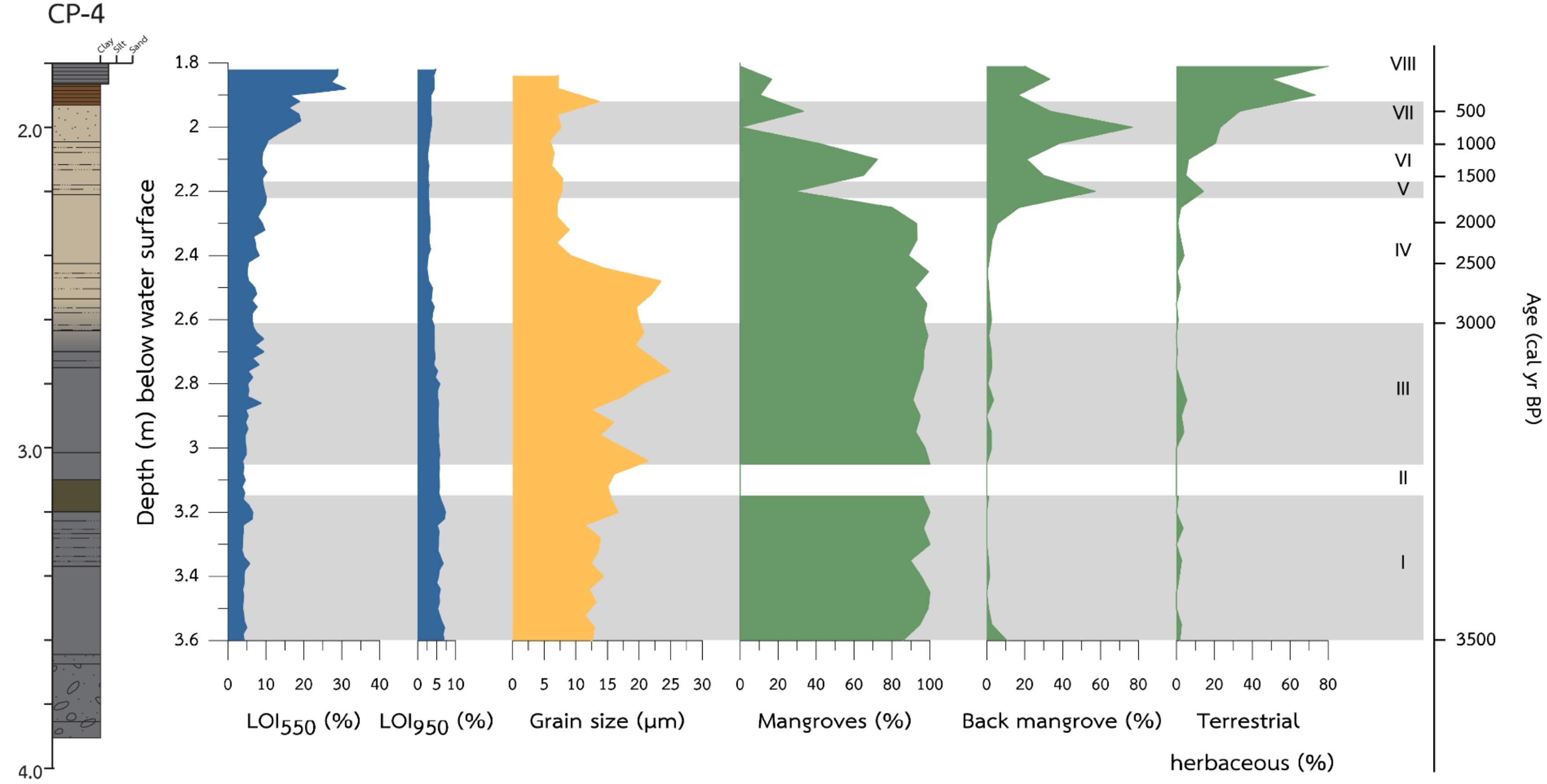


**Figure 28** SRY evolution stage according to LOI, grain size and pollen analysis

### 5.3 Sea level changes of the late Holocene

5.3.1 Sea level comparison of Sam Roi Yot area

Surakiatchai et al. (2018) provided the sea level reconstruction in Sam Roi Yot National Park based on Optically Stimulated Luminescence from beach ridge plain accompanied by radiocarbon dating of marine shells attached to sea notches (Figure 29).

Sea notch is efficiently indicated sea level stillstand (Maeda et al., 2004). The upper sea notch was developed at 6500 – 6000 cal year BP when this area was a coastal bay, beach ridge plain and tombolos. The geomorphological records suggest that sea level fall from 6000 to 3000 cal year BP. The environmental changes in stage I, II and III, which was from c. 3500 to 3000 cal year BP, in this study consists well in time with the late phase of regression. The geomorphology of coastal bay, beach ridge plain and tombolos corresponded with the marine-dominated coastline in SRY wetland in regarding to silt-dominated and low organic content sediments. The high deposition rate between 3500 and 3000 cal year BP can be explained by trap of sediments by mangrove forest. However, a temporary dry event based on the layer of oxidation and barren zone of pollen suggest that sea level suddenly declined at approximately 3300 cal year BP.

The middle sea notch indicates the stillstand of sea level c. 3000 – 1000 cal yr BP, when the geomorphology gradually transferred from coastal bay, beach ridge plain and tombolos to tidal flat. The limestone island was connected with mainland by tombolos that were continued from the previous period of regression. This period was concomitant with the reconstructed environment in stage IV, V, and VI. The reconstructed stillstand of sea level in SRY wetland can be referred by sediment and pollen records in stage IV (c. 3000 – 1700 cal yr BP). The decrease in grain size from silt- to clay-dominated sediments suggest a lower energy of sediment transport that consist well with an obviously decline in deposition rate during this period. Despite the sediment characteristicห changed, mangroves remained dominant in this stage. However, the slight fluctuation of sea level can be found in stage V and VI. The replacement of back mangrove together with a slight increase of $LOI_{550}$ in stage V indicated the short period of regression at c. 1700 – 1600 cal year BP. However, a slight sea level rise occurred between c. 1600 and 1000 cal year BP caused by the domination of *Avicennia* together with back mangrove taxa.

Surakiatchai et al. (2018) suggest a regression after 1000 cal yr BP that consists with the replacement of back mangrove and increase in terrestrial herbaceous plant in stage VII (1000 – 400 cal year BP). The marine influence gradually decreased in this stage. The change from beige clay to organic rich sediment and the prevailing of terrestrial herbaceous plant suggested that this area was completely transferred from tidal environment to freshwater wetland at approximately 400 cal yr BP.

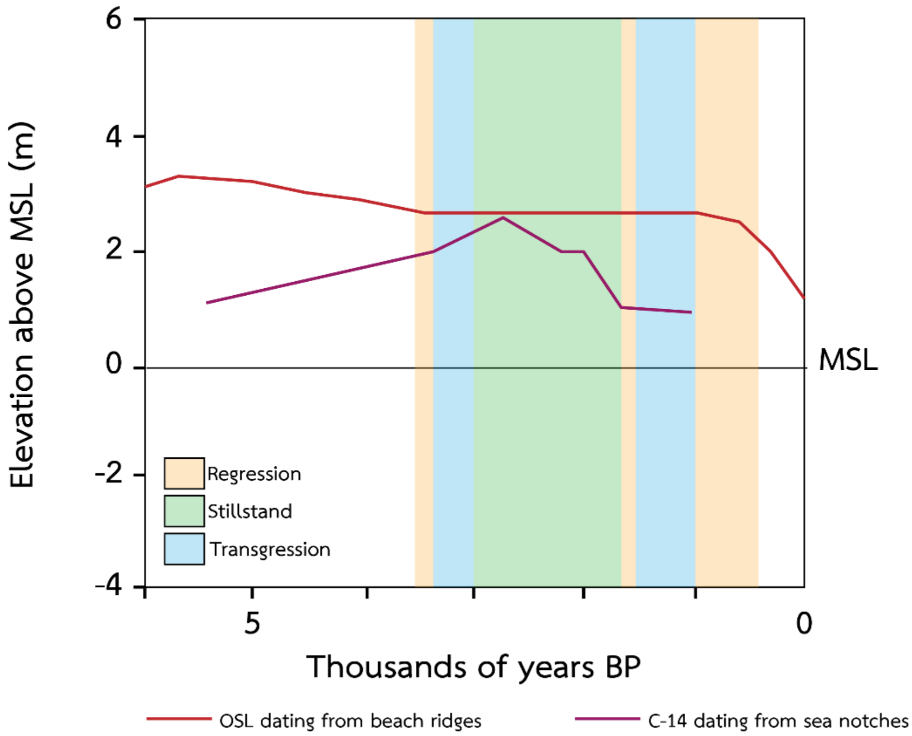


**Figure 29** Sea level reconstruction compared with Surakiatchai et al. (2018) represented by the red line

5.3.2 Sea level comparison around the Gulf of Thailand

Reconstructed sea level around the Gulf of Thailand from c. 3500 to 400 cal year BP were compared the results from this study. This interval has been generally considered to be a gradual falls in sea level after the mid Holocene highstand

(Choowong et al., 2004; Geyh et al., 1979; Hesp et al., 1998; Horton et al., 2005; Nimnate et al., 2015) (Figure 30). However, the reconstructed environment during 3500-400 cal year BP in this study can be divided into 8 stages of sea level fluctuation and 2 minor transgression (Figure 29). Furthermore, Sinsakul (1985) provided the sea level curve which is rather inverse from others since c. 3000 cal yr BP. The transgressions occurred when it was stillstand in this study at c. 3000 – 1700 cal yr BP. The result by Sinsakul (1985) was totally contrasted at c. 1600 – 1000 and 1000 - 400 cal yr BP. Sea level from SRY was transgressed while Sinsakul (1985) was regressed at approximately 1600 – 1000 cal yr BP, subsequent by a regression in this study but transgression in Sinsakul (1985) (Figure 30).

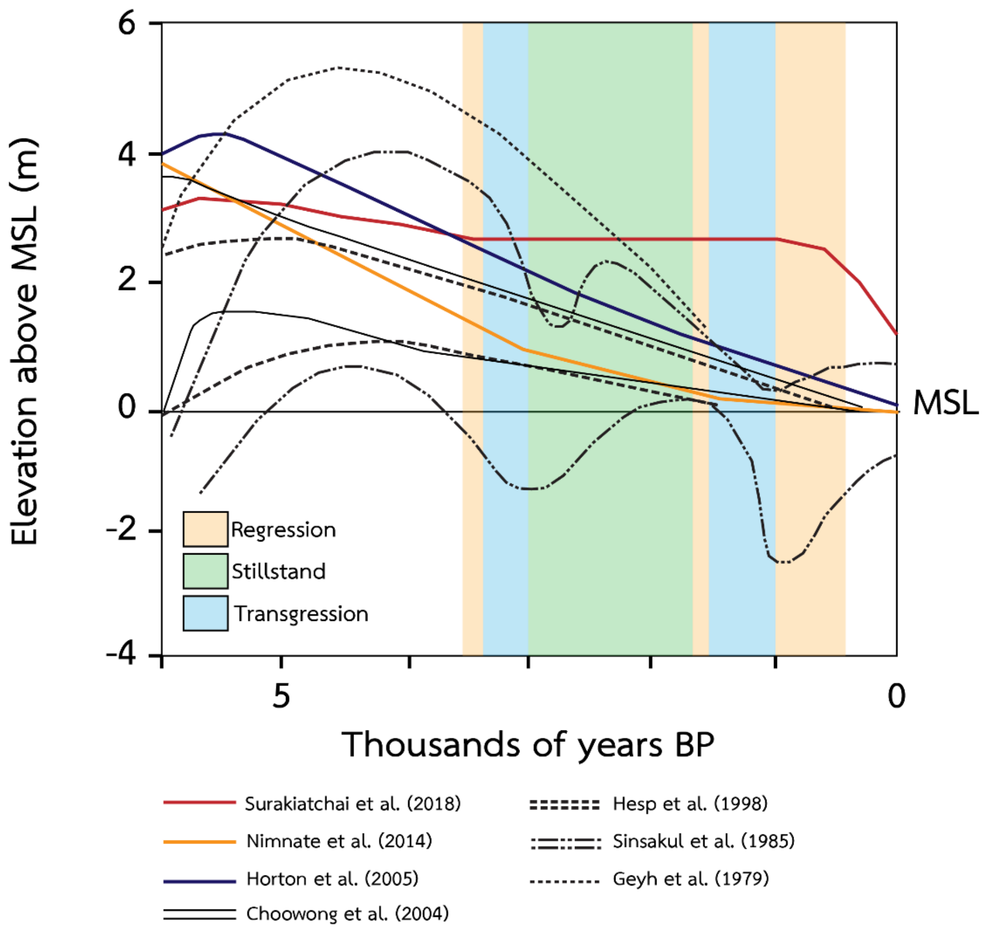


**Figure 30** Comparison of sea level fluctuation around the Gulf of Thailand

# CHAPTER 6 CONCLUSION

Sedimentary sequences obtained from SRY wetland has been divided into 3 units, comprised dark grey sediment in unit A, beige clay sediment in unit B, and gyttja sediment in unit C. An intensive analysis was focused on core CP-4 according to the most length and entire sedimentary unit composition. Environmental reconstruction was accomplished by pollen analysis, grain size analysis, Loss on Ignition (LOI) and radiocarbon dating.  The results altogether provided the environmental evolution that is an intertidal environment dominated by mangroves since c. 3500 - 1700  cal year BP with a temporary dry condition at c. 3300 cal year BP. Mangrove subsequently transferred to back mangroves at c. 1700 – 1600 cal year BP. Thereafter, mangrove zonation prograded seaward and effected this area prominent by back mangroves at c. 1000 -  400 cal year BP. Freshwater wetland was finally replaced at c. 400 cal year BP until present. The vegetation changes were suggested the marine regression since c. 3500 cal year BP followed by a minor transgression at c. 3300 cal year BP. Sea level became stable at c. 3000 cal year BP corresponded with Surakiatchai et al. (2018). Nevertheless, the fluctuation was found at c.  1700 – 1600 cal year BP which considered as a minor regression and 1600 – 1000 cal year BP which was determined as a minor transgression.  Thereafter, sea level was continuously fell at 1000 cal year BP to present, and can be negligible to this area since 400 cal year BP.

# REFERENCES

Bindoff, N. L., Willebrand, J., Artale, V., Cazenave, A., Gregory, J. M., Gulev, S., Hanawa, K., Le Quere, C., Levitus, S., and Nojiri, Y. 2007. Observations: oceanic climate change and sea level. In S. Solomon, D. Qin, M. Manning, Z. Chen, M. Marquis, K. B. Averyt, M. Tignor, and H. L. Miller (eds.), Climate change 2007: the physical science basis. Contribution of Working Group I, pp. 385-428. Cambridge: Cambridge University Press.

Bird, M. I., Fifield, L. K., Teh, T. S., Chang, C. H., Shirlaw, N., and Lambeck, K. 2007. An inflection in the rate of early mid-Holocene eustatic sea-level rise: A new sea-level curve from Singapore. Estuarine, Coastal and Shelf Science 71(3-4): 523-536.

Björck, S., and Wohlfarth, B. 2002. 14C Chronostratigraphic Techniques in Paleolimnology. pp. 205-245.

Blaauw, M., and Christen, J. A. 2005. Radiocarbon peat chronologies and environmental change. Journal of the Royal Statistical Society: Series C (Applied Statistics) 54(4): 805-816.

Blaauw, M., and Christen, J. A. 2011. Flexible paleoclimate age-depth models using an autoregressive gamma process. Bayesian analysis 6(3): 457-474.

Chaimanee, N. The transgression-regression event in Songkhla lake basin, southern Thailand. pp. 169-177.

Choowong, M. The geomorphology and assessment of indicators of sea-level changes to study coastal evolution from the Gulf of Thailand. pp. 207-220.

Choowong, M., Ugai, H., Charoentitirat, T., Charusiri, P., Daorerk, V., Songmuang, R., and Ladachart, R. 2004. Holocene Biostratigraphical Records in Coastal Deposits from Sam Roi Yod National Park, Prachuap Khiri Khan, Western Thailand. Tropical Natural History 4(2): 1-18.

Church, J., Clark, P., Cazenave, A., Gregory, J., Jevrejeva, S., Levermann, A., Merrifield, M., Milne, G., Nerem, R., Nunn, P., Payne, A., Pfeffer, W., Stammer, D., and Alakkat, U. 2013. Climate Change 2013: The Physical Science Basis. Contribution of

Working Group I to the Fifth Assessment Report of the Intergovernmental Panel on Climate Change. Sea Level Change: 1138-1191.

Culver, S. J., Leorri, E., Mallinson, D. J., Corbett, D. R., and Shazili, N. A. M. 2015. Recent coastal evolution and sea-level rise, Setiu Wetland, Peninsular Malaysia. Palaeogeography, Palaeoclimatology, Palaeoecology 417: 406-421.

De Vries, H., and Barendsen, G. 1952. A new technique for the measurement of age by radiocarbon. Physica 18

Dusitapirom, U., Choowong, M., and Daorerk, V. 2008. Analysis in genesis and pattern of limestone sea notches from Sam Roi Yot National Park, Prachuap Khiri Khan Province, Southern Thailand. Bulletin of Earth Sciences of Thailand 1: 35-39.

Ellison, J. C. 2008. Long-term retrospection on mangrove development using sediment cores and pollen analysis: A review. Aquatic Botany 89(2): 93-104.

Galbraith, H., Jones, R., Park, R., Clough, J., Herrod-Julius, S., Harrington, B., and Page, G. 2002. Global climate change and sea level rise: potential losses of intertidal habitat for shorebirds. Waterbirds 25(2): 173-183.

Geyh, M. A., Streif, H., and Kudrass, H. R. 1979. Sea-level changes during the late Pleistocene and Holocene in the Strait of Malacca. Nature 278(5703): 441-443.

Hanebuth, T., Stattegger, K., and Grootes, P. M. 2000. Rapid flooding of the Sunda Shelf: a late-glacial sea-level record. Science 288(5468): 1033-1035.

Hanebuth, T. J. J., Stattegger, K., and Bojanowski, A. 2009. Termination of the Last Glacial Maximum sea-level lowstand: The Sunda-Shelf data revisited. Global and Planetary Change 66(1-2): 76-84.

Hanebuth, T. J. J., Voris, H. K., Yokoyama, Y., Saito, Y., and Okuno, J. i. 2011. Formation and fate of sedimentary depocentres on Southeast Asia's Sunda Shelf over the past sea-level cycle and biogeographic implications. Earth-Science Reviews 104(1-3): 92-110.

Heiri, O., Lotter, A. F., and Lemcke, G. 2001. Loss on ignition as a method for estimating organic and carbonate content in sediments: reproducibility and comparability of results. Journal of paleolimnology 25(1): 101-110.

Hesp, P. A., Hung, C. C., Hilton, M., Ming, C. L., and Turner, I. M. 1998. A first tentative Holocene sea-level curve for Singapore. Journal of Coastal Research: 308-314.

Horton, B. P., Gibbard, P. L., Mine, G., Morley, R., Purintavaragul, C., and Stargardt, J. M. 2005. Holocene sea levels and palaeoenvironments, Malay-Thai Peninsula, southeast Asia. The Holocene 15(8): 1199-1213.

Hutangkura, T. 2012. Pollen analysis of the Holocene sedimentary sequences from the Lower Central Plain of Thailand and its implications for understanding palaeo-environmental and phytogeographical changes. Doctoral Thesis in History, University of Nice, France.

Kemp, A. C., Horton, B. P., Vane, C. H., Bernhardt, C. E., Corbett, D. R., Engelhart, S. E., Anisfeld, S. C., Parnell, A. C., and Cahill, N. 2013. Sea-level change during the last 2500 years in New Jersey, USA. Quaternary Science Reviews 81: 90-104.

Koskelainen, M. 2014. Paleobotanical and lithological changes in two lakes in Thailand – implications for hydrological changes and landscape management. Master's degree. Department of Geophysics and Geography University of Helsinki.

Li, Z., Saito, Y., Mao, L., Tamura, T., Li, Z., Song, B., Zhang, Y., Lu, A., Sieng, S., and Li, J. 2012. Mid-Holocene mangrove succession and its response to sea-level change in the upper Mekong River delta, Cambodia. Quaternary Research 78(2): 386-399.

Lugo, A. E., and Snedaker, S. C. 1974. The ecology of mangroves. Annual review of ecology and systematics 5(1): 39-64.

Maeda, Y., Siringan, F., Omura, A., Berdin, R., Hosono, Y., Atsumi, S., and Nakamura, T. 2004. Higher-than-present Holocene mean sea levels in Ilocos, Palawan and Samar, Philippines. Quaternary International 115: 15-26.

Michener, W. K., Blood, E. R., Bilstein, K. L., Brinson, M. M., and Garner, L. R. 1997. Climate change, hurricanes and tropical storms, and rising sea level in coastal wetlands. Ecological Applications 7(3): 770-801.

Milne, G. A., Gehrels, W. R., Hughes, C. W., and Tamisiea, M. E. 2009. Identifying the causes of sea-level change. Nature Geoscience 2(7): 471-478.

Nicholls, R. J., and Cazenave, A. 2010. Sea-level rise and its impact on coastal zones. science 328(5985): 1517-1520.

Nimnate, P., Chutakositkanon, V., Choowong, M., Pailoplee, S., and Phantuwongraj, S. 2015. Evidence of Holocene sea level regression from Chumphon coast of the

Gulf of Thailand. ScienceAsia 41(1)

Punwong, P. 2007. Pollen deposit in Bangkok clay from Ong Kharak District, Nakhon Nayok Province, and their implication on paleophytogeography. Master's thesis. Chulalongkorn University.

Qureshi, I. 1959. Botanical, silvicultural features of mangrove forests of Bombay State. Proc. Mangrove Sympos.(Calcutta)(1957): 20-25.

Reimer, P. J., Bard, E., Bayliss, A., Beck, J. W., Blackwell, P. G., Ramsey, C. B., Buck, C. E., Cheng, H., Edwards, R. L., and Friedrich, M. 2013. IntCal13 and Marine13 radiocarbon age calibration curves 0–50,000 years cal BP. Radiocarbon 55(4): 1869-1887.

Rowell, D. L. 2014. Soil science: Methods & applications. Routledge.

Rugmai, W., J. Grote, P., Chonglakmani, C., Zetter, R., and K. Ferguson, D. 2008. A Late Pleistocene palynoflora from the coastal area of Songkhla Lake, southern Thailand. ScienceAsia 34(2)

Santisuk, T. 1983. Taxonomy and distribution of terrestrial trees and shrubs in the mangrove formations in Thailand. Nat Hist Bull Siam Soc 5: 63-91.

Sinsakul, S. 1985. Holocene sea levels in Thailand: evidence and basis for interpretation. Journal of the Geological Society of Thailand 8: 1-12.

Sinsakul, S. 1992. Evidence of quarternary sea level changes in the coastal areas of Thailand: a review. Journal of Southeast Asian Earth Sciences 7(1): 23-37.

Somboon, J. 1988. Paleontological study of the recent marine sediments in the lower central plain, Thailand. Journal of Southeast Asian Earth Sciences 2(3-4): 201-210.

Surakiatchai, P., Choowong, M., Charusiri, P., Charoentitirat, T., Chawchai, S., PAILOPLEE, S., CHABANGBORN, A., Phantuwongraj, S., Chutakositkanon, V., and Kongsen, S. 2018. Paleogeographic Reconstruction and History of the Sea Level Change at Sam Roi Yot National Park, Gulf of Thailand. Tropical Natural History 18(2): 112-134.

Tam, C.-Y., Zong, Y., Hassan, K. b., Ismal, H. b., Jamil, H. b., Xiong, H., Wu, P., Sun, Y., Huang, G., and Zheng, Z. 2018. A below-the-present late Holocene relative sea level and the glacial isostatic adjustment during the Holocene in the Malay

Peninsula. Quaternary Science Reviews 201: 206-222.

Tamura, T., Saito, Y., Sieng, S., Ben, B., Kong, M., Sim, I., Choup, S., and Akiba, F. 2009. Initiation of the Mekong River delta at 8 ka: evidence from the sedimentary succession in the Cambodian lowland. Quaternary Science Reviews 28(3-4): 327-344.

Thiramongkol, N. 1984. Proceedings of the Third Meeting of the Working Group on Geomorphology of River and Coastal Plains, Chulalongkorn University, Bangkok, Thailand, December 11-17. Department of Geology, Chulalongkorn University.

Tjia, H. 1992. Holocene sea-level changes in the Malay-Thai Peninsula, a tectonically stable environment. Geol. Soc. Malaysia, Bulletin 31: 157-176.

Tjia, H. D. 1996. Sea-level changes in the tectonically stable Malay-Thai Peninsula. Quaternary International 31: 95-101.

Walker, M. J., Berkelhammer, M., Björck, S., Cwynar, L. C., Fisher, D. A., Long, A. J., Lowe, J. J., Newnham, R. M., Rasmussen, S. O., and Weiss, H. 2012. Formal subdivision of the Holocene Series/Epoch: a Discussion Paper by a Working Group of INTIMATE (Integration of ice-core, marine and terrestrial records) and the Subcommission on Quaternary Stratigraphy (International Commission on Stratigraphy). Journal of Quaternary Science 27(7): 649-659.

Watson, J. G. 1928. Mangrove forests of the Malay Peninsula. Malayan forest records ; no. 6. Singapore: Fraser & Neave.

# APPENDICES

## APPENDIX A
## CORE LOCATIONS

**Table 7** Core locations

| Core name | Latitude | Longitude | UTM (WGS) | |
|---|---|---|---|---|
| | | | X | Y |
| SRY CP-1 | 12.244640N | 99.930425E | 601197 | 1353780 |
| SRY CP-2 | 12.242838N | 99.928773E | 601018 | 1353580 |
| SRY CP-3 | 12.247110N | 99.927501E | 600878 | 1354052 |
| SRY CP-4 | 12.247312N | 99.931758E | 601341 | 1354076 |
| SRY CP-5 | 12.249895N | 99.929983E | 601147 | 1354361 |
| SRY CP-6 | 12.251215N | 99.927432E | 600869 | 1354506 |
| SRY CP-7 | 12.251590N | 99.931479E | 601309 | 1354549 |
| SRY CP-8 | 12.257124N | 99.931489E | 601308 | 1355161 |
| SRY CP-9 | 12.254691N | 99.931517E | 601312 | 1354892 |

# APPENDIX B
# STRATIGRAPHIC COLUMN

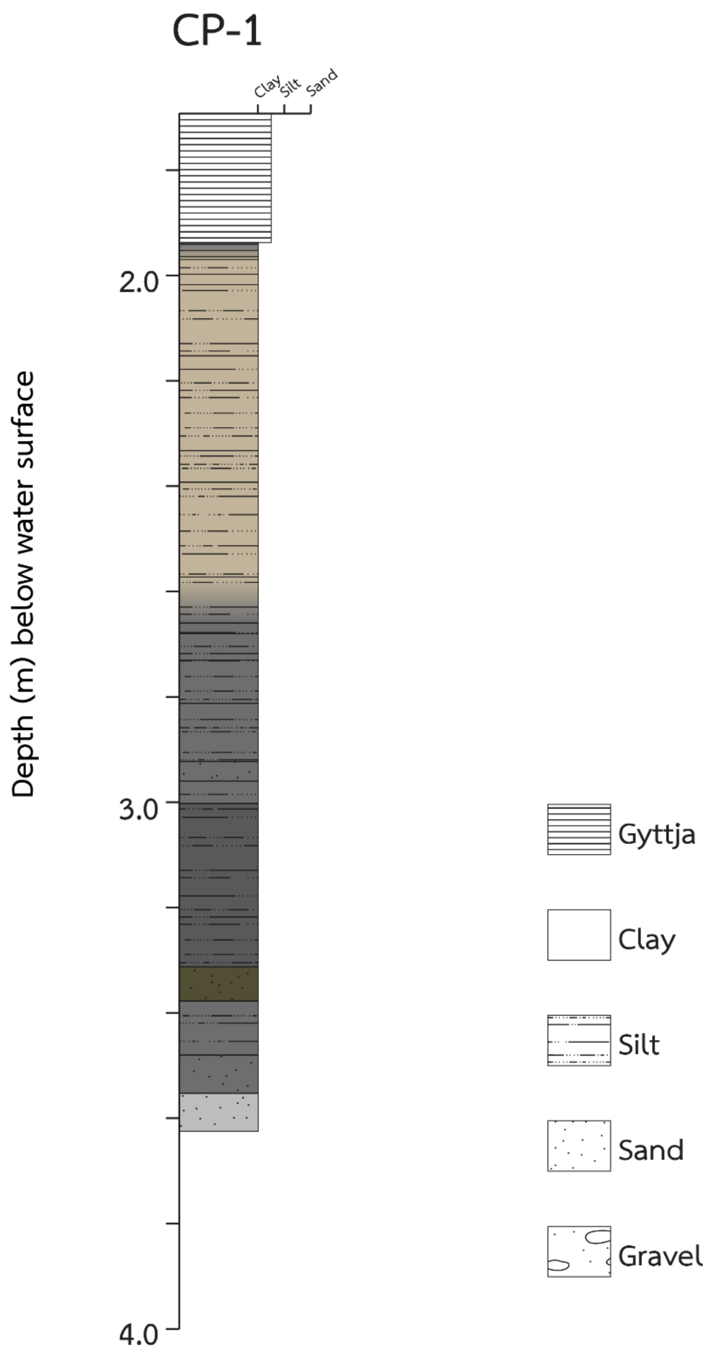


**Figure 31** Stratigraphic column of CP-1


**Figure 32** Stratigraphic column of CP-2

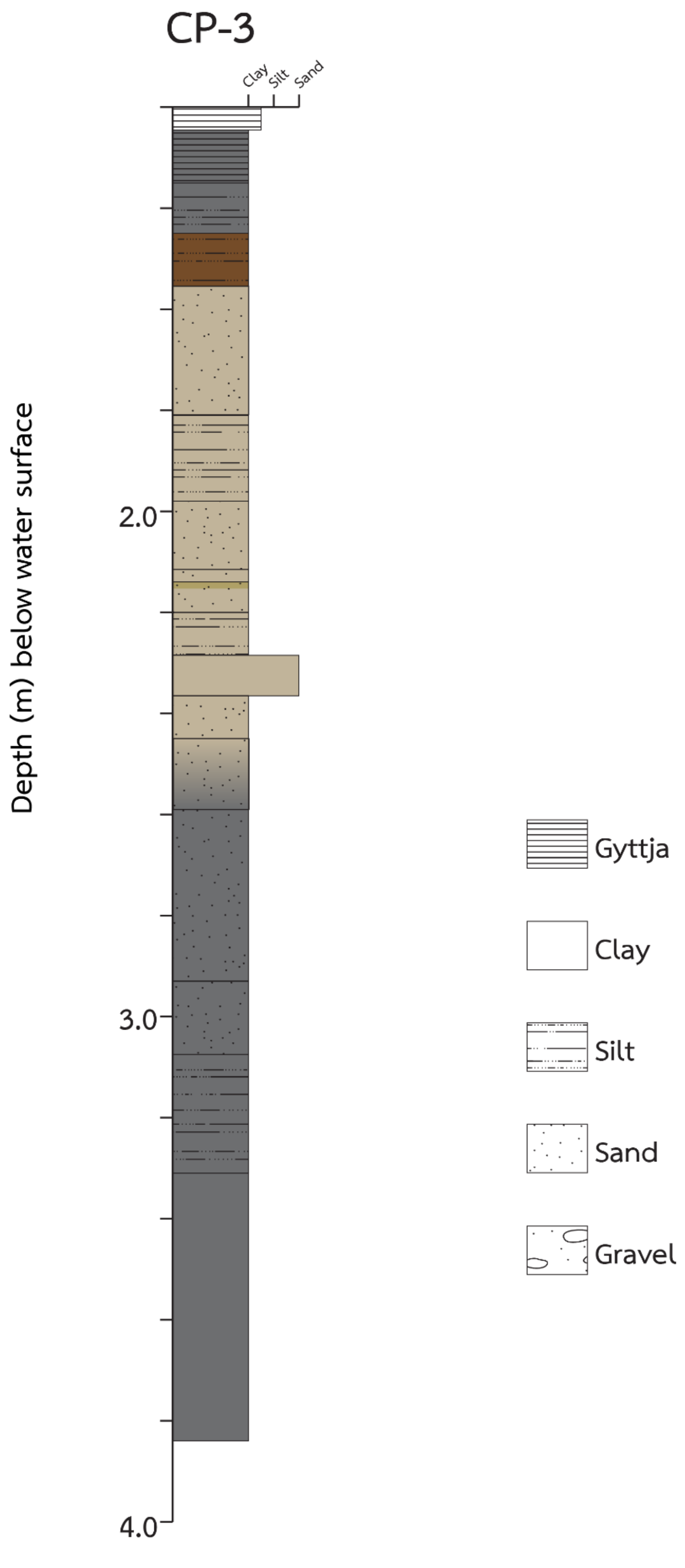


**Figure 33** Stratigraphic column of CP-3

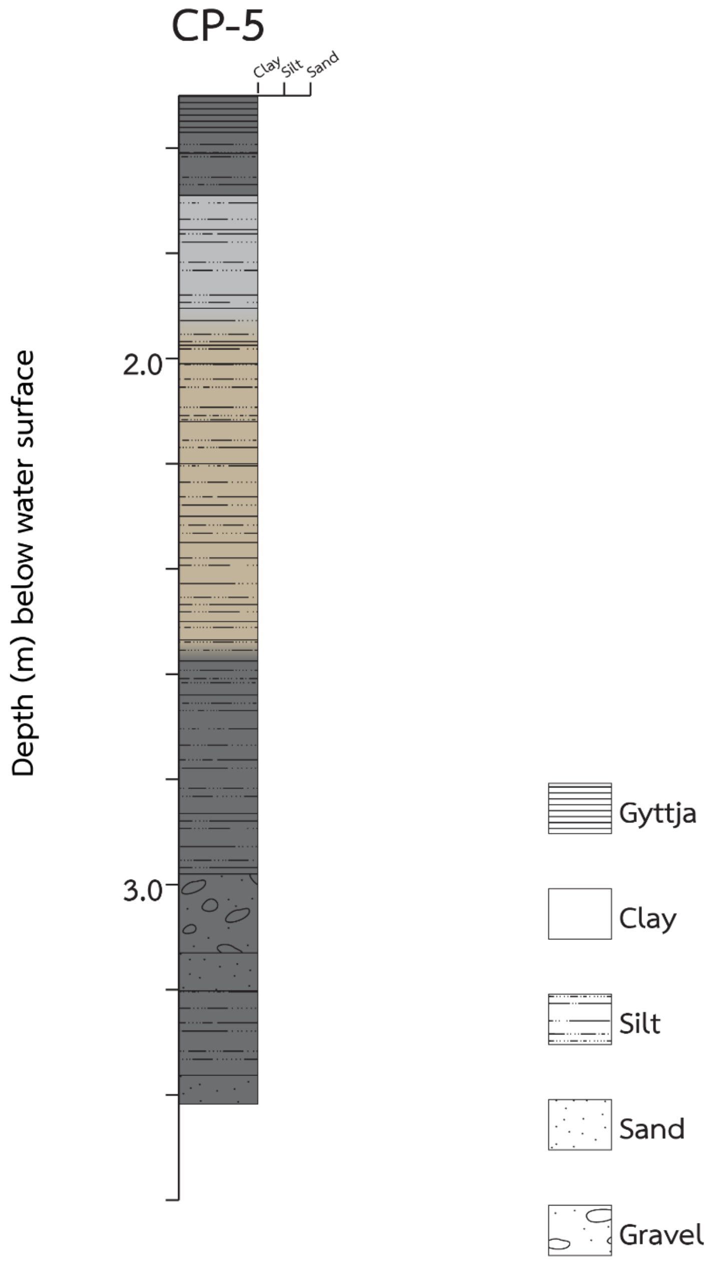


**Figure 34** Stratigraphic column of CP-5

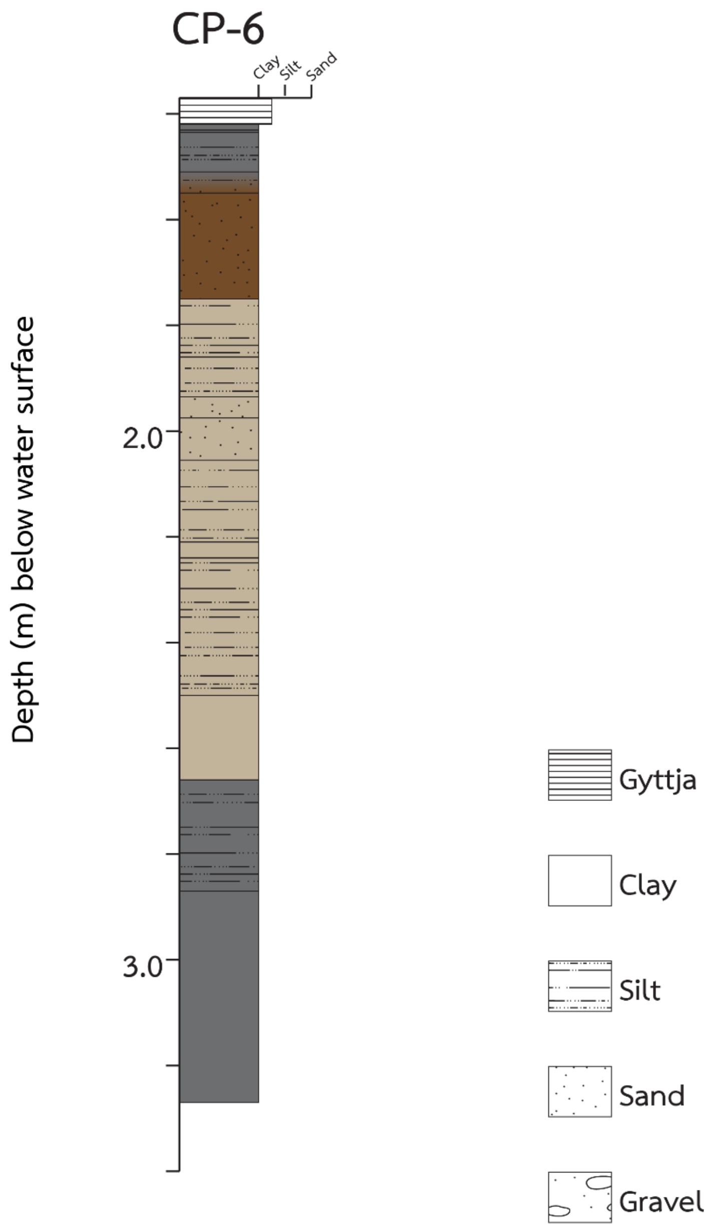


**Figure 35** Stratigraphic column of CP-6

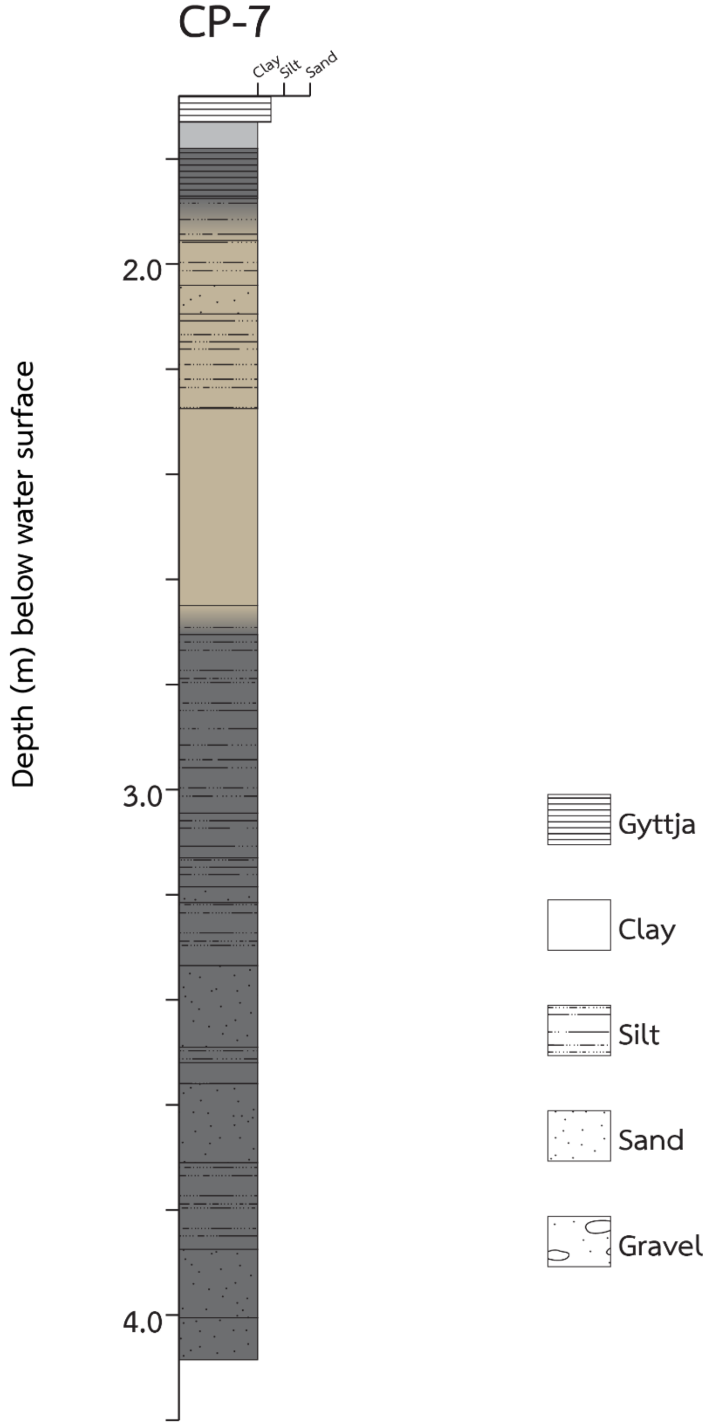


**Figure 36** Stratigraphic column of CP-7

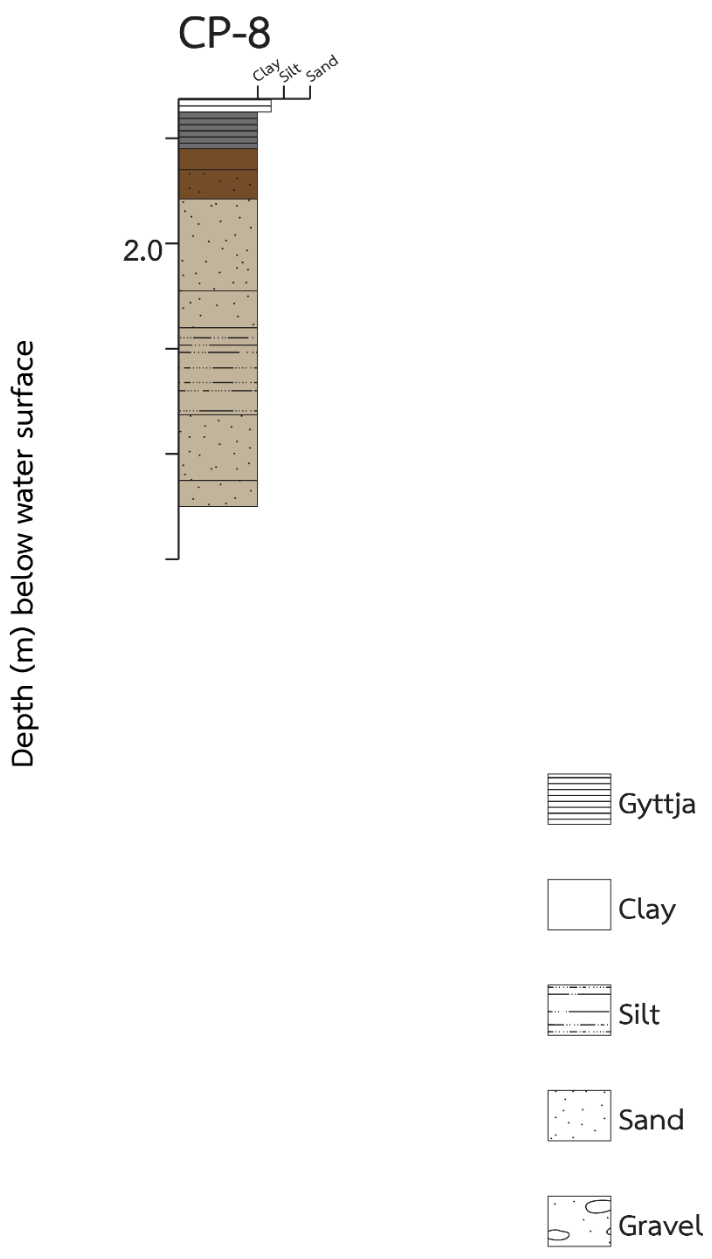


**Figure 37** Stratigraphic column of CP-8

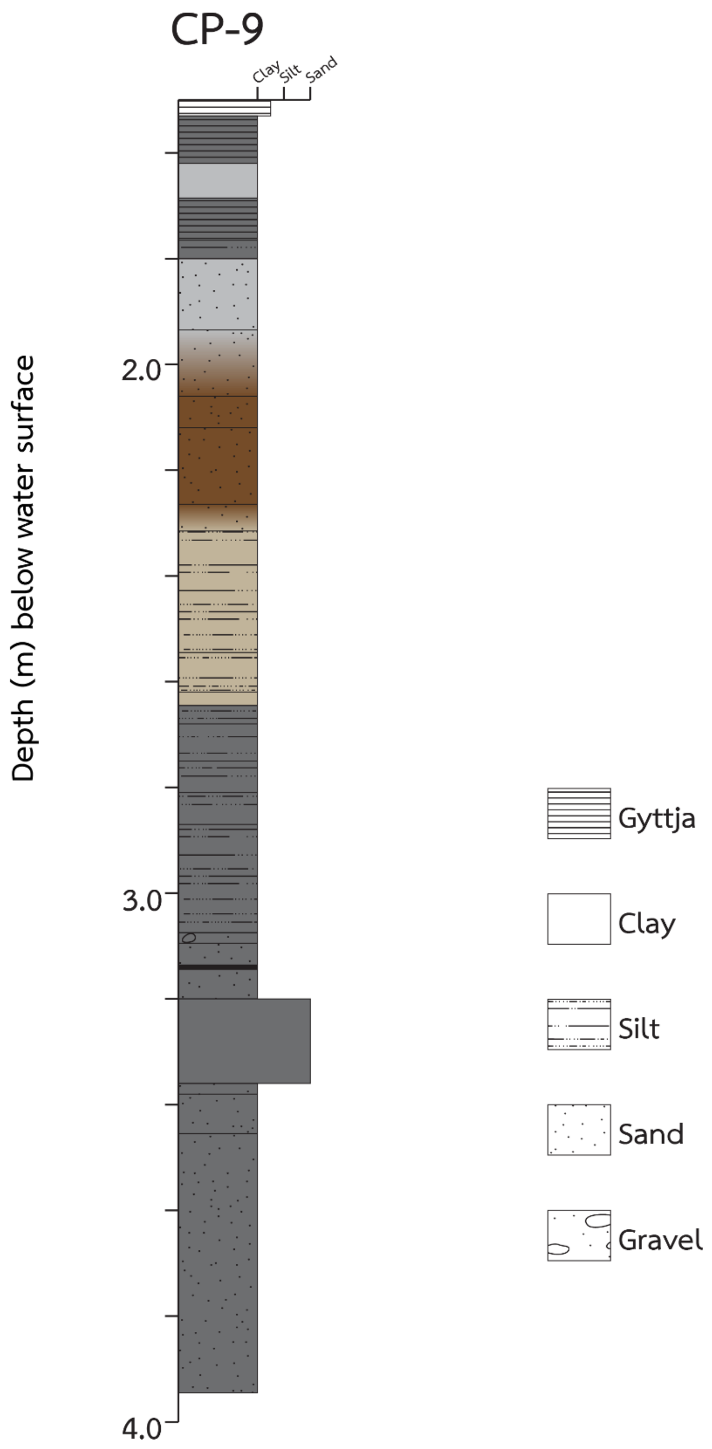


**Figure 38** Stratigraphic column of CP-9

# APPENDIX C
# LOSS ON IGNITION

**Table 8** Loss on Ignition data

| Sample No. | Depth (cm) below water surface | $DW_{105}$ | $DW_{550}$ | $DW_{950}$ | $LOI_{550}$ | $LOI_{950}$ |
|---|---|---|---|---|---|---|
| #2 | 181 – 182 | 1.459 | 1.037 | 0.968 | 28.92392 | 4.729267 |
| #4 | 183 - 184 | 1.594 | 1.136 | 1.071 | 28.73275 | 4.077792 |
| #6 | 185 – 186.5 | 1.756 | 1.28 | 1.206 | 27.10706 | 4.214123 |
| #8 | 187 – 188 | 1.621 | 1.119 | 1.05 | 30.96854 | 4.256632 |
| #10 | 189 - 190 | 2.017 | 1.693 | 1.624 | 16.06346 | 3.420922 |
| #12 | 191 – 192 | 2.253 | 1.831 | 1.753 | 18.73058 | 3.462051 |
| #14 | 193 – 194 | 2.389 | 2.013 | 1.931 | 15.7388 | 3.432398 |
| #16 | 195 – 196 | 2.418 | 1.968 | 1.885 | 18.61042 | 3.432589 |
| #18 | 197 – 198 | 2.13 | 1.725 | 1.648 | 19.01408 | 3.615023 |
| #20 | 199 - 200 | 2.612 | 2.19 | 2.099 | 16.1562 | 3.48392 |
| #22 | 201 - 202 | 2.879 | 2.502 | 2.413 | 13.09482 | 3.091351 |
| #24 | 203 – 204.5 | 2.786 | 2.492 | 2.409 | 10.55276 | 2.979182 |
| #26 | 205 - 206 | 3.084 | 2.782 | 2.696 | 9.792477 | 2.788586 |
| #28 | 207 – 208 | 2.837 | 2.581 | 2.508 | 9.023616 | 2.573141 |
| #30 | 209 - 210 | 2.256 | 2.057 | 2 | 8.820922 | 2.526596 |
| #32 | 211 – 212 | 3.169 | 2.886 | 2.797 | 8.930262 | 2.808457 |
| #34 | 213 – 214 | 3.082 | 2.771 | 2.689 | 10.09085 | 2.66061 |
| #36 | 215 - 216 | 3.194 | 2.906 | 2.823 | 9.016907 | 2.598622 |
| #38 | 217 – 218 | 3.265 | 2.965 | 2.873 | 9.188361 | 2.817764 |
| #40 | 219 – 220 | 3.247 | 2.936 | 2.848 | 9.578072 | 2.710194 |
| #42 | 221 - 222 | 3.098 | 2.788 | 2.703 | 10.00646 | 2.743706 |
| #44 | 223 – 224 | 2.952 | 2.663 | 2.578 | 9.789973 | 2.879404 |
| #46 | 225 – 226 | 3.15 | 2.878 | 2.789 | 8.634921 | 2.825397 |

| | | | | | | |
|---|---|---|---|---|---|---|
| #48 | 227 – 228 | 2.65 | 2.443 | 2.362 | 7.811321 | 3.056604 |
| #50 | 229 - 230 | 2.639 | 2.403 | 2.32 | 8.942781 | 3.145131 |
| #52 | 231 – 232 | 2.339 | 2.114 | 2.04 | 9.619496 | 3.163745 |
| #54 | 233 – 234 | 3.06 | 2.856 | 2.769 | 6.666667 | 2.843137 |
| #56 | 235 – 236 | 2.952 | 2.742 | 2.656 | 7.113821 | 2.913279 |
| #58 | 237 – 238 | 2.036 | 1.887 | 1.821 | 7.318271 | 3.24165 |
| #60 | 239 – 240 | 2.852 | 2.62 | 2.544 | 8.134642 | 2.664797 |
| #62 | 241.5 - 242 | 2.7 | 2.556 | 2.489 | 5.333333 | 2.481481 |
| #64 | 243 - 244 | 2.737 | 2.6 | 2.536 | 5.00548 | 2.338327 |
| #66 | 245 - 246 | 2.781 | 2.643 | 2.572 | 4.962244 | 2.553038 |
| #68 | 247 – 248 | 2.711 | 2.566 | 2.49 | 5.34858 | 2.803394 |
| #70 | 249 – 250 | 1.928 | 1.794 | 1.722 | 6.950207 | 3.73444 |
| #72 | 251 - 252 | 2.045 | 1.893 | 1.818 | 7.432763 | 3.667482 |
| #74 | 253.5 - 254 | 2.239 | 2.1 | 2.023 | 6.208129 | 3.439035 |
| #76 | 255 – 256 | 1.915 | 1.77 | 1.689 | 7.571802 | 4.229765 |
| #78 | 257 - 258 | 2.418 | 2.266 | 2.174 | 6.286187 | 3.804797 |
| #80 | 259 – 260 | 2.62 | 2.455 | 2.36 | 6.29771 | 3.625954 |
| #82 | 261 - 262 | 2.218 | 2.074 | 1.98 | 6.492335 | 4.238052 |
| #84 | 263.5 - 264 | 1.339 | 1.24 | 1.183 | 7.393577 | 4.256908 |
| #86 | 265 – 266 | 1.892 | 1.716 | 1.635 | 9.302326 | 4.281184 |
| #88 | 267 – 268 | 1.743 | 1.621 | 1.547 | 6.999426 | 4.245554 |
| #90 | 269 – 270 | 2.712 | 2.459 | 2.342 | 9.328909 | 4.314159 |
| #92 | 271 - 272 | 1.935 | 1.814 | 1.728 | 6.25323 | 4.444444 |
| #94 | 273 – 274 | 2.49 | 2.289 | 2.187 | 8.072289 | 4.096386 |
| #96 | 275 – 276 | 1.755 | 1.664 | 1.574 | 5.185185 | 5.128205 |
| #98 | 277 – 278 | 2.298 | 2.151 | 2.047 | 6.396867 | 4.525674 |
| #100 | 279 – 280 | 2.35 | 2.231 | 2.097 | 5.06383 | 5.702128 |
| #102 | 281 – 282 | 1.997 | 1.889 | 1.786 | 5.408112 | 5.157737 |
| #104 | 283 – 284 | 2.147 | 2.038 | 1.928 | 5.076851 | 5.123428 |
| #106 | 285 - 286 | 1.962 | 1.793 | 1.687 | 8.61366 | 5.40265 |

| | | | | | | |
|---|---|---|---|---|---|---|
| #108 | 287 - 288 | 2.523 | 2.408 | 2.275 | 4.558066 | 5.271502 |
| #110 | 289 – 290 | 2.598 | 2.463 | 2.326 | 5.196305 | 5.273287 |
| #112 | 291 – 292 | 2.215 | 2.115 | 1.999 | 4.514673 | 5.23702 |
| #114 | 293 – 294 | 1.794 | 1.702 | 1.606 | 5.128205 | 5.351171 |
| #116 | 295 – 296 | 2.564 | 2.45 | 2.31 | 4.446178 | 5.460218 |
| #118 | 297 – 298 | 2.786 | 2.662 | 2.512 | 4.450826 | 5.384063 |
| #120 | 299 - 300 | 2.222 | 2.118 | 1.995 | 4.680468 | 5.535554 |
| #122 | 301.5 - 302 | 1.946 | 1.854 | 1.743 | 4.727646 | 5.704008 |
| #124 | 303 – 304 | 2.149 | 2.069 | 1.951 | 3.722662 | 5.490926 |
| #126 | 305 – 306 | 3.009 | 2.886 | 2.717 | 4.087737 | 5.616484 |
| #128 | 307 – 308 | 2.466 | 2.372 | 2.237 | 3.811841 | 5.474453 |
| #130 | 309 – 310 | 2.014 | 1.924 | 1.812 | 4.468719 | 5.561072 |
| #132 | 311 – 312 | 1.922 | 1.853 | 1.745 | 3.59001 | 5.619147 |
| #134 | 313 - 314 | 2.561 | 2.45 | 2.311 | 4.334244 | 5.427567 |
| #136 | 315 – 316 | 2.648 | 2.545 | 2.387 | 3.889728 | 5.966767 |
| #138 | 317 – 318 | 2.255 | 2.131 | 1.981 | 5.498891 | 6.651885 |
| #140 | 319 – 320 | 1.607 | 1.504 | 1.388 | 6.409459 | 7.218419 |
| #142 | 321 - 322 | 1.934 | 1.811 | 1.677 | 6.359876 | 6.928645 |
| #144 | 323 – 324 | 2.122 | 2.04 | 1.933 | 3.864279 | 5.042413 |
| #146 | 325 – 326 | 2.447 | 2.351 | 2.216 | 3.923171 | 5.51696 |
| #148 | 327 – 328 | 2.254 | 2.169 | 2.048 | 3.771074 | 5.368234 |
| #150 | 329 – 330 | 2.169 | 2.089 | 1.973 | 3.688336 | 5.348087 |
| #152 | 331 – 332 | 1.993 | 1.921 | 1.817 | 3.612644 | 5.218264 |
| #154 | 333 – 334 | 2.361 | 2.263 | 2.123 | 4.150784 | 5.929691 |
| #156 | 335 – 336 | 2.093 | 1.975 | 1.837 | 5.63784 | 6.593407 |
| #158 | 337 – 338 | 2.199 | 2.103 | 1.981 | 4.365621 | 5.547976 |
| #160 | 339 – 340 | 1.917 | 1.838 | 1.735 | 4.121022 | 5.372979 |
| #162 | 341 – 342 | 2.535 | 2.429 | 2.304 | 4.18146 | 4.930966 |
| #164 | 343 – 344 | 2.233 | 2.149 | 2.019 | 3.761755 | 5.821764 |
| #166 | 345 – 346 | 2.591 | 2.488 | 2.346 | 3.975299 | 5.480509 |

| | | | | | | |
|---|---|---|---|---|---|---|
| #168 | 347 – 348 | 1.845 | 1.774 | 1.67 | 3.848238 | 5.636856 |
| #170 | 349 - 350 | 2.217 | 2.134 | 2.02 | 3.743798 | 5.142084 |
| #172 | 351 – 352 | 2.186 | 2.098 | 1.975 | 4.025618 | 5.626715 |
| #174 | 353 – 354 | 2.046 | 1.959 | 1.831 | 4.252199 | 6.256109 |
| #176 | 355 – 356 | 2.144 | 2.04 | 1.891 | 4.850746 | 6.949627 |
| #178 | 357 – 358 | 2.892 | 2.781 | 2.591 | 3.838174 | 6.569848 |
| #180 | 359 - 360 | 2.223 | 2.129 | 1.976 | 4.22852 | 6.882591 |

# APPENDIX D
# GRAIN SIZE DISTRIBUTION DATA

**Table 9** Grain size distribution data

| Sample no. | DBWS (cm) | $D_{10}$ (µm) | $D_{50}$ (µm) | $D_{90}$ (µm) | D[4,3] (µm) | D[3,2] (µm) | Laser Obscuration (%) |
|---|---|---|---|---|---|---|---|
| #4 | 183 – 184 | 0.91 | 3.88 | 18.2 | 7.14 | 2.31 | 18.7 |
| #4 | 183 – 184 | 0.903 | 3.82 | 18.3 | 7.28 | 2.29 | 18.55 |
| #4 | 183 – 184 | 0.89 | 3.73 | 18.3 | 7.04 | 2.25 | 18.44 |
| #8 | 187 – 188 | 0.964 | 4.19 | 17.3 | 7.22 | 2.43 | 13.4 |
| #8 | 187 – 188 | 0.964 | 4.19 | 17 | 7.08 | 2.42 | 13.3 |
| #8 | 187 – 188 | 0.966 | 4.2 | 16.8 | 7.05 | 2.43 | 13.32 |
| #12 | 191 – 192 | 1.65 | 8.46 | 31.4 | 13.7 | 4 | 25.41 |
| #12 | 191 – 192 | 1.65 | 8.38 | 31.2 | 13.6 | 3.98 | 25.41 |
| #12 | 191 – 192 | 1.64 | 8.3 | 30.9 | 13.4 | 3.96 | 25.41 |
| #16 | 195 – 196 | 1.06 | 4.19 | 17.3 | 6.96 | 2.56 | 14.86 |
| #16 | 195 – 196 | 1.06 | 4.19 | 17.5 | 7.03 | 2.56 | 15.04 |
| #16 | 195 – 196 | 1.06 | 4.18 | 17.4 | 6.97 | 2.56 | 15.06 |
| #20 | 199 – 200 | 1.05 | 5.05 | 14.9 | 7.65 | 2.69 | 18.3 |
| #20 | 199 – 200 | 1.05 | 5.07 | 14.7 | 7.56 | 2.69 | 18.37 |
| #20 | 199 – 200 | 1.05 | 5.07 | 14.5 | 7.52 | 2.68 | 18.45 |
| #24 | 203 – 204.5 | 0.873 | 3.73 | 14.4 | 5.9 | 2.2 | 23.24 |
| #24 | 203 – 204.5 | 0.869 | 3.7 | 14.2 | 5.83 | 2.19 | 23.21 |
| #24 | 203 – 204.5 | 0.867 | 3.69 | 14.1 | 5.81 | 2.19 | 23.18 |
| #28 | 207 – 208 | 1.05 | 4.4 | 15.5 | 6.52 | 2.57 | 15.07 |
| #28 | 207 – 208 | 1.05 | 4.38 | 15.3 | 6.48 | 2.57 | 15.07 |
| #28 | 207 - 208 | 1.05 | 4.39 | 15.4 | 6.49 | 2.57 | 15.08 |
| #32 | 211 – 212 | 1.03 | 4.19 | 14.4 | 6.13 | 2.5 | 16.31 |

| | | | | | | | |
|---|---|---|---|---|---|---|---|
| #32 | 211 – 212 | 1.03 | 4.19 | 14.4 | 6.12 | 2.5 | 16.31 |
| #32 | 211 – 212 | 1.03 | 4.19 | 14.3 | 6.11 | 2.5 | 16.32 |
| #36 | 215 – 216 | 0.938 | 4.2 | 13.6 | 7.78 | 2.39 | 17.68 |
| #36 | 215 – 216 | 0.939 | 4.2 | 13.6 | 7.83 | 2.39 | 17.69 |
| #36 | 215 – 216 | 0.939 | 4.22 | 13.5 | 7.9 | 2.39 | 17.74 |
| #40 | 219 – 220 | 0.885 | 4.31 | 16.7 | 7.75 | 2.33 | 22.12 |
| #40 | 219 – 220 | 0.892 | 4.38 | 16.7 | 7.77 | 2.35 | 22.24 |
| #40 | 219 – 220 | 0.894 | 4.42 | 16.5 | 7.71 | 2.36 | 22.33 |
| #44 | 223 – 224 | 0.93 | 4.56 | 16.8 | 7 | 2.44 | 13.47 |
| #44 | 223 – 224 | 0.928 | 4.55 | 16.8 | 6.98 | 2.44 | 13.45 |
| #44 | 223 - 224 | 0.927 | 4.54 | 16.6 | 6.92 | 2.43 | 13.44 |
| #48 | 227 – 228 | 0.948 | 4.65 | 16.7 | 7.02 | 2.49 | 16.63 |
| #48 | 227 – 228 | 0.948 | 4.64 | 16.6 | 6.96 | 2.49 | 16.65 |
| #48 | 227 – 228 | 0.95 | 4.65 | 16.7 | 7.03 | 2.49 | 16.74 |
| #52 | 231 – 232 | 0.985 | 5.09 | 18.8 | 8.87 | 2.6 | 24.21 |
| #52 | 231 – 232 | 0.987 | 5.1 | 18.6 | 8.83 | 2.61 | 24.24 |
| #52 | 231 – 232 | 0.99 | 5.13 | 18.7 | 8.95 | 2.62 | 24.34 |
| #56 | 235 – 236 | 0.995 | 5.22 | 15.2 | 6.87 | 2.63 | 18.94 |
| #56 | 235 – 236 | 0.998 | 5.25 | 15.1 | 6.86 | 2.64 | 19.03 |
| #56 | 235 – 236 | 0.999 | 5.26 | 14.9 | 6.82 | 2.64 | 19.09 |
| #60 | 239 – 240 | 0.994 | 5.25 | 19.4 | 9.14 | 2.65 | 16.15 |
| #60 | 239 – 240 | 1 | 5.26 | 19.3 | 9.17 | 2.66 | 16.24 |
| #60 | 239 – 240 | 0.999 | 5.23 | 18.8 | 8.91 | 2.65 | 16.26 |
| #64 | 243 – 244 | 2.1 | 11 | 32 | 14.8 | 4.9 | 17.51 |
| #64 | 243 – 244 | 2.05 | 10.7 | 30.8 | 14.3 | 4.79 | 17.52 |
| #64 | 243 – 244 | 2.01 | 10.5 | 30.2 | 14.1 | 4.73 | 17.5 |
| #68 | 247 – 248 | 2.61 | 14.8 | 55.3 | 23.7 | 5.89 | 21.02 |
| #68 | 247 – 248 | 2.48 | 14.3 | 53.3 | 23.1 | 5.69 | 20.97 |
| #68 | 247 – 248 | 2.44 | 14.3 | 54.9 | 23.3 | 5.63 | 20.97 |
| #72 | 251 – 252 | 2.63 | 14.9 | 47.8 | 22.1 | 5.98 | 21.86 |

| | | | | | | | |
|---|---|---|---|---|---|---|---|
| #72 | 251 – 252 | 2.59 | 14.9 | 47.1 | 21.9 | 5.93 | 22 |
| #72 | 251 – 252 | 2.58 | 14.9 | 46.7 | 21.7 | 5.92 | 22.04 |
| #76 | 255 – 256 | 1.99 | 12.9 | 42.7 | 19.5 | 4.96 | 17.88 |
| #76 | 255 – 256 | 1.98 | 12.9 | 42.5 | 19.4 | 4.95 | 17.92 |
| #76 | 255 – 256 | 1.98 | 12.9 | 42.6 | 19.6 | 4.95 | 18.07 |
| #80 | 259 – 260 | 2.12 | 12.4 | 48.1 | 20 | 5.08 | 19.17 |
| #80 | 259 – 260 | 2.12 | 12.4 | 47.5 | 19.8 | 5.06 | 19.23 |
| #80 | 259 – 260 | 2.12 | 12.5 | 47.5 | 19.9 | 5.08 | 19.37 |
| #84 | 263.5 – 264 | 2.47 | 15.8 | 45.3 | 20.8 | 5.73 | 24.36 |
| #84 | 263.5 – 264 | 2.45 | 15.6 | 44.9 | 20.7 | 5.69 | 24.6 |
| #84 | 263.5 – 264 | 2.41 | 15.3 | 44.1 | 20.5 | 5.62 | 24.91 |
| #88 | 267 – 268 | 2.15 | 11.9 | 42.9 | 19.5 | 5.03 | 18.02 |
| #88 | 267 – 268 | 2.05 | 11.7 | 42 | 19.1 | 4.88 | 17.95 |
| #88 | 267 – 268 | 2.03 | 11.8 | 42.3 | 19.3 | 4.85 | 17.93 |
| #96 | 275 – 276 | 2.08 | 16 | 65.3 | 24.9 | 5.31 | 17.28 |
| #96 | 275 – 276 | 2.08 | 16 | 65.2 | 24.8 | 5.31 | 17.42 |
| #96 | 275 – 276 | 2.1 | 16 | 65.5 | 24.7 | 5.34 | 17.8 |
| #100 | 279 – 280 | 2.02 | 13 | 44.7 | 20.2 | 4.98 | 17.57 |
| #100 | 279 – 280 | 2.02 | 13.1 | 44.9 | 20.3 | 5 | 17.74 |
| #100 | 279 – 280 | 2.03 | 13.3 | 45.1 | 20.5 | 5.03 | 17.98 |
| #104 | 283 – 284 | 1.61 | 10.8 | 42.8 | 17.2 | 4.15 | 16.98 |
| #104 | 283 – 284 | 1.6 | 10.7 | 42.9 | 17.3 | 4.13 | 17.03 |
| #104 | 283 – 284 | 1.57 | 10.4 | 42.1 | 17 | 4.05 | 17.09 |
| #108 | 287 – 288 | 1.66 | 7.44 | 28.1 | 12.1 | 3.87 | 11.44 |
| #108 | 287 – 288 | 1.65 | 7.37 | 28 | 12.3 | 3.84 | 11.43 |
| #108 | 287 – 288 | 1.63 | 7.27 | 27.5 | 12.4 | 3.8 | 11.41 |
| #112 | 291 – 292 | 1.61 | 8.65 | 34.2 | 16 | 3.91 | 16.48 |
| #112 | 291 – 292 | 1.57 | 8.4 | 33.3 | 15.8 | 3.83 | 16.49 |
| #112 | 291 – 292 | 1.55 | 8.25 | 32.9 | 15.9 | 3.78 | 16.48 |
| #116 | 295 – 296 | 1.57 | 8.6 | 31.7 | 13.9 | 3.87 | 12.82 |

| | | | | | | | |
|---|---|---|---|---|---|---|---|
| #116 | 295 – 296 | 1.53 | 8.33 | 30.8 | 13.7 | 3.78 | 12.83 |
| #116 | 295 – 296 | 1.49 | 8.08 | 30.2 | 13.6 | 3.7 | 12.83 |
| #124 | 303 – 304 | 1.56 | 10.5 | 55.4 | 22.3 | 4.05 | 18.72 |
| #124 | 303 – 304 | 1.53 | 9.96 | 53 | 21.4 | 3.96 | 18.99 |
| #124 | 303 – 304 | 1.51 | 9.6 | 50.8 | 20.3 | 3.91 | 18.9 |
| #128 | 307 – 308 | 1.64 | 10.8 | 38.3 | 16.1 | 4.18 | 13.35 |
| #128 | 307 – 308 | 1.63 | 10.7 | 37.9 | 16 | 4.16 | 13.38 |
| #128 | 307 – 308 | 1.62 | 10.6 | 37.7 | 15.9 | 4.14 | 13.42 |
| #132 | 311 – 312 | 1.35 | 7.96 | 35.8 | 15.4 | 3.47 | 19.22 |
| #132 | 311 – 312 | 1.3 | 7.49 | 34.1 | 14.6 | 3.35 | 18 |
| #132 | 311 – 312 | 1.28 | 7.36 | 34.7 | 15.1 | 3.31 | 18 |
| #136 | 315 – 316 | 1.59 | 8.93 | 37 | 15.8 | 3.99 | 15.03 |
| #136 | 315 – 316 | 1.58 | 8.83 | 36.4 | 15.5 | 3.97 | 15.11 |
| #136 | 315 – 316 | 1.57 | 8.74 | 36.1 | 15.4 | 3.94 | 15.18 |
| #140 | 319 – 320 | 1.82 | 11.4 | 39.2 | 16.6 | 4.55 | 9.44 |
| #140 | 319 – 320 | 1.8 | 11.2 | 39 | 16.5 | 4.51 | 9.47 |
| #140 | 319 – 320 | 1.8 | 11.3 | 39.4 | 16.7 | 4.52 | 9.54 |
| #144 | 323 – 324 | 1.43 | 7 | 25.6 | 11.2 | 3.49 | 19.11 |
| #144 | 323 – 324 | 1.42 | 6.95 | 25.7 | 11.3 | 3.47 | 19.2 |
| #144 | 323 – 324 | 1.45 | 6.94 | 25.8 | 11.4 | 3.61 | 19.34 |
| #148 | 327 – 328 | 1.71 | 9.19 | 32.4 | 13.8 | 4.17 | 15.42 |
| #148 | 327 – 328 | 1.71 | 9.19 | 32.5 | 13.7 | 4.17 | 15.43 |
| #148 | 327 – 328 | 1.71 | 9.19 | 32.6 | 13.9 | 4.18 | 15.42 |
| #152 | 331 – 332 | 1.9 | 11.1 | 29 | 13.5 | 4.57 | 19.87 |
| #152 | 331 – 332 | 1.89 | 11 | 29.1 | 13.6 | 4.56 | 19.92 |
| #152 | 331 – 332 | 1.88 | 10.9 | 28.8 | 13.4 | 4.53 | 19.99 |
| #156 | 335 – 336 | 1.87 | 10 | 26.1 | 12.4 | 4.45 | 11.01 |
| #156 | 335 – 336 | 1.86 | 10 | 26 | 12.3 | 4.43 | 11.05 |
| #156 | 335 – 336 | 1.86 | 9.97 | 26 | 12.3 | 4.42 | 11.08 |
| #160 | 339 – 340 | 1.55 | 9.57 | 34.3 | 14.3 | 3.96 | 21.53 |

| | | | | | | | |
|---|---|---|---|---|---|---|---|
| #160 | 339 – 340 | 1.54 | 9.42 | 34 | 14.2 | 3.92 | 21.88 |
| #160 | 339 – 340 | 1.55 | 9.51 | 34.5 | 14.4 | 3.94 | 21.74 |
| #164 | 343 – 344 | 1.62 | 7.83 | 27.4 | 12 | 3.91 | 13.7 |
| #164 | 343 – 344 | 1.62 | 7.77 | 27.1 | 11.9 | 3.89 | 13.76 |
| #164 | 343 – 344 | 1.62 | 7.76 | 27.2 | 12.1 | 3.89 | 13.83 |
| #168 | 347 – 348 | 1.49 | 8.62 | 31 | 13.1 | 3.8 | 21.79 |
| #168 | 347 – 348 | 1.49 | 8.53 | 30.8 | 13 | 3.78 | 21.89 |
| #168 | 347 – 348 | 1.48 | 8.44 | 30.9 | 13.3 | 3.75 | 22.06 |
| #172 | 351 – 352 | 1.4 | 6.85 | 24.1 | 11.4 | 3.42 | 13.98 |
| #172 | 351 – 352 | 1.38 | 6.72 | 23.6 | 11.3 | 3.38 | 14.07 |
| #172 | 351 – 352 | 1.37 | 6.64 | 23.4 | 11.3 | 3.36 | 14.12 |
| #176 | 355 – 356 | 1.58 | 8.3 | 30.5 | 12.8 | 3.91 | 20.17 |
| #176 | 355 – 356 | 1.58 | 8.25 | 30.5 | 12.9 | 3.89 | 20.29 |
| #176 | 355 – 356 | 1.57 | 8.16 | 30.3 | 13 | 3.87 | 20.37 |
| #180 | 359 – 360 | 1.44 | 7 | 25.9 | 12.4 | 3.51 | 18.44 |
| #180 | 359 – 360 | 1.44 | 7 | 26 | 12.5 | 3.51 | 18.48 |
| #180 | 359 – 360 | 1.45 | 7 | 26.1 | 12.6 | 3.52 | 18.55 |

APPENDIX E

PALYNOLOGY


Figure 39 *Rhizophora*


Figure 40 *Avicennia*


Figure 41 *Sonneratia*


Figure 42 *Bruguiera*


Figure 43 *Suaeda*


Figure 44 *Acrostichum*

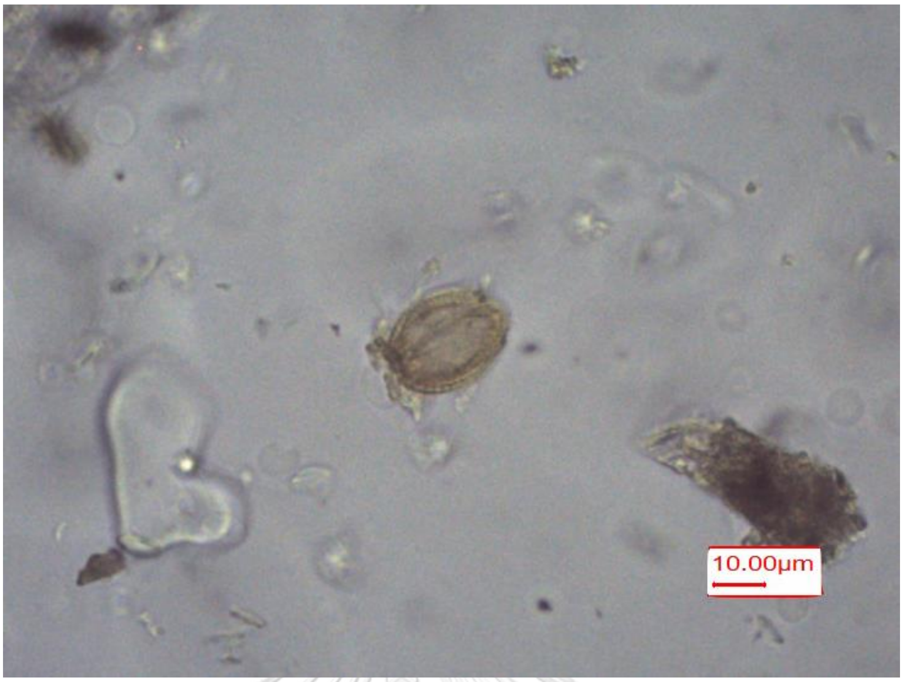


Figure 45 *Oncosperma*

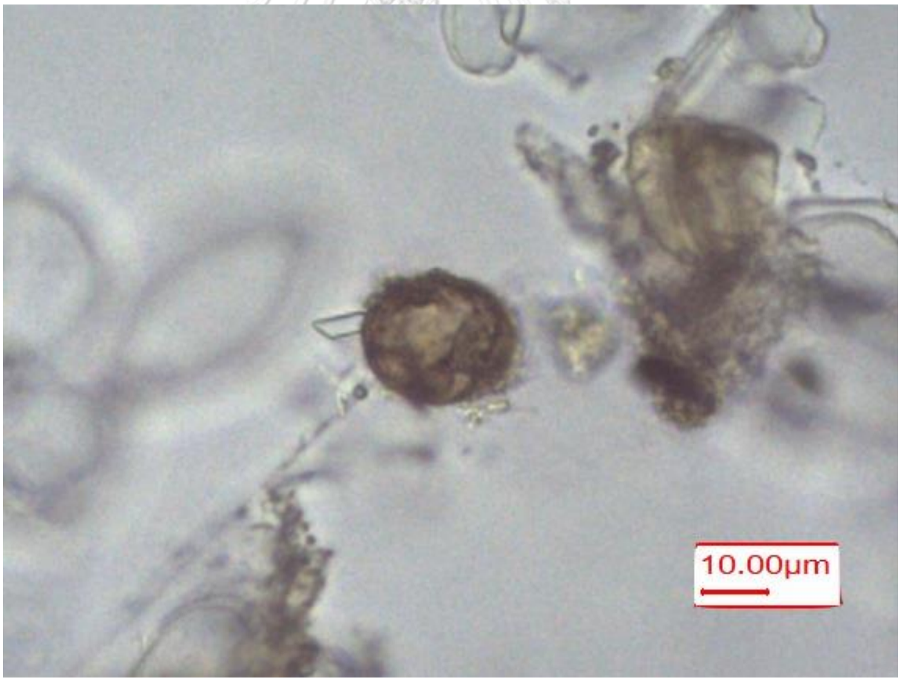


Figure 46 *Xylocarpus*

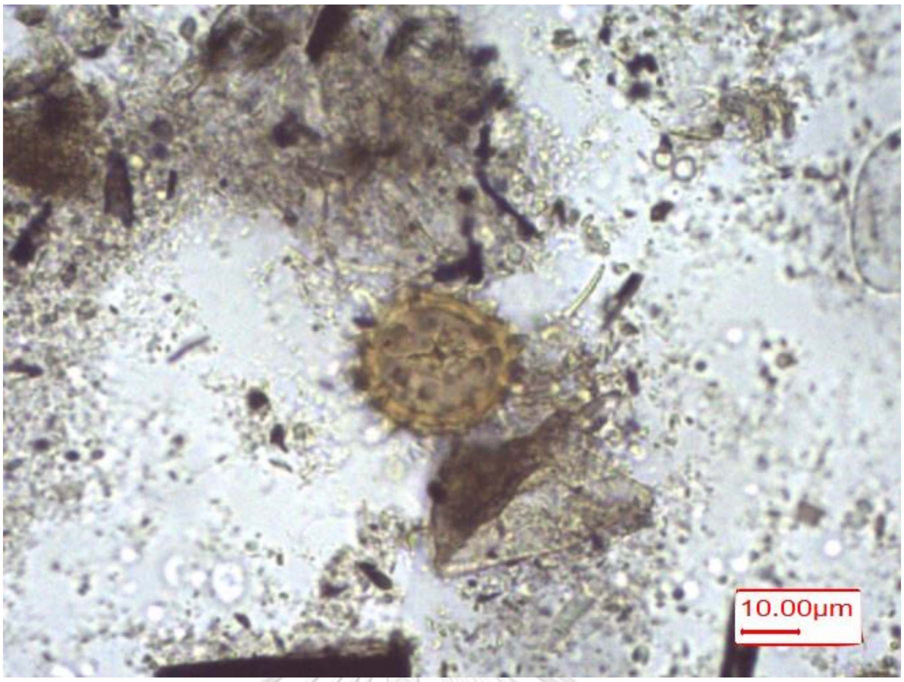


**Figure 47** Asteraceae

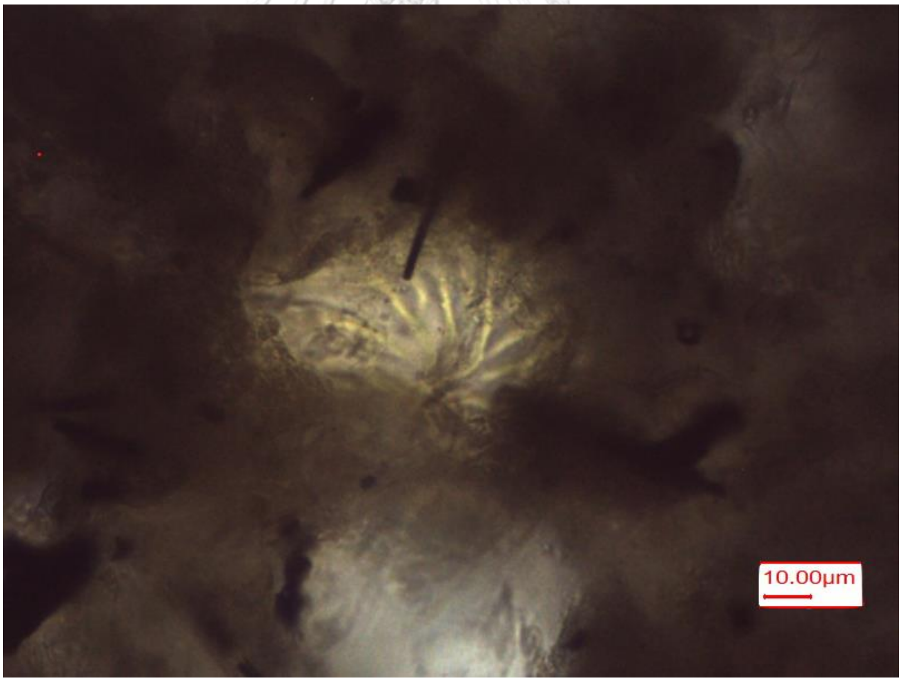


**Figure 48** *Ceratopteris*

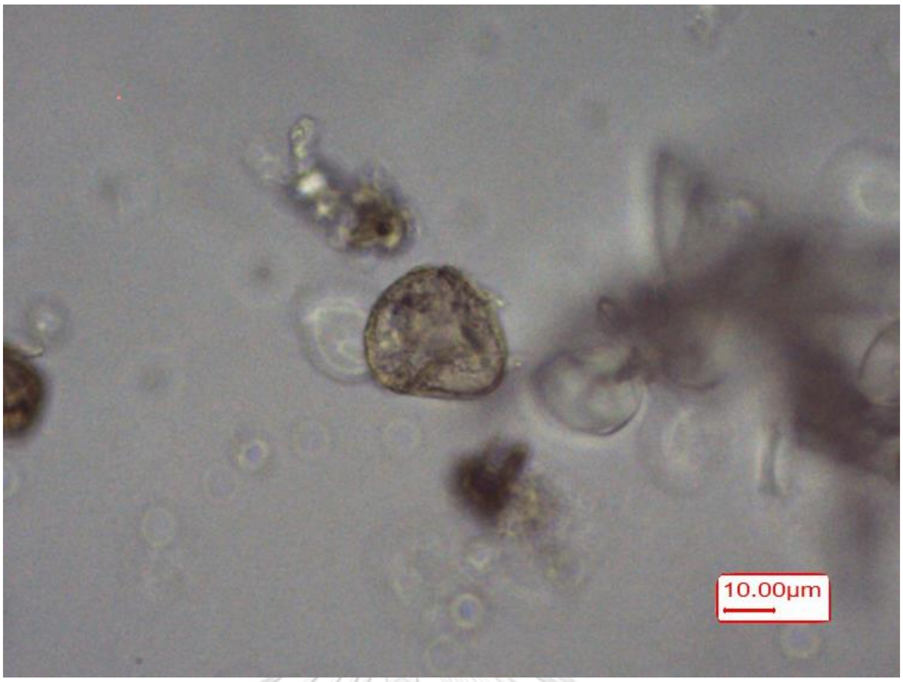


**Figure 49** Cyperaceae

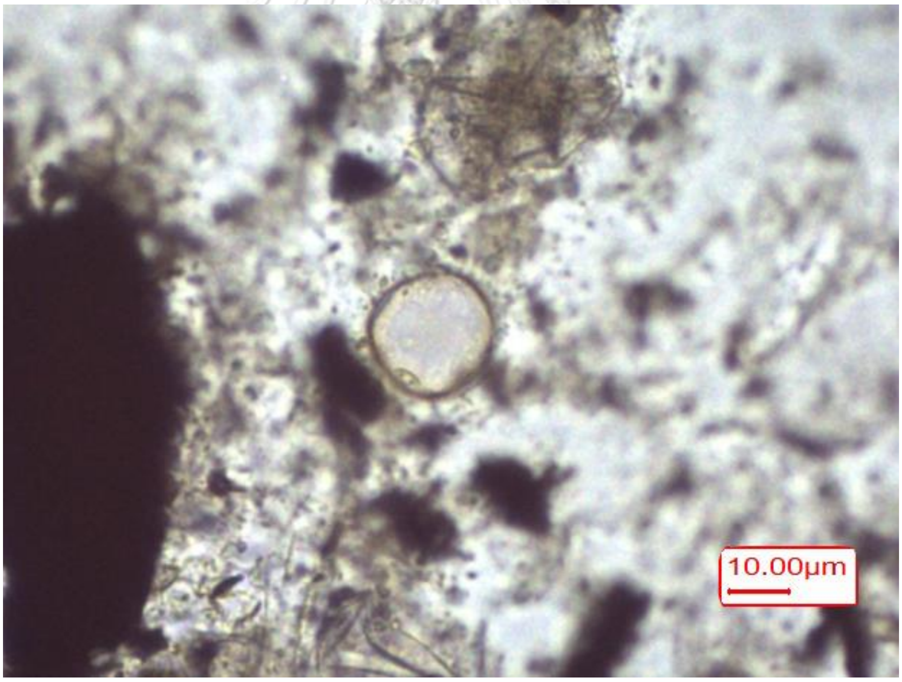


**Figure 50** Poaceae

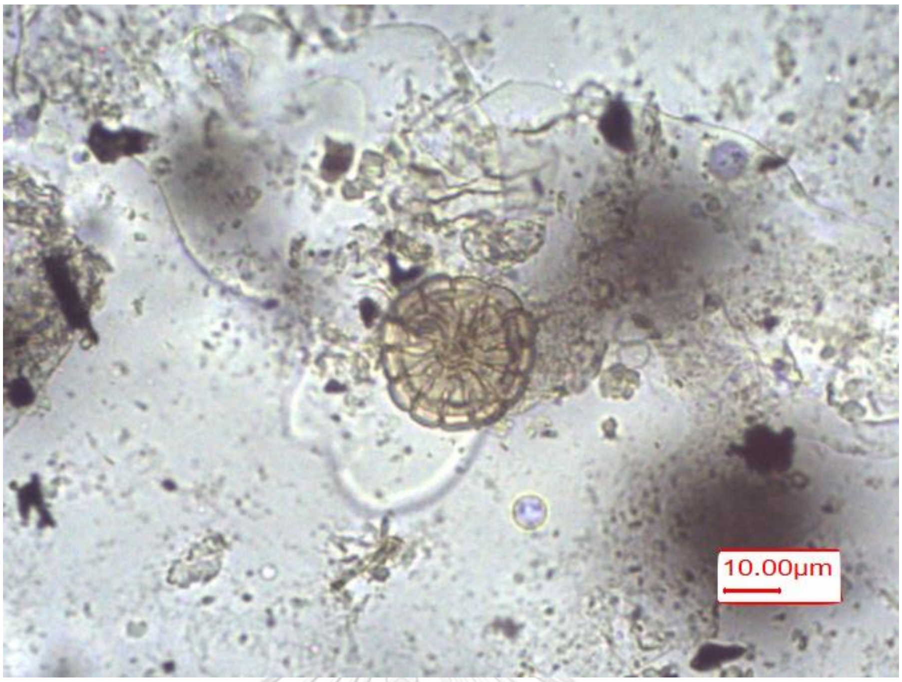


**Figure 51** Polygalaceae


**Figure 52** *Stenochlaena*


**Figure 53** *Casuarina*

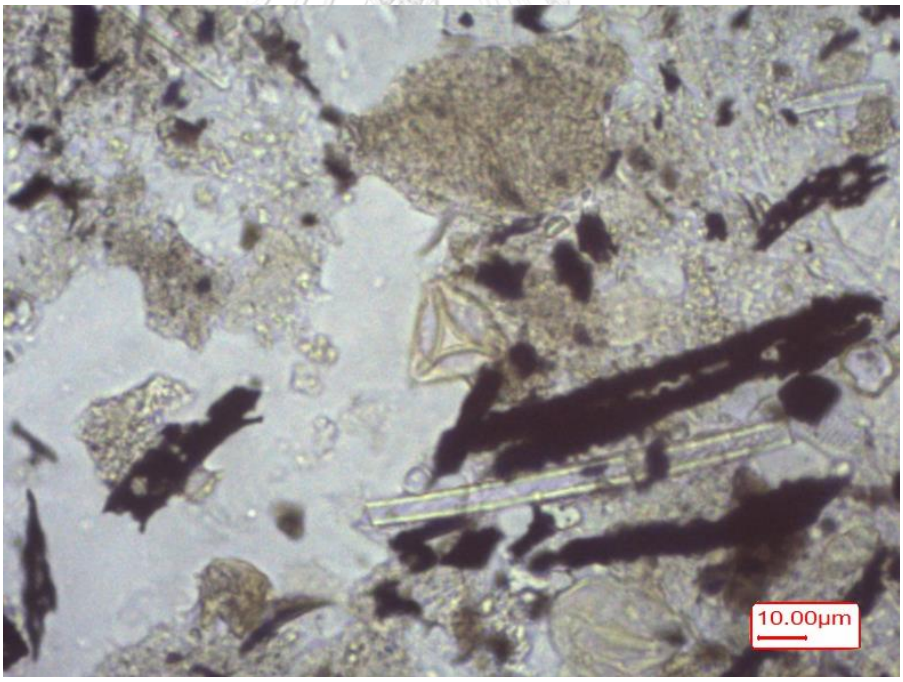


**Figure 54** Myrtaceae

# VITA

| | |
|---|---|
| **NAME** | Worakamon Nudnara |
| **DATE OF BIRTH** | 5 October 1994 |
| **PLACE OF BIRTH** | Bangkok, Thailand |
| **INSTITUTIONS ATTENDED** | Chulalongkorn University (B.Sc.) |
| **HOME ADDRESS** | 272/262, Soi 10, Sirunya Park village, Phahonyothin road, Tambon Thanon Yai, Amphoe Muang, Lopburi 15000 |